Neuroimaging assessment of Cortical Development and Corpus Callosum as predictive markers of neurodevelopmental outcome in small for gestational age fetuses

Gabriela Egaña Ugrinovic

PhD THESIS

Departament d'Obstetrícia i Ginecologia, Pediatria, Radiologia i Anatomía.

Programa de Doctorat de Medicina RD 1393/2007

NEUROIMAGING ASSESSMENT OF CORTICAL DEVELOPMENT AND CORPUS CALLOSUM AS PREDICTIVE MARKERS OF NEURODEVELOPMENTAL OUTCOME IN SMALL FOR GESTATIONAL AGE FETUSES

GABRIELA EGAÑA UGRINOVIC

For the degree of International Doctor in Medicine, May 2014

Directors:

Eduard Gratacós Solsona

Magdalena Sanz Cortés

BCNatal - Barcelona Center for Maternal-Fetal and Neonatal Medicine, Hospital Clínic and Hospital Sant Joan de Deu

PhD TESIS

Departament d'Obstetrícia i Ginecologia, Pediatria, Radiologia i Anatomía.

Programa de Doctorat de Medicina RD 1393/2007

EVALUACIÓN DEL DESARROLLO CORTICAL Y CUERPO CALLOSO COMO MARCADORES PREDICTIVOS DE NEURODESARROLLO EN FETOS PEQUEÑOS PARA LA EDAD GESTACIONAL

GABRIELA EGAÑA UGRINOVIC

Para obtener el grado de Doctor Internacional en Medicina, Mayo 2014

Directores:

Eduard Gratacós Solsona

Magdalena Sanz Cortés

BCNatal - Barcelona Center for Maternal-Fetal and Neonatal Medicine, Hospital Clínic and Hospital Sant Joan de Deu

Barcelona, May 2014.

Eduard Gratacós Solsona, Professor in Obstetrics and Gynecology

Magdalena Sanz Cortés, Microstructure and Metabolomic line coordinator

We confirm that **Gabriela Egaña Ugrinovic** has completed under our supervision the studies presented in the thesis **"Neuroimaging assessment of Cortical Development and Corpus Callosum as predictive markers of neurodevelopmental outcome in small for gestational age fetuses".**

The present thesis has been structured following the normative for PhD thesis as a compendium of publications for the degree of **International Doctor in medicine**, and that the mentioned studies are ready to be presented to the Tribunal.

Eduard Gratacós Solsona

Thesis director

Magdalena Sanz Cortés

Thesis director

ACKNOWLEDGMENTS

I wish to express my sincere gratitude to my tutors Eduard Gratacós who trusted in me and showed how to direct a research group based on the principle of excellence, and to Magda Sanz for her friendship and everlasting patience to guide me into the scientific publications.

I wish to thank all the mothers who participated in these studies and all parents who willingly gave their consent to enrolle their infants in the follow up of this project.

I am finally deeply grateful to my husband who was my support, inspiration and shelter in the diffult moments and to my parents and brothers who encourage me to fly higher and pursuit my objectives despite the distance.

Also, to my friends and collegues who generously shared their knowledge and became my new family.

Barcelona, May 2014

Gabriela Egaña Ugrinovic.

Acknowledgements for financial support: I which to thanks CONICYT, Chile for the financial support through Becas Chile (PFCHA/<Doctorado al Extranjero 4ª Convocatoria><72120071>)

CONTENTS

1. INTRODUCTION 9
1.1 SMALL FOR GESTATIONAL AGE 9
1.2 BRAIN DEVELOPMENT IN IUGR 10
1.2.1 CORTICAL DEVELOPMENT 12
1.2.2 CORPUS CALLOSUM 14
1.2.3 THE RELATIONSHIP BETWEEN CORTICAL DEVELOPMENT AND CORPUS CALLOSUM 16
1.3 NEUROIMAGING 17
1.3.1 FETAL MAGNETIC RESONANCE IMAGE 17
1.3.2 NEUROSONOGRAPHY 18
1.4 NEUROLOGICAL IMPAIREMENT 18
1.4.1 THE NEONATAL BEHAVIORAL ASSESSMENT SCALE TEST 19
1.4.2 BAYLEY SCALE FOR INFANTS AND TODDLER DEVELOPMENT 19
1.5 RELEVANCE AND JUSTIFICATION OF THE RESEARCH STUDY 21
2. HYPOTHESES 23
2.1 GENERAL HYPOTHESIS 23
2.2 SPECIFIC HYPOTHESES 23
3. OBJECTIVES 25
3.1 MAIN OBJECTIVE 25
3.2 SPECIFIC OBJECTIVES 25
4. METHODS 27
4.1 SETTINGS 27
4.2 STUDY TYPE 27
4.3 STUDY POPULATION 27
4.4 INTERVENTIONS 29
4.5 DESIGN 29
4.5.1 ETHICAL APPROVAL 29
4.5.2 EPIDEMIOLOGIC DATA 29
4.5.3 PERINATAL DATA 30
4.5.4 FETAL ULTRASOUND 30
4.5.5 NEUROIMAGING 31
4.6 MEASURES AND IMAGING POST PROCCESING 35
4.6.1 MRI ASSESSMENT 35
4.6.2 ULTRASOUND IMAGING ASSESSMENT 44
4.7 MANAGEMENT 46

4.8 NEURODEVELOPMENT ASSESSMENT 46
4.9 PREDICTIVE VARIABLES 48
4.10 OUTCOME VARIABLES 48
4.11 STATISTICAL ANALYSIS 49
5. STUDIES 51
5.1 STUDY 1 52
5.2 STUDY 2 61
5.3 STUDY 3 89
5.4 STUDY 4 115
5.5 STUDY 5 142
6. RESULTS 169
6.1 CORTICAL DEVELOPMENT DIFFERENCES IN LATE IUGR (STUDY 1) 169
6.2 INSULAR CORTICAL MORPHOMETRY IN LATE IUGR (STUDY 2) 174
6.3 CORPUS CALLOSUM ASSESSMENT BY MRI IN SGA AND ITS ASSOCIATION WITH NEUROBEHAVIOR (STUDY 3) 178
6.4 CORPUS CALLOSUM ASSESSMENT BY NEUROSONOGRAPHY IN SGA (STUDY 4) 180
6.5 CORRELATION BETWEEN FETAL BRAIN ASSESSMENT AND NEURODEVELOPMENTAL OUTCOME AT 2 YEARS (STUDY 5) 183
7. DISCUSSION 187
8. CONCLUSIONS 195
9. ABBREVIATIONS 196
10. REFERENCES 197

1. INTRODUCTION

1.1 SMALL FOR GESTATIONAL AGE (SGA)

Intrauterine growth restriction (IUGR) is a frequent condition in perinatal medicine, accounting between 5-8% prevalence from live newborn babies (Gardosi 2009). IUGR is a major contributor of perinatal and long term morbidity (Ley 1996; Doctor 2001; Lindqvist 2005), including neurological deficits which are considered one of the most consistently reported sequelae in this population (Arcangeli 2012; Savchev 2013; Figueras 2009). In clinical practice a fetus is considered small when the estimated fetal weight is below the 10^{th} centile (Hadlock 1985; Chauhan 2009), in absence of genetic syndromes or fetal infections. Once this suspicion is made, all efforts will be displayed to differentiate between true growth restriction and a constitutionally small fetus. Traditionally, an abnormal umbilical artery Doppler ultrasound measurement was considered the benchmark to differentiate between fetuses exposed to a placental insufficiency in case of an abnormality and "constitutionally small" fetuses or the so called small for gestational age fetuses (SGA)(Marconi 2008). However, several studies have recently shown how this notion should be reconsidered (Savchev 2012; Cruz-Martinez 2009). Indeed, SGA neonates have shown worse perinatal outcomes (Savchev 2013), poorer neurobehavioral scores (Figueras 2009) and worse neurodevelopmental outcome (Arcangeli 2012) compared to adequate for gestational age fetuses (AGA). Due to its high prevalence and its potential impact in public health, different attempts have been made in order to identify the

subpopulation of SGA fetuses that suffer true forms of placental insufficiency and that cannot be detected by umbilical artery Doppler. Small fetuses that present signs of vascular redistribution expressed by abnormal middle cerebral artery Doppler or cerebro-placental ratio are those that present worse perinatal results and neurodevelopment outcomes (Cruz-Martinez 2009). Furthermore, those SGA that are especially small (<3rd centile) and those that present an abnormal uterine artery Doppler are also considered to present worse perinatal and neurodevelopment results (Savchev 2012; Severi 2002). Due to this evidence, it has been recently proposed a classification in which those SGA fetuses with signs of brain redistribution, an estimated fetal weight below the 3rd centile or an abnormal uterine artery Doppler should be considered as a subgroup that may be suffering true forms of late-onset growth restriction (Figueras 2014).

However an optimal identification of those small fetuses at risk for an abnormal neurodevelopment still remains unclear and constitutes one of the main challenges of fetal medicine nowadays.

1.2 BRAIN DEVELOPMENT IN IUGR

Modern neuroimaging has evolved during the last years, improving imaging resolution by ultrasound and magnetic resonance imaging (MRI). Also, advanced sequences of MRI such as spectroscopy or diffusion tensor imaging can report information of brain metabolism and microstructure respectively and have been used to assess fetal brain development (Mailath-Pokorny 2012; Limperopoulos 2009). However, the impact of IUGR on brain

development is still poorly characterized. Some of the brain reorganizational changes that occur under placental insufficiency have been identified and their association with neurodevelopmental deficits has started to be explored (Egana-Ugrinovic 2013; Tolsa 2004; Dubois 2008). Once the right imaging biomarkers are identified and can be implemented in our current practice, infants at risk for an abnormal neurodevelopment will be detected at a very early stage. A thoughtful use of targeted interventions and strategies during the first three years of life, which is considered an important window of opportunity, may improve the functional, intellectual and learning performance of these infants (Als 2012; McAnulty 2010).

We hypothesized that brain microstructural changes may be present also in milder forms of growth restriction, the so called SGA fetuses. These microstructural changes could represent the impact of an adverse environment conferred by a chronic placental insufficiency. Brain sulcation and corpus callosum development are affected in similar adverse in-utero conditions, therefore could be considered good imaging biomarkers candidates to monitor brain maturation under chronic hypoxia (Dubois 2008; Clouchoux 2013; Goldstein 2011; Moses 2000). Moreover, there is a close relationship between the developments of both structures. Indeed, the corpus callosum is topographycally organized according to cortical-callosal connections (Witelson 1989).

We hypothesized that the parameters obtained from the analysis of cortical development and corpus callosum morphometry could predict neurobehavioral and neurodevelopment outcome.

1.2.1 CORTICAL DEVELOPMENT

The development of the fetal cerebral cortex closely reflects brain maturation (Zhang 2010). The formation of cortical sulci is a complex process that begins around 14 weeks of gestation and continues until the end of pregnancy or even after birth. From a completely smooth surface at 22 weeks, it develops into a complex array of sulci and gyri resembling the adult brain by the end of gestation (Cohen-Sacher 2006).

The period from 26 to 36 weeks of gestation has been defined as a critical period for cortical folding (Dubois 2008). Primary sulci become progressively deeply infolded developing side branches, designated as secondary sulci, and as gyration proceeds the tertiary sulci emerge from these last ones (Chi 1977). The timing of the appearance of these different types of sulci is so precise that neuropathologists consider gyration to be a reliable estimate of gestational age and consequently a good marker of fetal brain maturation (Zhang 2010; Garel 2001). Compared to neuropathology findings, neuroimaging has a delay in detecting the apparition of the different fissures, by means of one week on MRI (Garel 2001) and two weeks by brain ultrasound (Cohen-Sacher 2006; Ruiz 2006). The exact mechanisms underlying cortical development are still not understood, although several hypotheses have been proposed such as genetic control, active growth of convolutions during gyrogenesis, differential growth between the inner v/s outer layers of the cortex, cytoarchitectonic differentiation, cortical growth and tension from white matter axonal fibers pulling radially on the developing cortex (Glenn 2009). Besides this coordinated cortical maturation, it is remarkable that there is a normal asymmetry in the formation of sulci between the right and left cerebral hemispheres

(Kasprian 2011; Pistorius 2010); finding for example that left lateral fissure is deeper than the right one in normal intrauterine conditions (Dubois 2010). This structural asymmetry is thought to precede the later expression of some lateralized functions, such as language and handedness (Dubois 2009), and abnormalities in its development have been described as an important predisposition factor for common neurologic and psychiatric diseases (Kasprian 2011).

While this harmonious anatomical brain development is partly related to the cortical functional organization, local perturbations in cortical morphology are of interest to identify an abnormal neurodevelopment (Rajagopalan 2011). Some of these cortical abnormalities have been observed in certain developmental and neuropsychiatric disorders. For example autism spectrum disorder individuals have been described to present a generalized cerebral cortical enlargement (Hazlett 2011), a loss of brain asymmetry and reduced interhemispheric connectivity (Lo 2011). In subjects diagnosed with schizophrenia, a reduced sulcation, irrespective of age at onset of the disease has been reported, with a special impact on the left collateral sulcus (Penttila 2008). Furthermore, severe IUGR preterm newborns show an abnormal sulcation pattern and abnormal cortical development which was considered a good marker of their functional outcome (Dubois 2008). Therefore, we think that it is plausible that late-onset IUGR fetuses could present subtle changes in their cortical development and that cortical morphology at term may represent an early endophenotype of later neurodevelopment.

1.2.2 CORPUS CALLOSUM

Corpus callosum is a thick plate of dense myelinated fibers. Its formation, which follows an anterior to posterior directionality, is initiated in the embryonic period during the 5th week of gestation and is completed by 18–20 weeks (Kier 1996). Fetal corpus callosum serves as a sensitive indicator for normal brain development and maturation (Goodyear 2001). A comprehensive evaluation of corpus callosum development during normal human fetal gestation is essential to detect and understand subtle abnormalities of fetal neurodevelopment. On this matter, normal appearance and reference growth values for the different gestational ages during the second half of pregnancy have been reported on transvaginal sonograms (Bornstein 2010; Garel 2011; Malinger 1993; Achiron 2001; Hofer 2006). Corpus callosum continues its growth postnatally and it is not until puberty that reaches its maximum fiber directionality and by the age of 25 completes its adult size (Pujol 1993). The most anterior regions of the corpus callosum are the rostrum and the genu, that connect higher-order prefrontal cortical functions with smaller diameter fibers (Barkovich 1988). Moving caudally, the successive callosal areas are the body and the splenium which connect from anterior to posterior through larger diameter fiber the premotor and sensory cortex, and the occipital cortex (Gilliam 2011).

Due to the connectivity that underlies the corpus callosum with different parts of the brain, it is considered an interesting target when different neuropsychiatric conditions are studied. Attention deficit hyperactivity disorder subjects have shown to present smaller corpus callosum total area, and smaller anterior midbody and isthmus. Furthermore, their microstructure was also abnormal, finding reduced fractional anisotropy of the isthmus

compared to controls (Cao 2010). In autism spectrum disorders, smaller corpus callosum volumes, high mean diffusivity and low fractional anisotropy values have been described, suggesting microstructure abnormalities as well (Alexander 2007). Patients diagnosed with schizophrenia have shown low fractional anisotropy values in the genu and the splenium of the corpus callosum (Davenport 2010). These findings further support the relationship between abnormal corpus callosum maturation and the susceptibility to develop neuropsychiatric conditions later on. Another group of interest is very low birth weight children because they are at high risk of perinatal white matter injury (Counsell 2008). Indeed, preterm-born adolescents with very low birth weight present reduced fractional anisotropy values in the corpus callosum which was further associated with perceptual, cognitive, motor and mental health impairments, supporting that perinatal injury of white matter tracts may persist with clinical significance into adolescence (Allin 2007; Skranes 2007).

Subtle abnormalities in the maturation of the corpus callosum could appear in response to an adverse environment, and these reorganizational changes could constitute a more vulnerable phenotype to develop neurological deficits during childhood (Huppi 2008). On this matter, abnormalities in the thickness of the corpus callosum have been associated not only to the presence of additional brain malformations such as ventriculomegaly, vermian agenesis and abnormal sulcation, but also to neurodevelopmental impairments such as mental retardation and neonatal seizures (Volpe 2006; Lerman-Sagie 2009). Consequently, corpus callosum could be considered both a reliable surrogate marker of

white matter growth, and a sensitive indicator of normal brain development and maturation (Goodyear 2001).

Therefore knowledge of fetal callosal size and morphology could be key to understand subtle changes in those SGA fetuses exposed to chronic placental insufficiency which may represent an early endophenotype of later neurodevelopment outcome.

1.2.3 THE RELATIONSHIP BETWEEN CORTICAL DEVELOPMENT AND CORPUS CALLOSUM

Although most of the previous studies focus on the assessment of the cortical development or corpus callosum independently, it is remarkable the existence of a delicate association between these two structures (Moses 2000). In the agenesis of the corpus callosum, it has been described a disruption of the normal cortical folding pattern (Warren 2010) and a higher incidence of gyral malformations, which are among the most common additional malformation seen in the agenesis of the corpus callosum (Brisse 1998). Furthermore, it has been reported a general delayed sulcation process in fetuses diagnosed with corpus callosum agenesis (Warren 2010) which could be explained most likely as a consequence of a failed commisuration due to a diffuse white matter dysgenesis in these fetuses (Tang 2009). Probably this synergism between cortical development and corpus callosum maturation involves a combination between mechanical theories in the gyrification processes and genetic factors guiding brain development (Toro 2005).

These findings support the theory that an integral corpus callosum facilitates optimal gyral development and that minor alterations of the corpus callosum may induce subtle differences in the cortical development.

1.3 NEUROIMAGING

1.3.1 FETAL MAGNETIC RESONANCE IMAGE

To date, fetal MRI has been used primarily for the qualitative morphologic evaluation of the fetal brain. However, recent applications of advanced MRI techniques have provided an unprecedented opportunity to investigate the developing brain *in vivo* (Limperopoulos 2009). The ability to begin a reliable investigation of brain development in the healthy and compromised fetus promises a range of new quantitative biomarkers that can be applied clinically, and that will help to formulate a better understanding of brain development and lead to improved management of high-risk pregnancies (Limperopoulos 2009). Fetal MRI has several advantages when assessing brain development: not being hampered by fetal presentation or oligohydramnios; better characterization of the brain cortex and it can evaluate diffuse white matter abnormalities better than ultrasound (Hagmann 2008). Nevertheless it has disadvantages: its high cost and the fact that it is not always available; it may be hampered by fetal motion artifacts and marked maternal obesity; and it doesn't provide information about the maternal-fetal circulation (Hagmann 2008).

1.3.2 NEUROSONOGRAPHY

This sonographic exam consists on a dedicated fetal ultrasound scan to assess the fetal brain. It can be performed trasabdominally, although the transvaginal approach provides excellent visualization of brain structures during the second half of the pregnancy. The ultrasound scan is the screening modality of choice for the detection of fetal abnormalities (Hagmann 2008). Even if we acknowledge that the transvaginal approach could be challenging, this difficulty can be overcome with proper training (Malinger 1994). Moreover, the ultrasound approach shows several advantages: is widely available and low cost; it is a real-time imaging allowing dynamic assessment of the fetus and multiplanar reconstruction can be performed; it is an easily accepted technique that can be frequently repeated; it has excellent spatial resolution, and offers the possibility to evaluate the maternal-fetal circulation (Hagmann 2008). Nevertheless, it has some disadvantages: it may be hampered by fetal presentation, oligohydramnios and maternal obesity; it has poor contrast resolution and therefore, poor evaluation of diffuse white matter abnormalities; and the cortical morphometry is not easily assessable (Hagmann 2008).

1.4 NEUROLOGICAL IMPAIRMENT

An increasing number of neurodevelopmental disorders in childhood and adult life are thought to have a prenatal origin (Barker 1995; Kok 1998; Toft 1999). Fetal growth restriction is a well-recognized risk factor for perinatal morbidity and long term consequences (Savchev 2012; Ley 1996; Leitner 2007). Indeed, 20-40% of IUGR children will experience cognitive challenges and learning disabilities (Geva 2006; Jugovic 2007;

Walker 2008). Exposure to chronic placental insufficiency inducing an undernourished and hypoxic environment may impact the developing brain of small fetuses (Tolsa 2004; Huppi 2008), resulting in a spectrum of neurological disabilities. Neurological impairment can be assessed by different tests according to the infants´s age and to the spectrum of the neurodevelopmental issue that is aimed to be explored:

1.4.1 THE NEONATAL BEHAVIORAL ASSESSMENT SCALE (NBAS) TEST

This test was developed in 1973 by Dr. T. Berry Brazelton (Brazelton 1995; Brazelton 2004). It evaluates a wide range of behaviors landmarks that enables us to describe developmental and behavioral maturation, central nervous system integrity, and the kinds of stress responses. Moreover, it has been reported that early developmental status is associated with later developmental outcome through infancy, particularly neonatal general irritability was a predictor of mental development at 12 months, and neonatal self-regulation behaviors were predictors of psychomotor development, verbal and total intelligence quotient at 6 years (Canals 2011).

1.4.2 BAYLEY SCALE FOR INFANT AND TODDLER DEVELOPMENT (BAYLEY-III)

This is an internationally recognized scale to evaluate the neurodevelopmental status of children aged 1 to 42 months (Milne 2012). This test can be performed even in non-verbal children. The Bayley-III is an individually administered instrument that assesses infant development across five domains, including cognitive, language and motor competencies.

Parent reported questionnaires are incorporated into the Bayley-III to assess social-emotional and adaptive behaviors.

Therefore, we hypothesized that term SGA subjects might have an abnormal neurobehavioral and neurodevelopmental outcome attributable to disrupted brain maturational process.

1.5 RELEVANCE AND JUSTIFICATION OF THE RESEARCH STUDY

Fetal growth restriction affects up to 5-8% of fetuses in developed countries, with over half a million cases per year in Europe and the USA (MacDorman 2010). IUGR is considered an independent risk factor for the development of neuropsychiatric diseases and neurocognitive deficits (Geva 2006). Therefore, these neurodevelopment deficits are thought to be the result of fetal brain reorganizational changes (Sanz-Cortes 2010; Batalle 2012). However, the impact of fetal growth restriction on brain development is still poorly characterized. The identification of brain imaging biomarkers associated to a sustained undernutrition and chronic hypoxia in-utero could become predictive tools of abnormal neurodevelopment in fetuses at risk.

Abnormalities in cortical and corpus callosum development have been described in early and severe IUGR (Goldstein 2011; Dubois 2008); therefore, these structures might provide valuable information about the influence of prenatal conditions on brain maturation. But the presence of cortical and callosal abnormalities in term small fetuses has not been explored yet, nor the potential association with the neurodevelopmental outcome.

Identifying fetuses at risk for abnormal neurodevelopment in fetal medicine lays the basis to perform specific strategies to potentially improve both pre and postnatal management, such as timely delivery, careful support for breastfeeding and a thoughtful use of this window of opportunity to improve their neurocognitive outcome through specific strategies of early stimulation during the first years of life.

2. HYPOTHESES

2.1 GENERAL HYPOTHESIS

Term SGA fetuses present cortical developmental and corpus callosum differences when compared to controls. These brain structural differences correlate with their neurobehavior and neurodevelopmental outcome.

2.2 SPECIFIC HYPOTHESES

1. SGA present a different pattern of brain sulcation that correlates with neonatal neurobehavioral performance.

2. SGA present differences in their corpus callosum morphology that correlates with neonatal neurobehavioral performance.

3. A predictive model using cortical development and corpus callosum features can be constructed to obtain an algorithm for early identification of those infants at highest risk of abnormal neurodevelopment.

3. OBJECTIVES

3.1 MAIN OBJECTIVE

To evaluate cortical development and corpus callosum parameters in term SGA compared to control fetuses and to assess their correlation with their neurobehavior and neurodevelopmental outcome.

3.2 SPECIFIC OBJECTIVES

1. To compare cortical development assessment by fetal brain MRI between term SGA and AGA fetuses and to evaluate its correlation with neonatal neurobehavioral outcome
2. To compare corpus callosum morphometry assessed by fetal brain MRI between term SGA and AGA fetuses and to evaluate its correlation with neonatal neurobehavioral outcome
3. To compare corpus callosum morphometry assessed by neurosonography between late-onset IUGR and AGA fetuses
4. To explore the correlation between brain cortical development and corpus callosum parameters with the neurodevelopmental outcome of term SGA born infants.

4. METHODS

4. 1. SETTING

BCNatal - Barcelona Center for Maternal-Fetal and Neonatal Medicine (Hospital Clínic and Hospital Sant Joan de Deu), Institut d'Investigacions Biomediques August Pi i Sunyer (IDIBAPS), Centre for Biomedical Research on Rare Diseases (CIBER-ER), and University of Barcelona, Barcelona, Spain.

4. 2. STUDY TYPE: Prospective cohort study.

4. 3. STUDY POPULATIONS

Pregnant women were classified in the following groups:

1. Group: AGA
2. Group: SGA
3. Group: late-onset IUGR

Inclusion criteria:

1. Group AGA:
   - Normal pregnancies with an estimated fetal weight $\geq 10^{th}$ centile (Chauhan 2009), according customized growth curves (Figueras 2008), confirmed postnatally

2. Group SGA:

   - Estimated fetal weight <10th centile (Chauhan 2009), according to customized growth curves (Figueras 2008), confirmed postnatally
   - Normal umbilical artery Doppler (pulsatily index (PI) <95th centile) (Arduini 1990)

3. Group late-onset IUGR:

   - Estimated fetal weight <10th centile (Chauhan 2009), according to customized growth curves (Figueras 2008), confirmed postnatally
   - Normal umbilical artery Doppler (PI <95th centile) (Arduini 1990)
   - At least one of the following criteria (Figueras 2014): abnormal cerebroplacental ratio (Bahado-Singh 1999) and/or estimated fetal weight <3rd centile for the gestational age (Savchev 2012) and/or abnormal uterine Doppler (Severi 2002)

Exclusion criteria:

- Evidence of fetal structural or chromosomal abnormalities
- Absence of maternal pathologies (Diabetes Mellitus type 1 or 2, preeclampsia and/or chronic hypertension, autoimmune disease and obesity)
- Perinatal infection
- Multiple gestation
- Breech presentation
- Obesity defined by a maternal body mass index >30 (calculated as pregestational weight in kg/[height cm]^2)

- Contraindications for MRI such as claustrophobia, pacemaker, anxiety or panic attacks

4.4 INTERVENTIONS

- Signature of maternal consent to enrollment in the study for all study groups
- Collection of epidemiological data
- Fetal brain MRI and ultrasound
- Collection of perinatal data
- Neonatal neurobehavioral assessment: NBAS test
- Neurodevelopment assessment of the children at 2 years: Bayley-III test

4.5. DESIGN

4.5.1 ETHICAL APPROVAL

The protocol was approved by the hospital ethics committee and written consent was obtained from all mothers (Institutional Review Board Committee on 12th June, 2008; 2008/4422).

4.5.2 EPIDEMIOLOGICAL DATA

Maternal age, weight, height, body mass index, smoking status (number of cigarettes per day), parity, ethnicity, educational level, and socioeconomic status defined by never worked, unemployed, independent worker or employed (United Kingdom National

Statistics Socio-economic Classification).

4.5.3 PERINATAL DATA

Last menstrual period corrected by the first trimester crown-rump length (Robinson 1975), pregnancy complications, requirement for induction of labor, gestational age at delivery and way of delivery, requirement of emergency cesarean section, neonatal gender, Apgar score at 1 and 5 minutes, cord arterial and venous pH, birth weight and birth weight centile, and days in neonatal intensive care unit.

4.5.4 FETAL ULTRASOUND

- **BASIC ULTRASOUND**

Determination of fetal presentation and biometry assessment of fetal growth using the Hadlock formula (Hadlock 1985) were estimated, including the measurement of the biparietal diameter (BPD), head and abdominal circumferences and femur length.

- **DOPPLER STUDY**

It was obtained one week from the MRI scan. In small fetuses, examination was performed every one or two weeks using a Siemens Sonoline Antares (Siemens Medical Systems, Malvern, PA, USA), or General Electric Voluson E8 (GE Medical Systems, Zipf, Austria) ultrasound machine equipped with a 6–2-MHz linear curved-array transducer. Doppler recordings were performed in the absence of fetal movements and voluntary maternal suspended breathing. Pulsed Doppler parameters were performed automatically from three or more consecutive waveforms, with the angle of insonation as close to 0º as

possible (Arduini 1990).

Umbilical artery PI: was performed from a free-floating cord loop and considered abnormal when >95th centile (Arduini 1990).

Middle cerebral artery PI: was obtained in a transversal view of the fetal head, at the level of its origin from the circle of Willis. The cerebroplacental ratio was calculated dividing the middle cerebral artery PI by the umbilical artery PI. Middle cerebral artery PI and cerebroplacental ratio values <5th centile were considered indicative of cerebral blood flow redistribution (Baschat 2003).

Uterine arteries PI: in a sagittal section of the uterus the transducer was gently tilted from side to side and color flow mapping was used to identify the uterine artery. The PI was obtained bilaterally from the ascending branch of the uterine artery. The mean PI of the left and right arteries was calculated and considered abnormal when >95th (Gomez 2008).

4.5.5 NEUROIMAGING

- **NEUROSONOGRAPHY**

A detailed fetal brain scan was performed one or two weeks after the diagnosis of fetal growth restriction in a dedicated neurosonographic unit. In order to compare our neurosonographic data, control fetuses were recruited from our general population matching them with our cases by gestational age in which the neurosonography was performed. All structural images were reviewed for the presence of anatomical abnormalities. The methodology used in our neurosonographic assessment included the acquisition of specific slices from the three orthogonal planes based on the guidelines

proposed by the International Society of Ultrasound in Obstetrics and Gynecology (ISUOG 2007):

Axial Plane: two axial planes were routinely obtained:

-Transventricular plane: as used for the measurement of the BPD (ISUOG 2007). The anatomical landmarks were the anterior horns, the presence in the anterior third of the cavum septi pellucidi which appears as an image depicted by two parallel lines that separate the anterior horns, the atrium, the posterior horns of the lateral ventricles and the choroid plexus to discard an oblique plane (Alonso 2010) (Figure 1).

-Supraventricular plane: is a more cephalad plane from the transventricular plane (Fig. 2).

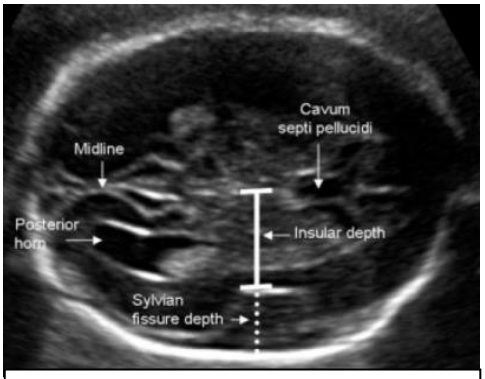

Figure 1: Transventricular plane

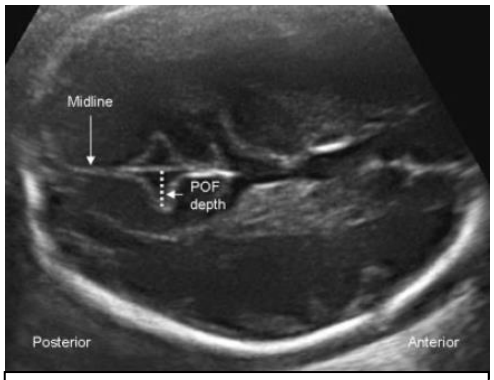

Figure 2: Supraventricular plane

Midsagittal plane: this plane is mainly acquired for the assessment of the fetal corpus callosum which can be visualized as a hypoechoic structure bound by two echogenic lines (Pashaj 2013). In this plane the sulcus of the corpus callosum, the cingulate gyrus, and the cavum septi pellucidi and cavum vergae have to be present (Achiron 2001). The slice containing a clear view of the fornix, the anterior commissure, the fastigium and the lamina cuadrigemina will be selected for post processing analysis (Stancak 2003). Absence of the fetal orbits also must be present (Figure 3).

Figure 3: Midsagittal plane

Coronal Plane: this plane is mainly acquired for the assessment of the posterior fossa. Two coronal planes were obtained:

-Transcaudal plane: was defined as where the corpus callosum disrupts the interhemispheric fissure. It includes the cavum septi pellucidi, the anterior horns of the lateral ventricles and the lateral fissures (Pistorius 2010) (Figure 4).

-Transcerebellar plane: in order to assess the posterior fossa and to obtain a coronal view, the probe was turned 90° from the transcaudal plane, identifying the anterior horns, thalami, cerebellum, tentorium and cisterna magna (Alonso 2010) (Figure 5).

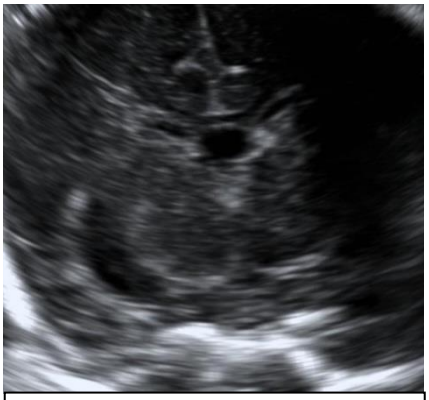

Figure 4: Transcaudal plane

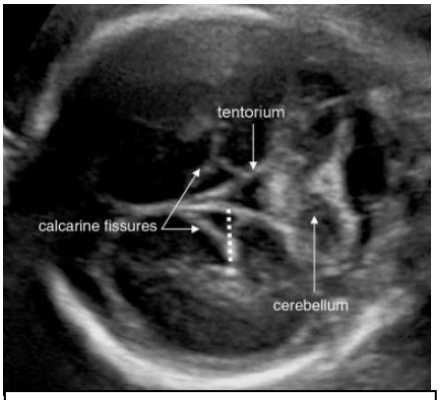

Figure 5: Transcerebellar plane

- **FETAL MAGNETIC RESONANCE IMAGE**

We designed a protocol in which anatomical and diffusion sequences were obtained:

- Localizer sequence
- T2 half-Fourier acquisition single-shot turbo spin-echo (HASTE) axial, coronal and sagittal planes for anatomical assessment
- Diffusion tensor imaging: anisotropy diffusion coefficient and fractional anisotropy

Fetal brain MRI scan was performed at 37±1 weeks of gestational age on a clinical magnetic resonance system using the Institut d'Investigacions Biomediques August Pi i Sunyer image platform, operating at 3.0 Tesla (Siemens Magnetom Trio Tim syngo MR B15, Siemens, Germany) without fetal sedation and following the American College of Radiology guidelines for use of medical imaging during pregnancy and lactation (Tremblay 2012). A body coil with 8 elements was wrapped around the mother's abdomen. Routine fetal imaging consisted on single-shot, fast spin echo T2-weighted sequences (TR 990ms, TE 137 ms, slice thickness 3.5mm, no gap, field of view 260mm, voxel size 1.4 x 1.4 x 3.5mm, matrix 192 x 192, flip angle 180o, acquisition time 24 seconds) acquired in the axial, sagittal and coronal planes. If the quality of the images was suboptimal, sequences were repeated. Subsequently, a 12-direction diffusion tensor imaging acquisition was obtained (TR 9300ms, TE 94ms, diffusion weighting b-value 1000s/mm^2, slice thickness 2.2mm, no gap, field of view 220mm, voxel size 2.2×2.2×2.2mm, matrix 100x100, flip angle 90º, acquisition time 2.30 minutes).

Structural images were reviewed for the presence of anatomical abnormalities by an experienced specialist in neuroradiology blinded to group membership.

4. 6. MEASURES AND IMAGING POST PROCESSING

4.6.1 MRI ASSESSMENT

All measurements were performed using Analyze 9.0 software (Analyze TM, Biomedical Imaging Resource, Mayo Foundation ©1999-2009).

- **CORTICAL DEVELOPMENT**

Fissures depth, total brain, intracranial and opercular volumes were assessed in the anatomical acquisitions.

1. Brain biometric and fissure assessment:

To avoid the bias of having smaller measurements in smaller heads, a normalization of the biometric measurements was performed using the BPD obtained by MRI (Reichel 2003).

a. **BPD** was measured in the transthalamic plane as described for ultrasound by ISUOG (ISUOG 2007) (Figure 9A). To avoid the bias of smaller BPD in smaller head, the BPD was corrected by birth weight.

b. **Cortical fissure depths** were measured bilaterally (Figure 9):

    i. Parietoccipital fissure was measured in the axial slice above the

transthalamic plane used for the BPD assessment, tracing a perpendicular line from the interhemispheric fissure to the apex of the parietoccipital fissure (Alonso 2010) (Figure 9B).

ii. Lateral fissure depth was measured in the axial slice located immediately below the anterior commissure and the cavum septi pellucidi, with a continuing line starting from the most external border of the insular cortex to the interface conformed between the subarachnoid space and the skull (Alonso 2010) (Figure 9C).

iii. Insular depth was measured in the same plane described above, tracing a perpendicular line from the interhemispheric fissure to the most external border of the insular cortex (Alonso 2010) (Figure 9D).

iv. Cingulate fissure was measured in the midcoronal plane, tracing a perpendicular line from the median longitudinal fissure to the apex of the cingulate fissure (Pistorius 2010) (Figure 9E).

v. Calcarine fissure was measured in the coronal transcerebellar plane (ISUOG 2007), tracing a perpendicular line from the interhemispheric fissure to the apex of the calcarine fissure (Alonso 2010) (Figure 9F).

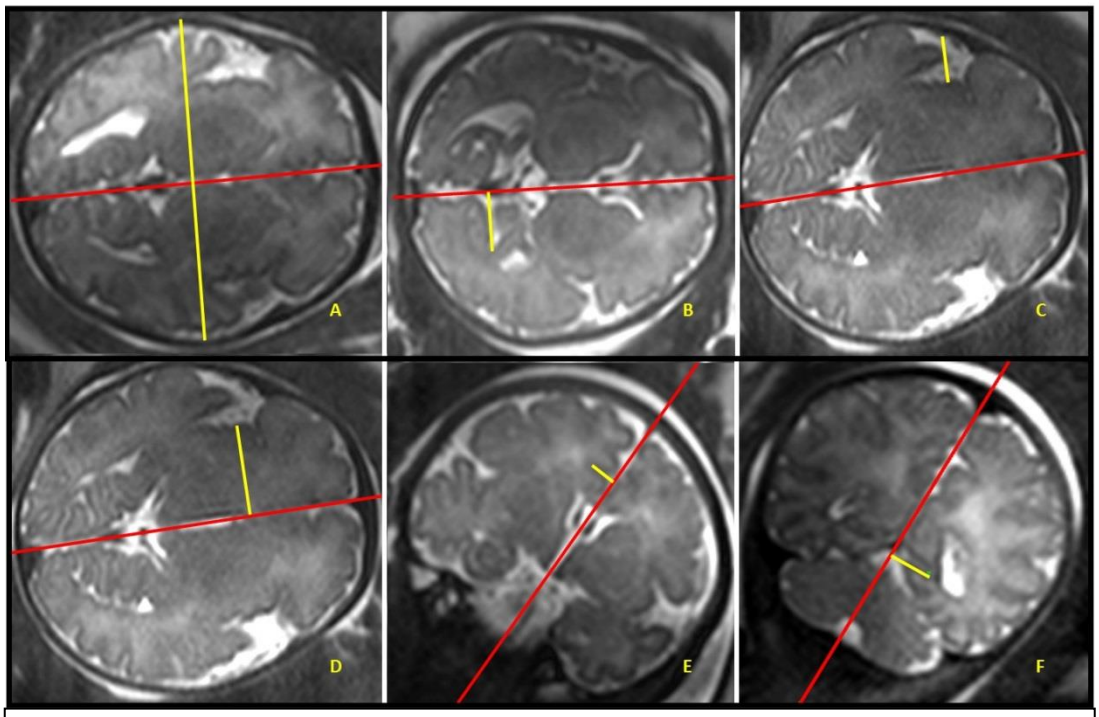

Figure 9: Cortical Development assessment

2. Brain volumetric analysis:

All volumetric estimations were obtained using Cavalieri´s principle (Clatterbuck 1997) by a multiplanar analysis considering a slice thickness of 3.5mm with no gap interval between them. To avoid bias of smaller measurements in smaller heads, total intracranial volume and total brain volume were adjusted by birth weight and the opercular volumes were adjusted by the total brain volume.

a. **Total intracranial volume** was successively delineated including the extra and intraventricular cerebrospinal fluid, cerebral, cerebellar, and brain stem (Limperopoulos 2010) (Figure 10A).

b. **Total brain volume** was successively delineated including intraventricular

cerebrospinal fluid, cerebral, cerebellar and brain stem parenchyma, but excluding the extraventricular cerebrospinal fluid (Limperopoulos 2010) (Figure 10B).

c. **Opercular volumes** were delineated bilaterally in all slices in which the operculums were identified, following the opercular cortex until the external borders of the lateral fissures, thus closing the volume by a straight line joining the anterior and posterior edges of the fissure. A methodology reported by Nakamura *et al.* was adapted and followed (Nakamura 2004) (Figure 10C).

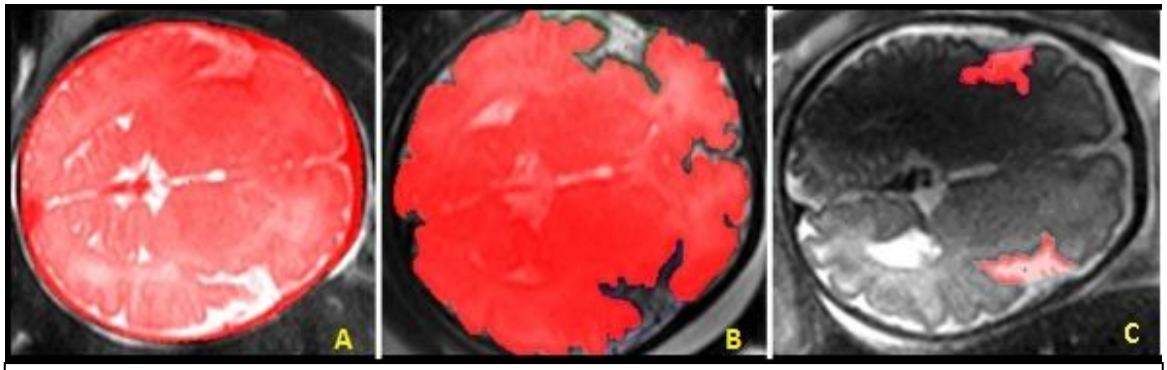

Figure 10: Brain volumes assessment

3. Brain Asymmetry:

In order to assess the degree of **brain asymmetry**, we applied a previously reported asymmetry index (Dubois 2008) expressed by asymmetry index = (R–L)/(R+L) to compare right (R) and left (L) fissures and opercular measurements.

- **INSULAR CORTICAL MORPHOLOGY**

The cortical plate was identified by the intensity threshold defined as the T2-weighted hypointense rim delineating the brain surface (Righini 2012).

1. Biometric Measurements:

   a. **Insular cortical thickness**: was measured bilaterally in the axial plane located immediately below the plane of the anterior commissure and the cavum of the septi pellucidi. Anterior, middle and posterior thickness of the insular cortex were manually delineated from its inner-to-external cortical border. Every measurement was performed three times and the mean of each one was used for further analysis. The anterior and posterior insular cortical thicknesses were traced on the limiting portion with the frontal and temporal operculum respectively (Chen 1995). Middle insular cortical thickness was measured equidistantly from the anterior and posterior measurements (Figure 11A).

   b. **Insular depth**: was measured as described above in cortical development post-processing (Alonso 2010). Insular depth was obtained to correct the insular cortical thickness for differences in head size (Figure 11B).

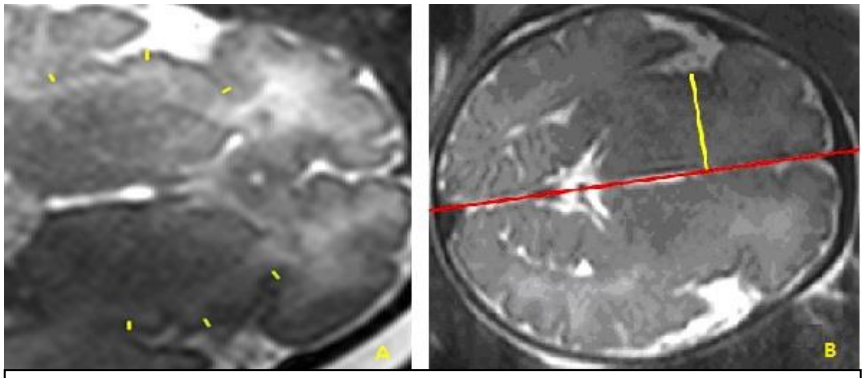

Figure 11: Insular biometric assessment

2. Volumetric measurements:

Volumes were delineated through cursor-guided free-hand trace. The region-of-interest traced on each image created an area that was multiplied by the slice thickness in order to produce a volume. Volumes from successive slices were then summed to yield the volume of the full extent from the desired region-of-interest (Cohen 2010).

a. **Insular cortical volume**: the whole insular cortex was traced bilaterally in the coronal plane. The anatomical boundaries chosen for delineation were (Crespo-Facorro 2000; Takahashi 2004) (Figure 12A):

    i. Anteriorly the most rostral slice containing the insular cortex

    ii. Posteriorly the fusion of the superior and inferior circular insular sulci in the coronal plane

    iii. Superiorly by the superior circular insular sulcus, and

    iv. Inferiorly by the inferior circular insular sulcus or the orbitoinsular sulcus.

b. **Total brain volume** was delineated as described above in cortical development post-processing (Limperopoulos 2010). Total brain volume was obtained to correct the insular cortical volume for differences in head size (Figure 12B).

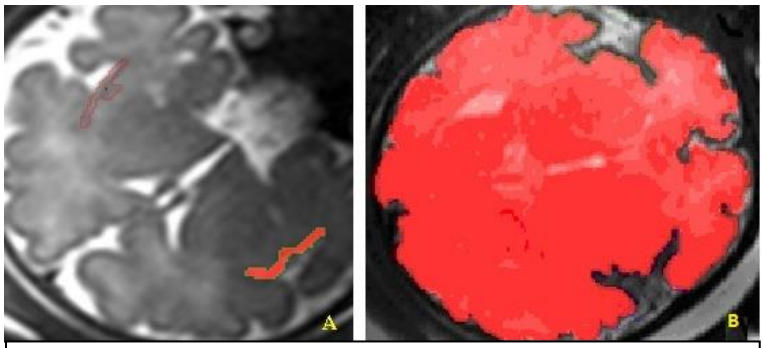

Figure 12: Insular and total brain volume assessment

3. Asymmetry indices: an **asymmetry coefficient** for insular cortical thickness and insular cortical volume size was calculated using the following formula asymmetry index = (R–L)/(R+L) to compare right (R) and left (L), where a negative value indicated a larger left-sided structure (Dubois 2008).

4. Fractional anisotropy: **fractional anisotropy maps** were analyzed using the ITK-SNAP 2.4 software. A region-of-interest of 43mm^3 was traced at the level of the corresponding anterior, middle and posterior insular cortex measurements bilaterally in order to obtain fractional anisotropy values. Mean fractional anisotropy values and standard deviations were used for further analysis (Figure 13).

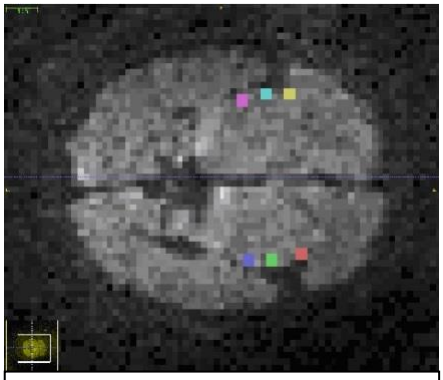

Figure 13: Fractional anisotropy

- **CORPUS CALLOSUM MORPHOMETRY**

Corpus callosum was identified in the midsagittal plane as a slightly curved horizontal T2-weighted hypointense structure (Harreld 2011). The slice chosen for corpus callosum measurements had to accomplish strict quality criteria defined in the midsagittal plane (Achiron 2001; Stancak 2003). Furthermore, a clear visualization of the body, splenium,

genu, and rostrum of the corpus callosum was required. Length, thickness and areas were delineated.

To avoid the bias of having smaller corpus callosum measurements in smaller heads, a normalization of all measures was performed using the cephalic index. The cephalic index was calculated applying a previously reported formula: cephalic index=BPD/occipitofrontal diameter*100 (Lim 2004).

1. Linear measurements

   a. **Corpus callosum length** was measured from the most anterior part of the genu to the most posterior part of the splenium tracing a straight rostro-caudal line between the two points, known as the outer-to-outer callosal length (Harreld 2011) as shown by the red line in Figure 14. Length was measured three times and the mean value was used for further analysis.

   b. **Corpus callosum thickness** was measured in its anterior, middle and posterior portions corresponding to the genu, body and splenium thickness (Witelson 1989; Lerman-Sagie 2009). The thickness of the genu and splenium were measured at the same level where the line for callosal length was traced, and body thickness was measured equidistantly from the genu and splenium (Witelson 1989). These measurements were obtained three times and the mean value was used for further analysis. They are shown by yellow lines in Figure 14.

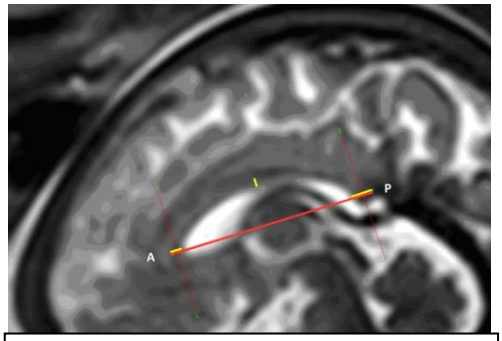

Figure 14: CC linear measures

2. Area measurements

a. **Total corpus callosum area** was delineated through cursor-guided free-hand traces. It limited superiorly by the cingulate gyrus which was identified as a hyperintense curved shaped line and inferiorly, by the cavum septi pellucidi and cavum vergae (Witelson 1989; Boger-Megiddo 2006) (Figure 15A).

b. **Corpus callosum** was subdivided in **seven areas** described by Witelson *et al* in order to measure the rostrum, genu, rostral body, anterior midbody, posterior midbody, isthmus and splenium areas (Witelson 1989) (Figure 15B).

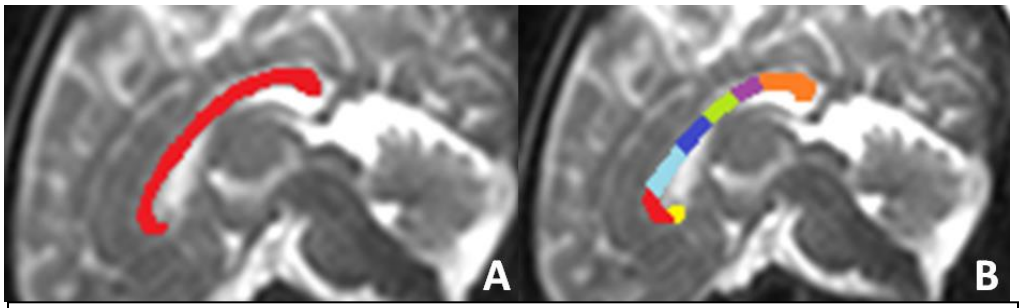

Figure 15: Total corpus callosum area and its subdivisions

4.6.2. ULTRASOUND IMAGING ASSESSMENT

All measurements were performed using Analyze 9.0 software (Analyze TM, Biomedical Imaging Resource, Mayo Foundation ©1999-2009).

- **CORPUS CALLOSUM MORPHOMETRY**

Corpus callosum was identified in the midsagittal plane as a slightly curved hypoechoic structure. The slice chosen for measurements had to accomplish strict quality criteria defined in the midsagittal plane (Pashaj 2013). Furthermore, a clear visualization of the body, splenium, genu, and rostrum of the callosum had to be accomplished. Length, thickness and areas were measured.

To avoid the bias of having smaller corpus callosum measurements in smaller heads, a normalization of all measures was performed using the cephalic index. The cephalic index was calculated applying a previously reported formula: cephalic index=BPD/occipitofrontal diameter*100 (Lim 2004).

1. Linear measurements

    a. **Corpus callosum length** was measured from the most anterior part of the genu to the most posterior part of the splenium tracing a straight rostrocaudal line between the two points, as shown by the straight red line in Figure 6 (Harreld 2011). This measurement was obtained three times and the mean value was used for further analysis.

b. **Corpus callosum thickness** was measured in its anterior, middle and posterior portions corresponding to the genu, body and splenium thickness (Lerman-Sagie 2009). The thickness of the genu and splenium were measured at the same level where the line for corpus callosum length was traced (Witelson 1989) and body thickness was measured equidistantly from the genu and splenium as shown by the yellow lines in Figure 6. These measurements were obtained three times and the mean value was used for further analysis.

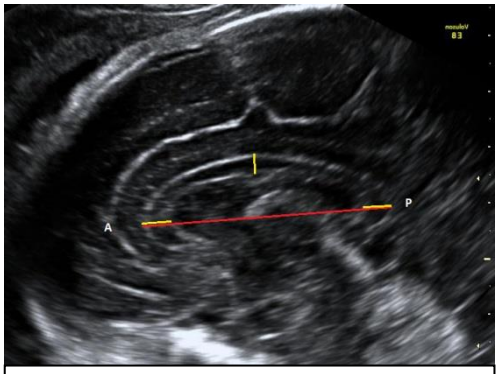

Figure 6: CC linear measures

2. <u>Area measurements</u>

a. **Total corpus callosum area** was delineated through cursor-guided free-hand traces limited superiorly by the hyperechoic sulcus of the corpus callosum and the cingulate gyrus and inferiorly, by the cavum septi pellucidi and cavum vergae (Figure 7) (Pashaj 2013).

b. **Corpus callosum** was subdivided in **seven areas** described by Witelson *et al.* (Figure 8) (Witelson 1989) in order to measure, from anterior to posterior, the rostrum, genu, rostral body, anterior midbody, posterior midbody, isthmus and

splenium area.

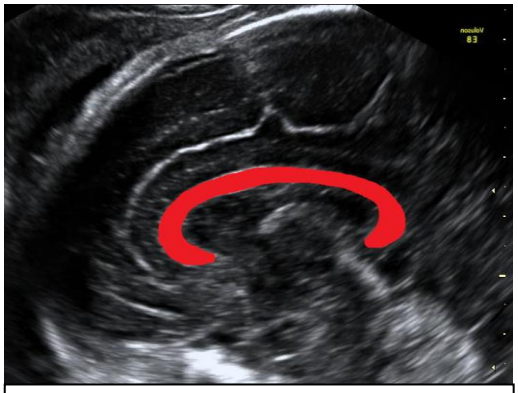

Figure 7: Total corpus callosum area

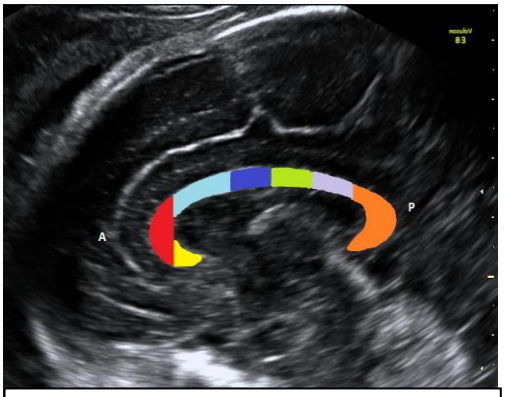

Figure 8: Corpus callosum subdivision

4.7. MANAGEMENT

Labor induction was performed at term (≥37 weeks) for all SGA cases by cervical ripening with a slow release of vaginal prostaglandin E_2 (10 mg). If the onset of labor did not occur within twelve hours, oxytocin induction was performed. All deliveries were attended by a staff obstetrician. For the SGA cases the decision at what gestational age to effect delivery, as well as the mode of delivery was taken in accordance to the institution protocols, taking into account the possible complications of prematurity versus the risk of continued intrauterine stay.

4.8. NEURODEVELOPMENT ASSESSMENT

4.8.1 NEONATAL NEUROBEHAVIORAL ASSESSMENT

The NBAS test was prospectively performed in all cases at 42-43 weeks by one of three

observers accredited by The Brazelton Institute (Harvard Medical School, Boston, USA). The observers were blinded to the Doppler results. The examination consisted on 6 behavioral areas rated on a 1 to 9 scale where 9 is the best performance for some areas and for others this is represented by the central score of 5 (Brazelton 1995). With the newborn between two feedings, in a small and quiet semi-dark room, with a temperature between 22-27°C and in the presence of at least one parent, the following areas were analyzed: social-interactive (which include response to visual and acoustic stimuli), organization of state (which include peak of excitement, rapidity of build-up, irritability and lability of states) and motor (which include general tone, motor maturity, pull-to-sit, defensive movements and level of activity). Following a recent report by the original authors of the NBAS, individual items were clustered to assess the attention capacity (which includes alertness, quality of alert responsiveness and cost of attention) (Sagiv 2008). The behavioral items were converted into centiles according to normal curve references for our population (Costas-Moragas 2007), and each area was considered abnormal at a score <5th centile.

4.8.2 NEURODEVELOPMENTAL OUTCOME AT 2-YEARS

Developmental function was evaluated at 24 months using the Bayley-III, 3rd Edition, which is a revision of the prior edition (Bayley 2006). The Bayley-III is an instrument that assesses infant development across five domains, including cognitive, language and motor competencies. Parent reported questionnaires are incorporated into the Bayley-III to assess social-emotional and adaptive behaviors. All evaluations were performed by one of

three trained psychologists, blinded to the study group and perinatal outcomes. According to the test manual, abnormal result for each domain was defined as a Bayley-III score below 1 SD (<85). We considered a pathological neurodevelopmental outcome at the presence of at least one abnormal domain.

4.9. PREDICTIVE VARIABLES

Main predictive variables: study group, measurements of cortical development and corpus callosum

Secondary predictive variables: parental smoking; maternal body mass index; socioeconomic and educational status; ethnicity; gestational age at MRI; neonatal gender; neonatal complications; age at Bayley-III and breastfeeding.

4.10. OUTCOME VARIABLES

Primary outcome variable: abnormal cortical and corpus callosum development in term SGA fetuses and abnormal neurodevelopment in the neonatal period and at 2 years.

Secondary outcome variables:

-Abnormal fetal brain development: Different sulcation pattern, smaller brain volumes, thinner cortex, smaller corpus callosum

-Abnormal neurodevelopment: abnormal neurobehavior (results below 1 Z-score

according to normal local curves in the neonatal period assessed by the NBAS test) and abnormal neurodevelopment (at least one abnormal domain below 1 Z-score in the Bayley-III according to manual at 24 month of age).

4.11. STATISTICAL ANALYSES

Student's t-test and Pearson Chi-squared test or exact Fisher test were used to compare quantitative and qualitative data, respectively.

The primary analysis was focused on the evaluation of the existence of differences in the predictive variables and primary outcomes among study groups using a Multivariate analysis of covariance (MANCOVA), or Student *T*- test.

As secondary analysis, linear regression was used to evaluate the relationship between the predictive variables (cortical development and corpus callosum) with postnatal neurodevelopment. Results were adjusted by several potentially confounding variables (study group, gender, gestational age at the neuroimaging scan, maternal BMI, maternal socioeconomic and educational status, parental smoking and breastfeeding). The relationship between the independent variables (fissures depth; brain volumes; insular cortical thickness; insular cortical volume; and corpus callosum length, thickness and areas) with outcome variables (abnormal neonatal neurobehavior and neurodevelopment outcome at 2 years) were modeled by binary logistic regression analysis.

Then, a composite score was obtained using a combination between the independent

variables from brain development that provided the best classification model of being a term-SGA fetus. This composite score was constructed according to the formula obtained by the logistic regression: Composite score= $e^{-(Y)}$/ (1 + $e^{-(Y)}$). The ROC curve of the model was then obtained. This same analysis was performed to construct a composite score to predict abnormal neurodevelopment at 2 years, using a combination of the best variables of brain development that predicted an abnormal neurodevelopment according to the regression analysis and to the principal component analysis. The ROC curve of the model was then obtained.

Statistical anlyses were performed using the Statistical package for the Social Sciences (SPSS for Windows version 17.0, Chicago, Illinois, USA) statistical software.

5. STUDIES

The projects included in this thesis belong to the same research line leading to five articles already published or submitted for publication in international journals:

1. Egaña-Ugrinovic G, Sanz-Cortes M, Figueras F, Bargalló N, Gratacós E. Differences in cortical development assessed by fetal MRI in late-onset intrauterine growth restriction. *Am J Obstet Gynecol. 2013; 209: 126.e1-8.*

2. Egaña-Ugrinovic G, Sanz-Cortes M, Figueras F, Couve-Perez C, Gratacós E. Fetal MRI Insular Cortical Morphometry and its Association with Neurobehavior in Late-Onset Small For Gestational Age Fetuses. *Ultrasound Obstet Gynecol. 2014 Mar 10. doi: 10.1002/uog.13360.*

3. Egaña-Ugrinovic G, Sanz-Cortés M, Couve-Pérez C, Figueras F, Gratacós E. Corpus callosum differences assessed by fetal MRI in late-onset intrauterine growth restriction and its association with neurobehavior. *Prenat Diagn. 2014 Apr 7. doi: 10.1002/pd.4381.*

4. Egaña-Ugrinovic G, Savchev, S, Bazán-Arcos C, Puerto B, Gratacós E, Sanz-Cortés Neurosonographic assessment of the corpus callosum as a potential biomarker of abnormal neurodevelopment in late-onset fetal growth restriction. *Submitted Fetal Diagnosis and Therapy 2014.*

5. Egaña-Ugrinovic G, Sanz-Cortés M, Bazán-Arcos C, Couve-Pérez C, Gratacós E. Correlation between structural brain abnormalities assessed by fetal MRI and neurodevelopmental outcome at 2 years in infants born small for gestational age.. *Submitted Am J Obstet Gynecol 2014.*

5.1 STUDY 1

Differences in cortical development assessed by fetal MRI in late-onset intrauterine growth restriction

Egaña-Ugrinovic G, Sanz-Cortes M, Figueras F, Bargalló N, Gratacós E.

Am J Obstet Gynecol. 2013

State: Published

Impact factor: 3.877

Quartile: 1st

OBSTETRICS

Differences in cortical development assessed by fetal MRI in late-onset intrauterine growth restriction

Gabriela Egaña-Ugrinovic, MD; Magdalena Sanz-Cortes, PhD; Francesc Figueras, PhD; Nuria Bargalló, PhD; Eduard Gratacós, PhD

OBJECTIVE: The objective of the study was to evaluate cortical development parameters by magnetic resonance imaging (MRI) in late-onset intrauterine growth—restricted (IUGR) fetuses and normally grown fetuses.

STUDY DESIGN: A total of 52 IUGR and 50 control fetuses were imaged using a 3T MRI scanner at 37 weeks of gestational age. T2 half-Fourier acquisition single-shot turbo spin-echo anatomical acquisitions were obtained in 3 planes. Cortical sulcation (fissures depth corrected by biparietal diameter), brain volumetry, and asymmetry indices were assessed by means of manual delineation and compared between cases and controls.

RESULTS: Late-onset IUGR fetuses had significantly deeper measurements in the left insula (late-onset IUGR: 0.293 vs control: 0.267; $P = .02$) and right insula (0.379 vs 0.318; $P < .01$) and the left cingulate fissure (0.096 vs 0.087; $P = .03$) and significantly lower intracranial (441.25 cm^3 vs 515.82 cm^3; $P < .01$), brain (276.47 cm^3 vs 312.07 cm^3; $P < .01$), and left opercular volumes (2.52 cm^3 vs 3.02 cm^3; $P < .01$). IUGR fetuses showed significantly higher right insular asymmetry indices.

CONCLUSION: Late-onset IUGR fetuses had a different pattern of cortical development assessed by MRI, supporting the existence of in utero brain reorganization. Cortical development could be useful to define fetal brain imaging-phenotypes characteristic of IUGR.

Key words: brain volumetry, cortical sulcation, fetal brain imaging

Cite this article as: Egaña-Ugrinovic G, Sanz-Cortes M, Figueras F, et al. Differences in cortical development assessed by fetal MRI in late-onset intrauterine growth restriction. Am J Obstet Gynecol 2013;209:126.e1-8.

Late-onset intrauterine growth restriction (IUGR) accounts for the majority of clinical forms of growth restriction and affects approximately 10% of the general population.[1] For a long time considered as a relatively benign condition with a majority of constitutionally small fetuses, recent evidence has demonstrated that late-onset growth restriction is strongly associated with adverse pregnancy and long-term outcomes.[2] Abnormal neurodevelopment in newborns and children is among the most relevant consequences of late-onset IUGR.[3-8]

Neurodevelopmental deficits associated with this condition are thought to be the result of brain reorganizational changes, as suggested by studies demonstrating differences in brain metabolism and microstructure,[3,9] morphology,[10] and connectivity.[11] However, the impact of late-onset IUGR on brain development is still poorly characterized. There is a need to develop imaging biomarkers that help identifying the patterns of neurodevelopment associated with sustained undernutrition in utero.

Evaluation of cortical development (CD) may provide valuable information about the influence of prenatal conditions on brain maturation. Cortical sulcation is a continuous process that occurs mainly during fetal life and results in the intricate array of brain fissures and sulci as present in term fetuses.[12] The progress of sulcation can be used as a reliable estimate of gestational age and a good marker of fetal cortical maturation.[13]

An altered convolution pattern has been demonstrated in preterm newborns diagnosed with severe early-onset IUGR,[14,15] but the existence of differences in late-onset IUGR fetuses has not been evaluated. Aside from sulcation, normal CD during intrauterine life

From the Department of Maternal-Fetal Medicine, Institut Clínic de Ginecologia, Obstetrícia i Neonatologia, Fetal and Perinatal Medicine Research Group, Institut d'Investigacions Biomediques August Pi i Sunyer, and Centro de Investigación Biomédica en Red de Enfermedades Raras, Hospital Clínic, Universitat de Barcelona (Drs Egaña-Ugrinovic, Sanz-Cortes, Figueras, and Gratacós), and the Department of Radiology, Hospital Clínic, and Centre de Diagnostic per la Imatge, Institut d'Investigacions Biomediques August Pi i Sunyer (Dr Bargalló), Barcelona, Spain.

Received Nov. 14, 2012; revised March 6, 2013; accepted April 4, 2013.

This work was supported by grants from the Cerebra Foundation for the Brain-Injured Child, Carmarthen, Wales, UK; the Thrasher Research Fund, Salt Lake City, UT; Obra Social "la Caixa," Barcelona, Spain; and Banca Cívica de Caja Navarra (Proyecto TETD). G.E.-U. was supported by CONICYT (PFCHA/Doctorado al Extranjero 4ª Convocatoria, grant 72120071), Chile. M.S.-C. was supported by the Instituto de Salud Carlos III Rio Hortega (grant CM10/00222), Spain.

The authors report no conflict of interest.

Partial results from this study were presented in oral format at the 22nd World Congress on Ultrasound in Obstetrics and Gynecology, Copenhagen, Denmark, Sept. 9-13, 2012; the 11th World Congress of the Fetal Medicine Foundation, Kos, Greece, June 24-28, 2012; and the 23rd European Congress of Perinatal Medicine, Paris, France, June 13-16, 2012.

Reprints not available from the authors.

0002-9378/$36.00 • • http://dx.doi.org/10.1016/j.ajog.2013.04.008

results in a physiological brain asymmetry.[16,17] Abnormal brain asymmetry has been described in childhood conditions characterized by altered neurodevelopment, such as autism spectrum disorders, attention deficit-hyperactivity disorder (ADHD), dyslexia, and schizophrenia.[14,18] It seems plausible that term late-onset IUGR fetuses could show differences in their CD pattern because the most relevant changes in brain sulcation and expression of asymmetry occur during late third trimester.[16,17]

The aim of this study was to evaluate the existence of individual or combined CD differences in fetuses with late-onset IUGR compared with controls. We evaluated the depth of brain fissures, brain volumetries, and the asymmetry indices by fetal brain magnetic resonance imaging (MRI) in late-onset IUGR and adequate-for-gestational-age (AGA) fetuses at term.

Materials and Methods

Subjects

This study is part of a larger prospective research program on IUGR involving fetal, neonatal, and long-term postnatal follow-up. The specific protocol of this study was approved by the institutional ethics committee (institutional review board no. 2008/4422), and all participants gave written informed consent.

A total of 102 singleton fetuses were included in our cohort, classified in 52 late-onset IUGR and 50 AGA fetuses. Pregnancies were dated according to the first-trimester crown-rump length measurement.[19] IUGR was defined by an estimated and postnatally confirmed fetal weight less than the 10th centile, according to local standards[20] with normal umbilical Doppler (umbilical artery pulsatility index less than the 95th centile).[21] AGA subjects were defined as normal term fetuses with an estimated and postnatally confirmed fetal weight of the 10th centile or greater, according to local standards.[20] Exclusion criteria included congenital malformations, chromosomal abnormalities, perinatal infections, chronic maternal pathology, contraindications for MRI, and noncephalic presentations.

Clinical and ultrasound data

IUGR patients were followed up in our fetal growth restriction unit from diagnosis until delivery. The entire sample underwent serial Doppler ultrasound scans using a General Electric Voluson E8, 6-2 MHz curved-array transducer (GE Medical Systems, Zipf, Austria). Fetal umbilical artery and middle cerebral artery pulsatility index (PI) were measured in 3 or more consecutive waveforms, with the angle of insonation as close as possible to 0° and in the absence of fetal or maternal movements and used for the calculation of the cerebroplacental ratio (CPR). Abnormal CPR was defined as a value below the fifth centile according to previously published reference values.[22] Uterine artery (UtA) PI was measured transabdominally as previously described,[23] and values were considered abnormal when greater than the 95th centile.[23] All fetuses in this study had at least 1 scan within 1 week of delivery. Maternal and perinatal data were prospectively recorded in all study patients.

Fetal MRI imaging acquisition

MRI was performed at 37 weeks of gestational age on a clinical magnetic resonance system using the IDIBAPS image platform, operating at 3.0 Tesla (Siemens Magnetom Trio Tim syngo MR B15; Siemens, Munich, Germany) without fetal sedation and following the American College of Radiology guidelines for the use of medical imaging during pregnancy and lactation.[24] A body coil with 8 elements was wrapped around the mother's abdomen. Routine fetal imaging took from 15 to 20 minutes and consisted of single-shot, fast spin echo T2-weighted sequences (repetition time 990 milliseconds, echo time 137 milliseconds, slice thickness 3.5 mm, no gap, field of view 260 mm, voxel size 1.4 × 1.4 × 3.5mm, matrix 192 × 192, flip angle 180°, and acquisition time 24 seconds) acquired in the 3 orthogonal planes. If the quality of the images was suboptimal, sequences were repeated.

Structural MRI images were reviewed for the presence of anatomical abnormalities by an experienced specialist in neuroradiology blinded to group membership.

Fetal imaging after processing and delineation

Offline analyses of brain biometric and volumetric measurements were performed using the semiautomatic Analyze 9.0 software (Biomedical Imaging Resource; Mayo Clinic, Kansas City, KS) by 2 experienced examiners blinded to group membership. Cortical fissure delineations in the fetal MRI were performed adapting previously described methodology to assess CD on prenatal ultrasound.[25,26] All volumetric estimations were obtained using Cavalieri's principle[27] by a multiplanar analysis considering a slice thickness of 3.5 mm with no gap interval between them.

Both biometric and volumetric measurements showed optimal quality to perform CD analysis in 97% of the cases and in 98% of controls.

Brain biometric and sulcation analysis

Cortical fissure depths were measured bilaterally as shown in Figure 1 and corrected by biparietal diameter (BPD), obtaining a ratio (fissure/BPD) for each fissure measurement to perform the statistical analysis as follows.

- BPD was measured in the transthalamic axial plane as described for ultrasound by the International Society of Ultrasound in Obstetrics and Gynecology.[28,29]
- Parietoccipital fissures were measured in an axial slice above the transthalamic plane used for the BPD assessment,[26,28] tracing a perpendicular line from the longitudinal fissure to the apex of the parietoccipital fissures.
- Insular depths were measured in the axial slice located immediately below the anterior commissure and the cavum septum pellucidum, tracing a perpendicular line from the median longitudinal fissure to the most external border of the insular cortex.[26]
- Lateral fissure depths were measured in the same plane described above, with a continuing line starting from

the most external border of the insular cortex to the interface conformed between the subarachnoid space and the skull.[26,30]

- Cingulate fissures were measured in the midcoronal plane,[25,28] tracing a perpendicular line from the median longitudinal fissure to the apex of the cingulate fissures.
- Calcarine fissures were measured in the coronal transcerebellar plane as described in ultrasound by the International Society of Ultrasound in Obstetrics and Gynecology,[26,28] tracing a perpendicular line from the median longitudinal fissure to the apex of the calcarine fissures.

Brain volumetric analysis

For the statistical analysis, total intracranial volume and total brain volume were adjusted by birthweight centile, and the opercular volumes were adjusted by total brain volume (TBV) (Figure 2).

- Total intracranial volume (TIC) was successively delineated including the extra- and intraventricular cerebrospinal fluid (CSF), cerebral, cerebellar, and brain stem.[31]
- TBV was successively delineated including intraventricular CSF, cerebral, cerebellar, and brain stem parenchymal volumes but excluding the extraventricular CSF volume.[31]
- Opercular volumes were delineated bilaterally in all the slices in which the operculums were identified, following the opercular cortex until the external borders of the lateral fissures, thus closing the volume by a straight line joining the anterior and posterior edges of the fissure. A methodology reported by Nakamura et al[32] was adapted and followed.

Brain asymmetry

To assess the degree of brain asymmetry, we applied a previously reported asymmetry index[33] expressed by the following: asymmetry index = (R−L)/(R+L) to compare right (R) and left (L) fissures and opercular measurements.

Interobserver variability

To establish both biometric and volumetric measurement reproducibility, a total of 15 cases were completely assessed independently by 2 experienced examiners blinded to group membership. Bland-Altman plots were used to assess interobserver variability with a significance level set at 5% ($P < .05$) for all measurements.

FIGURE 1
Illustrative figures of brain biometric and sulcation assessment in different brain sections

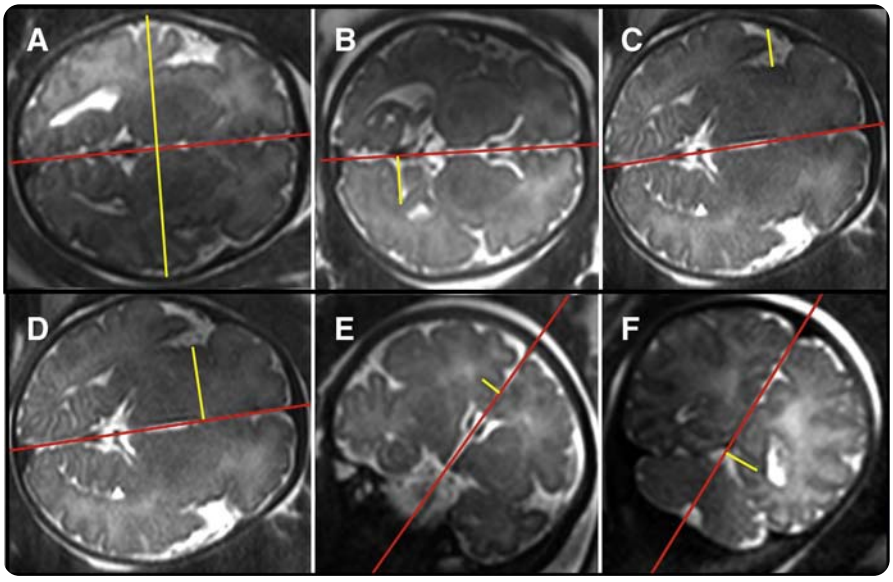

Red line indicates the interhemispheric fissure and *yellow line* indicates the measure of interest in T2-weighted magnetic resonance images of a fetus at 37 weeks of gestational age. **A,** The biparietal diameter and a unilateral example of each fissure assessed are shown. **B,** Right parietoccipital fissure depth, **C,** left lateral fissure depth, and **D,** left insular depth are shown in the axial plane. **E,** The left cingulate fissure depth and the **F,** right calcarine fissure depth are shown in the coronal plane.

Egaña-Ugrinovic. Cortical development analysis in late-onset IUGR fetuses. Am J Obstet Gynecol 2013.

Statistical analysis of clinical and CD data

Student *t* test for independent samples and Pearson's χ^2 tests were used to compare quantitative and qualitative data, respectively, between late-onset IUGR and controls. Multivariate analyses of

FIGURE 2
Brain volumetric assessment by semiautomatic delineation

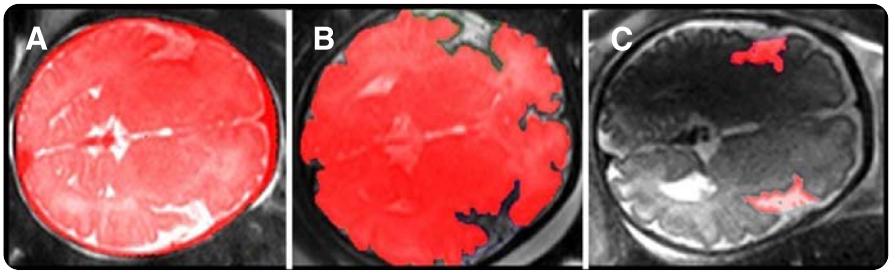

A, Total intracranial volume, **B,** total brain volume, and **C,** opercular volume in using axial T2-weighted magnetic resonance images in a fetus at 37 weeks of gestational age using the Analyze software (Biomedical Imaging Resource; Mayo Clinic, Kansas City, KS) are shown.

Egaña-Ugrinovic. Cortical development analysis in late-onset IUGR fetuses. Am J Obstet Gynecol 2013.

TABLE 1
Maternal characteristics of the study groups

Charactertistic	IUGR (n = 52)	AGA (n = 50)	*P* value[a]
Maternal age, y	31.8 ± 6.2	32.2 ± 4.3	.64
Maternal smoking	15.4%	6%	.13
Maternal height, m	1.58 ± 0.05	1.65 ± 0.06	< .01
Maternal weight, kg	56.9 ± 10.1	63.2 ± 11.3	.01
Maternal BMI, kg/m^2	22.7 ± 3.7	23.2 ± 3.9	.49
Primiparity	65%	64%	.88
Caucasian ethnicity	79%	68%	.18
GA at MRI, wks	37.5 ± 0.8	37.7 ± 0.8	.30

Results are expressed as mean ± SD or percentage as appropriate.

AGA, adequate-for-gestational-age; *BMI*, body mass index; *GA*, gestational age; *IUGR*, intrauterine growth–restricted; MRI, magnetic resonance imaging.

[a] Student *t* test for independent samples or Pearson's χ^2 test.

Egaña-Ugrinovic. Cortical development analysis in late-onset IUGR fetuses. Am J Obstet Gynecol 2013.

covariance were conducted for biometric and volumetric measurements, adjusting by sex, gestational age at MRI, and maternal body mass index as covariants. Furthermore, a classified model was constructed by means of a logistic regression including all cortical parameters to explore the existence of combined patterns that classified the study groups better than the top individual parameter.

Finally, a subanalysis was conducted to explore the existence of differences in relation with previously described predictors of poorer perinatal outcome, namely abnormal CPR, UtA Doppler before birth, or a birthweight less than the third centile in the last scan before delivery.[4,34]

The software package SPSS 17.0 (SPSS, Chicago, IL) and the MedCalc 8.0 (Broekstraat, Belgium) were used for the statistical analyses.

TABLE 2
Perinatal outcome of the study groups

Variable	IUGR (n = 52)	AGA (n = 50)	*P* value[a]
GA at birth, wks	38.8 ± 1.0	40.0 ± 1.0	< .01
Birthweight, g	2488 ± 247	3452 ± 311	< .01
Birthweight percentile	3.9 ± 6.6	55.2 ± 24.2	< .01
Male sex	62%	52%	.34
Labor induction	77.1%	14.3%	< .01
Emergency cesarean section	31%	6%	< .01
Neonatal acidosis[b]	19.6%	5%	.04
Apgar score less than 7 at 5 minutes	5.8%	0%	.04
NICU stay length, d	0.3	0	.09

Results are expressed as mean ± SD or percentage as appropriate.

AGA, adequate-for-gestational-age; *GA*, gestational age; *IUGR*, intrauterine growth–restricted; *NICU*, neonatal intensive care unit.

[a] Student *t* test for independent samples or Pearson's χ^2 test; [b] Neonatal acidosis: umbilical artery pH less than 7.15 and base excess greater than 12 mEq/L.

Egaña-Ugrinovic. Cortical development analysis in late-onset IUGR fetuses. Am J Obstet Gynecol 2013.

RESULTS

Clinical characteristics in the study population

All 102 fetuses from our sample (52 late-onset IUGR and 50 AGA) underwent fetal MRI at 37 weeks of gestational age. Maternal characteristics and time of MRI scans did not differ between cases and controls (Table 1). As expected, IUGR fetuses were delivered earlier with higher rates of labor induction, emergency cesarean section, neonatal acidosis, and lower Apgar scores at 5 minutes of life (Table 2).

Interobserver agreement

Overall CD measurements showed a good interobserver reproducibility. Regarding the sulcation analysis, the coefficients of variation were 4.4% for the left insular depth, 13.5% for the right insular depth, 19.7% for the left lateral fissure depth, 18.7% for the right lateral fissure depth, 21.5% for the left parietoccipital fissure depth, 22.6% for the right parietoccipital fissure depth, 25.2% for the left cingulate fissure depth, 30.7% for the right cingulate fissure depth, 32.6% for the left calcarine fissure depth, and 21.3% for the right calcarine fissure depth . The coefficient of variation for the volumetric analysis was 3.4%.

Brain biometric and sulcation analysis

IUGR fetuses showed smaller BPD measurements (IUGR: 94.33 mm ± 2.76 vs AGA: 100.63 mm ± 3.1; $P < .01$). IUGR fetuses showed significantly deeper fissure measurements in the right and left insula and the left cingulate fissure (Table 3).

Brain volumetric analysis

The IUGR group had smaller TIC and TBV (441.25 cm^3 ± 56.01 vs 515.82 cm^3 ± 36.63; $P < .01$; and 276.47 cm^3 ± 52.61 vs 312.07 cm^3 ± 40.85; $P < .01$, respectively) and smaller left opercular volumes (2.52 cm^3 ± 0.69 vs 3.02 cm^3 ± 0.71; $P < .01$) (Table 4 and Figure 3).

Asymmetry indices analysis

Brain asymmetry indices for biometric and volumetric measurements were analyzed. IUGR fetuses showed a more pronounced right insular asymmetry compared with controls (asymmetry index: 0.13 ± 0.11 vs 0.07 ± 0.12; $P = .03$). No statistically significant differences in asymmetry were found for the other fissures or for opercular volumes.

Differences among IUGR fetuses according to severity

The existence of differences according to the presence or absence of factors associated with poor perinatal outcome, as defined in the previous text, was explored. There were no significant differences for any of the analyzed measurements in relation with the presence or absence of signs of poor perinatal outcome (Figure 4).

TABLE 3
Brain biometric parameters in the study groups

Variable	IUGR (n = 52)	AGA (n = 50)	*P* value[a]
LID/BPD	0.293 ± 0.052	0.267 ± 0.029	.02
RID/BPD	0.379 ± 0.066	0.318 ± 0.075	< .01
Left lateral fissure/BPD	0.154 ± 0.042	0.151 ± 0.024	.81
Right lateral fissure/BPD	0.151 ± 0.037	0.154 ± 0.042	.82
Left parietooccipital fissure/BPD	0.139 ± 0.029	0.132 ± 0.036	.18
Right parietooccipital fissure/BPD	0.138 ± 0.029	0.132 ± 0.036	.22
Left cingulate fissure/BPD	0.096 ± 0.016	0.087 ± 0.019	.03
Right cingulate fissure/BPD	0.093 ± 0.019	0.088 ± 0.018	.19
Left calcarine fissure/BPD	0.180 ± 0.039	0.182 ± 0.040	.56
Right calcarine fissure/BPD	0.179 ± 0.038	0.187 ± 0.041	.14

Results are expressed as mean ± SD.

AGA, adequate-for-gestational-age; *BMI*, body mass index; *BPD*, biparietal diameter; *GLM*, general linear model; *IUGR*, intrauterine growth–restricted; *LID*, left insular depth; *MRI*, magnetic resonance imaging; *RID*, right insular depth.

[a] GLM adjusted for sex, gestational age at MRI, and maternal BMI.

Egaña-Ugrinovic. Cortical development analysis in late-onset IUGR fetuses. Am J Obstet Gynecol 2013.

Classified model analysis

Regression analysis suggested that a combination of left (LID) and right insular depth (RID) corrected for BPD (LID/BPD and RID/BPD, respectively) and left parietoccipital fissure depth (LPOD)/BPD provided the best classification model, accounting for 30% of the uncertainty of being late-onset IUGR (Figure 5). A composite score (ranging from 0 to 1) was constructed using a combination of these variables according to the following formula obtained by logistic regression: composite score $= e^{-(Y)}/(1 + e^{-(Y)})$, where $Y = 6.259 + [(\text{LID/BPD} * \text{RID/BPD} * -41.264) + (\text{LPOD/BPD} * -16.247)]$. The composite score achieved a higher discrimination performance as compared with any of the individual parameters previously analyzed (Figure 5). The receiver-operating characteristic curve of the model resulted in an area under the curve of 79% (95% confidence interval, 70–88%).

Comment

These results provide evidence that late-onset IUGR fetuses present a different pattern of CD compared with normally grown fetuses, with deeper fissures, smaller brain volumes, and a more pronounced right asymmetry. The data add to previous evidence suggesting abnormal brain maturation and reorganization in this condition.[3,9-11,35] CD assessment is feasible in utero and could be of help in the definition of brain biomarkers to identify imaging phenotypes characteristic of fetal undernutrition and growth restriction in utero.

Concerning sulcation and brain volumetries, the results suggest similar alterations to those reported in early-onset IUGR. Previous studies have shown that severe early-onset IUGR neonates presented a disrupted cortical developmental profile with increased gyrification.[14,15] The authors suggested that this increased cortical sulcation in proportion to brain surface might reflect a thinner thickness of the cortex.[14] Likewise, decreased brain volumes have been reported in early-onset IUGR fetuses by ultrasound[36] and in neonates by MRI.[15]

In the present study, late-onset IUGR fetuses had cortical sulcational differences in the insula and cingulate fissure. Both areas play an important role in the limbic system,[37] which is responsible for interoceptive awareness and higher cognitive functions. These areas may be particularly more vulnerable to sustained undernutrition and/or hypoxia because of their late in-utero maturational time courses.[38] This contention is

TABLE 4
Brain volumes in the study groups

Variable	IUGR (n = 52)	AGA (n = 50)	*P* value[a]
Total intracranial volume, cm^3	441.25 ± 56.01	515.82 ± 36.63	< .01
Total brain volume, cm^3	276.47 ± 52.61	312.07 ± 40.85	< .01
Left opercular volume, cm^3[b]	2.52 ± 0.69	3.02 ± 0.71	< .01
Right opercular volume, cm^3[b]	3.13 ± 3.48	3.06 ± 1.47	.26

Results are expressed as mean ± SD.

AGA, adequate-for-gestational-age; *BMI*, body mass index; *IUGR*, intrauterine growth–restricted; *MRI*, magnetic resonance imaging; *TBV*, total brain volume.

[a] General linear model adjusted for birthweight centile, sex, gestational age at MRI, and maternal BMI; [b] Adjusted also for TBV.

Egaña-Ugrinovic. Cortical development analysis in late-onset IUGR fetuses. Am J Obstet Gynecol 2013.

FIGURE 3
Total brain and opercular volumes in late-onset IUGR and AGA

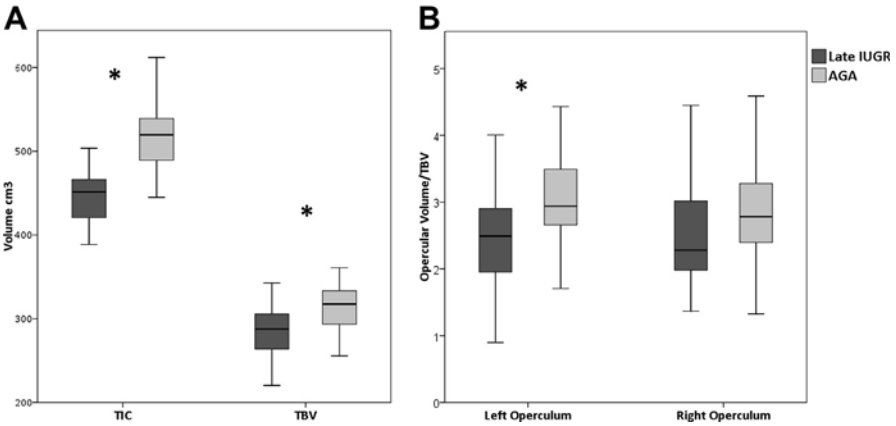

A, Total brain volumes and **B,** opercular volumes in late-onset IUGR and AGA are shown. **A,** TIC and TBV, adjusted for sex, gestational age at MRI, and maternal BMI. **B,** Adjusted for TBV, sex, gestational age at MRI, and maternal BMI. *Asterisk* indicates $P < .05$.

AGA, adequate-for-gestational-age; *BMI*, body mass index; *IUGR*, intrauterine growth—restricted; *MRI*, magnetic resonance imaging; *TBV*, total brain volume; *TIC*, total intracranial volume.

Egaña-Ugrinovic. Cortical development analysis in late-onset IUGR fetuses. Am J Obstet Gynecol 2013.

FIGURE 4
Differences among IUGR fetuses

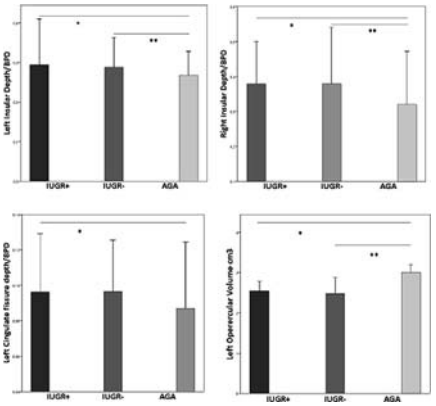

Differences among IUGR fetuses according to severity in globally significant cortical development parameters. The figure demonstrates the polynomial contrast analysis showing the differences between IUGR-positive (IUGR with signs of poor perinatal outcome defined as CPR less than the fifth centile, the UtA Doppler before birth greater than the 95th centile, or a birthweight less than the third centile), IUGR-negative (IUGR without signs of poor perinatal outcome described previously), and AGA. The *bars* depict the mean within each group. *Asterisk* and *double asterisk* indicate $P < .05$.

AGA, adequate-for-gestational-age; *CPR*, cerebroplacental ratio; *IUGR*, intrauterine growth—restricted; *UtA*, uterine artery.

Egaña-Ugrinovic. Cortical development analysis in late-onset IUGR fetuses. Am J Obstet Gynecol 2013.

in line with neurodevelopmental studies in late-onset IUGR infants, which show differences in complex functions regulated by the limbic system and frontal lobe such as working memory and emotions.[38,39]

Another finding of this study was decreased brain volumetric measurements in IUGR fetuses, even after adjusting for birthweight centile. These differences might reflect reductions in brain cellularity, as described in experimental models of IUGR.[40]

Physiological brain asymmetry has been well documented in fetuses and neonates,[16,17] but it had not been investigated in IUGR. In normal conditions, antenatal asymmetry shows a clear dominance of the right hemisphere. Human embryologic[17] as well as functional neuroimaging studies[18] suggest that asymmetry results from a physiological 2 week maturational lag between right and left hemispheres. Physiological brain asymmetry is particularly evident in the superior temporal sulcus and perisylvian region.[16]

The findings of the present study are in line with other studies reporting differences in asymmetry between hemispheres in disorders associated with abnormal neurodevelopment, such as autism spectrum disorders, ADHD, dyslexia, and schizophrenia.[14,18] This lateralization in brain development associated with increased susceptibility to changes in cerebral blood flow along the delicate sulcation process could be an explanation of the unilateral affection in the cingulate fissure and left operculum. Brain asymmetry, a phenomenon essentially developing before birth, has actually been considered as supporting evidence for the current theories suggesting a prenatal origin in some of these conditions.[14,41]

From a clinical perspective, the results of this study provide further evidence of the existence of brain reorganization in late-onset IUGR. This form of IUGR is far more prevalent than the early-onset form, and it affects thousands of infants yearly.[42] Consequently, late-onset IUGR might represent a public health opportunity for tackling neurodevelopmental disorders in a remarkable proportion of the population. In addition, the findings support further research on CD assessment to explore the development of reproducible biomarkers of abnormal neurodevelopment in IUGR and possibly other fetal diseases.

In most conditions associated with subtle brain damage or reorganization, structural abnormalities are detectable long before the appearance of functional symptoms.[14,43] This offers the possibility of developing biomarkers based on brain imaging, but it requires modern techniques capable of detecting subtle differences in brain microstructure, such as MRI spectroscopy[35] or diffusion.[44,45] However, such MRI approaches entail complex acquisition settings and are very sensitive to motion artifacts, which represent serious drawbacks for its clinical use in human fetuses. In contrast, CD assessment is based on a more simple principle, it can be performed in 2-dimensional images, and consequently it is feasible with fetal MRI acquisition protocols currently used in clinical practice. The results provide evidence that composite scores including more

FIGURE 5
Classified model between IUGR and AGA fetuses

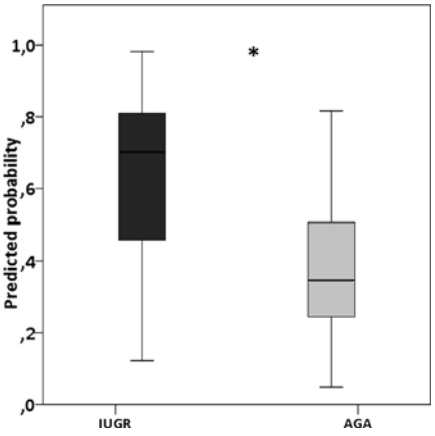

Composite score obtained by logistic regression. The score contains a combination of left and right insular depth and left parietoccipital fissure depth, all corrected by BPD. *Asterisk* indicates $P < .01$.

AGA, adequate-for-gestational-age; *BPD*, biparietal diameter; *IUGR*, intrauterine growth—restricted.

Egaña-Ugrinovic. Cortical development analysis in late-onset IUGR fetuses. Am J Obstet Gynecol 2013.

than 1 CD measure could be useful to characterize brain reorganization patterns associated with IUGR.

We acknowledge some limitations in this study. Measures were carried out by manual delineation because there are no automatic softwares for these purposes. To counter this problem, we used previously reported sonographic fissures and confirmed that interobserver agreement was within acceptable values. We measured only previously reported brain fissures, and consequently, not all brain sulci at term were explored. We can not exclude that further detailed analysis might detect differences that have been missed by this study.

Among the strengths of the study, the study groups were prospectively recorded and cases represent a homogeneous sample that is highly representative of the condition of interest. The use of the 2-dimensional-measurement approach with half-Fourier acquisition single-shot turbo spin-echo images assured a reproducible and non—motion-distorted method to analyze the images, supported by the interobserver agreement.

To conclude, late-onset IUGR fetuses showed differences in CD, which further support the notion that this condition is associated with disrupted brain maturation that can already be detected in utero. Further research involving long-term follow-up is warranted to evaluate the role of imaging biomarkers based on CD in the prediction of abnormal neurodevelopment in fetuses with IUGR. ■

ACKNOWLEDGMENTS

G.E.-U. thanks Carles Falcón from the Neuroimage Laboratory Institut d'Investigacions Biomediques August Pi i Sunyer (Barcelona, Spain) for the technical support using Analyze software and Rudolf Zupan image after processing for interobserver agreement analysis.

REFERENCES

1. Gardosi J. Clinical strategies for improving the detection of fetal growth restriction. Clin Perinatol 2011;38:21-31, v.

2. Figueras F, Eixarch E, Meler E, et al. Small-for-gestational-age fetuses with normal umbilical artery Doppler have suboptimal perinatal and neurodevelopmental outcome. Eur J Obstet Gynecol Reprod Biol 2008;136:34-8.

3. Sanz-Cortes M, Figueras F, Bargallo N, Padilla N, Amat-Roldan I, Gratacos E. Abnormal brain microstructure and metabolism in small-for-gestational-age term fetuses with normal umbilical artery Doppler. Ultrasound Obstet Gynecol 2010;36:159-65.

4. Savchev S, Figueras F, Cruz-Martinez R, Illa M, Botet F, Gratacos E. Estimated weight centile as a predictor of perinatal outcome in small-for-gestational-age pregnancies with normal fetal and maternal Doppler indices. Ultrasound Obstet Gynecol 2012;39:299-303.

5. Baschat AA. Neurodevelopment following fetal growth restriction and its relationship with antepartum parameters of placental dysfunction. Ultrasound Obstet Gynecol 2011;37:501-14.

6. Arcangeli T, Thilaganathan B, Hooper R, Khan KS, Bhide A. Neurodevelopmental delay in small babies at term: a systematic review. Ultrasound Obstet Gynecol 2012;40:267-75.

7. Pylipow M, Spector LG, Puumala SE, Boys C, Cohen J, Georgieff MK. Early postnatal weight gain, intellectual performance, and body mass index at 7 years of age in term infants with intrauterine growth restriction. J Pediatr 2009;154:201-6.

8. Strauss RS, Dietz WH. Growth and development of term children born with low birth weight: effects of genetic and environmental factors. J Pediatr 1998;133:67-72.

9. Sanz-Cortés M, Figueras F, Bonet-Carne E, et al. Fetal brain MRI texture analysis identifies different microstructural patterns in adequate- and small-for-gestational-age fetuses at term. Fetal Diagn Ther 2013;33:122-9.

10. Pueyo V, Oros D, Valle S, et al. Axonal loss and cognitive deficits in term infants born small for gestational age with normal umbilical artery Doppler. Ultrasound Obstet Gynecol 2012;40:297-303.

11. Batalle D, Eixarch E, Figueras F, et al. Altered small-world topology of structural brain networks in infants with intrauterine growth restriction and its association with later neurodevelopmental outcome. Neuroimage 2012;60:1352-66.

12. Chi JG, Dooling EC, Gilles FH. Gyral development of the human brain. Ann Neurol 1977;1:86-93.

13. Garel C, Chantrel E, Brisse H, et al. Fetal cerebral cortex: normal gestational landmarks identified using prenatal MR imaging. AJNR Am J Neuroradiol 2001;22:184-9.

14. Dubois J, Benders M, Borradori-Tolsa C, et al. Primary cortical folding in the human newborn: an early marker of later functional development. Brain 2008;131:2028-41.

15. Tolsa CB, Zimine S, Warfield SK, et al. Early alteration of structural and functional brain development in premature infants born with intrauterine growth restriction. Pediatr Res 2004;56:132-8.

16. Dubois J, Hertz-Pannier L, Cachia A, Mangin JF, Le Bihan D, Dehaene-Lambertz G. Structural asymmetries in the infant language and sensori-motor networks. Cereb Cortex 2009;19:414-23.

17. Kasprian G, Langs G, Brugger PC, et al. The prenatal origin of hemispheric asymmetry: an in utero neuroimaging study. Cereb Cortex 2011;21:1076-83.

18. Toga AW, Thompson PM. Mapping brain asymmetry. Nat Rev Neurosci 2003;4:37-48.

19. Robinson HP, Fleming JE. A critical evaluation of sonar "crown-rump length" measurements. Br J Obstet Gynaecol 1975;82:702-10.

20. Figueras F, Meler E, Iraola A, et al. Customized birthweight standards for a Spanish population. Eur J Obstet Gynecol Reprod Biol 2008;136:20-4.

21. Arduini D, Rizzo G. Normal values of pulsatility index from fetal vessels: a cross-sectional study on 1556 healthy fetuses. J Perinat Med 1990;18:165-72.

22. Baschat AA, Gembruch U. The cerebroplacental Doppler ratio revisited. Ultrasound Obstet Gynecol 2003;21:124-7.

23. Gomez O, Figueras F, Fernandez S, et al. Reference ranges for uterine artery mean pulsatility index at 11-41 weeks of gestation. Ultrasound Obstet Gynecol 2008;32:128-32.

24. Tremblay E, Therasse E, Thomassin-Naggara I, Trop I. Quality initiatives: guidelines for use of medical imaging during pregnancy and lactation. Radiographics 2012;32:897-911.

25. Pistorius LR, Stoutenbeek P, Groenendaal F, et al. Grade and symmetry of normal fetal cortical development: a longitudinal two- and

three-dimensional ultrasound study. Ultrasound Obstet Gynecol 2010;36:700-8.
26. Alonso I, Borenstein M, Grant G, Narbona I, Azumendi G. Depth of brain fissures in normal fetuses by prenatal ultrasound between 19 and 30 weeks of gestation. Ultrasound Obstet Gynecol 2010;36:693-9.
27. Clatterbuck RE, Sipos EP. The efficient calculation of neurosurgically relevant volumes from computed tomographic scans using Cavalieri's Direct Estimator. Neurosurgery 1997; 40:339-42; discussion 343.
28. The International Society of Ultrasound in Obstetrics and Gynecology. Sonographic examination of the fetal central nervous system: guidelines for performing the "basic examination" and the "fetal neurosonogram." Ultrasound Obstet Gynecol 2007;29:109-16.
29. Reichel TF, Ramus RM, Caire JT, Hynan LS, Magee KP, Twickler DM. Fetal central nervous system biometry on MR imaging. AJR Am J Roentgenol 2003;180:1155-8.
30. Mittal P, Goncalves LF, Kusanovic JP, et al. Objective evaluation of sylvian fissure development by multiplanar 3-dimensional ultrasonography. J Ultrasound Med 2007;26: 347-53.
31. Limperopoulos C, Tworetzky W, McElhinney DB, et al. Brain volume and metabolism in fetuses with congenital heart disease: evaluation with quantitative magnetic resonance imaging and spectroscopy. Circulation 2010;121:26-33.
32. Nakamura K, Kawasaki Y, Suzuki M, et al. Multiple structural brain measures obtained by three-dimensional magnetic resonance imaging to distinguish between schizophrenia patients and normal subjects. Schizophr Bull 2004;30: 393-404.
33. Habib M. Anatomical asymmetries of the human cerebral cortex. Int J Neurosci 1989;47: 67-80.
34. Cruz-Martinez R, Figueras F, Hernandez-Andrade E, Oros D, Gratacos E. Fetal brain Doppler to predict cesarean delivery for nonreassuring fetal status in term small-for-gestational-age fetuses. Obstet Gynecol 2011; 117:618-26.
35. Makhoul IR, Soudack M, Goldstein I, Smolkin T, Tamir A, Sujov P. Sonographic biometry of the frontal lobe in normal and growth-restricted neonates. Pediatr Res 2004; 55:877-83.
36. Benavides-Serralde A, Hernandez-Andrade E, Fernandez-Delgado J, et al. Three-dimensional sonographic calculation of the volume of intracranial structures in growth-restricted and appropriate-for-gestational age fetuses. Ultrasound Obstet Gynecol 2009;33: 530-7.
37. Allen GV, Saper CB, Hurley KM, Cechetto DF. Organization of visceral and limbic connections in the insular cortex of the rat. J Comp Neurol 1991;311:1-16.
38. Hernandez-Andrade E, Figueroa-Diesel H, Jansson T, Rangel-Nava H, Gratacos E. Changes in regional fetal cerebral blood flow perfusion in relation to hemodynamic deterioration in severely growth-restricted fetuses. Ultrasound Obstet Gynecol 2008;32:71-6.
39. Geva R, Eshel R, Leitner Y, Fattal-Valevski A, Harel S. Memory functions of children born with asymmetric intrauterine growth restriction. Brain Res 2006;1117:186-94.
40. Uno H, Lohmiller L, Thieme C, et al. Brain damage induced by prenatal exposure to dexamethasone in fetal rhesus macaques. I. Hippocampus. Brain Res Dev Brain Res 1990; 53:157-67.
41. Huppi PS. Neuroimaging of brain development—discovering the origins of neuropsychiatric disorders? Pediatr Res 2008;64: 325.
42. Gardosi J, Madurasinghe V, Williams M, Malik A, Francis A. Maternal and fetal risk factors for stillbirth: population based study. BMJ 2013;346:f108.
43. Ming GL, Brustle O, Muotri A, Studer L, Wernig M, Christian KM. Cellular reprogramming: recent advances in modeling neurological diseases. J Neurosci 2011;31:16070-5.
44. Evans AC. The NIH MRI study of normal brain development. Neuroimage 2006;30: 184-202.
45. Dubois J, Dehaene-Lambertz G, Mangin JF, Le Bihan D, Huppi PS, Hertz-Pannier L. [Brain development of infant and MRI by diffusion tensor imaging]. Neurophysiol Clin 2012;42:1-9.

5.2 STUDY 2

Fetal MRI Insular Cortical Morphometry and its Association with Neurobehavior in Late-Onset Small for Gestational Age Fetuses

Egaña-Ugrinovic G, Sanz-Cortes M, Figueras F, Couve-Perez C, Gratacós E.

Ultrasound Obstet Gynecol. 2014

State: Published

Impact factor: 3.557

Quartile: 1st

FETAL MRI INSULAR CORTICAL MORPHOMETRY AND ITS ASSOCIATION WITH NEUROBEHAVIOR IN LATE-ONSET SMALL FOR GESTATIONAL AGE FETUSES.

Gabriela EGAÑA-UGRINOVIC, MD[1]; Magdalena SANZ-CORTES, PhD[1]; Francesc FIGUERAS, PhD[1]; Constanza COUVE-PEREZ, MD[1]; Eduard GRATACÓS, PhD[1].

[1] Maternal-Fetal Medicine Department, Institut Clínic de Ginecologia, Obstetrícia i Neonatologia (ICGON); Fetal and Perinatal Medicine Research Group, Institut d'Investigacions Biomediques August Pi i Sunyer (IDIBAPS) and Centro de Investigación Biomédica en Red de Enfermedades Raras (CIBERER). Hospital Clínic, Universitat de Barcelona, Barcelona, Spain.

Corresponding author:

Eduard Gratacós

Maternal-Fetal Medicine Department

Hospital Clínic – Maternitat

Sabino de Arana, 1

08028 Barcelona, Spain

Telephone: +34 93 227 9333

Fax: +34 93 227 5612

Email: gratacos@clinic.ub.es

Disclosure statement

None of the authors have a conflict of interest

This article has been accepted for publication and undergone full peer review but has not been through the copyediting, typesetting, pagination and proofreading process, which may lead to differences between this version and the Version of Record. Please cite this article as doi: 10.1002/uog.13360

ABSTRACT

Objective

To evaluate insular cortical morphometry assessed by Magnetic Resonance Imaging (MRI) in late-onset small for gestational age (SGA) fetuses compared to controls and its association with neurobehavioral outcome.

Methods

65 late-onset SGA and 59 normally grown fetuses were imaged by MRI at 37 weeks of gestation. T2 HASTE anatomical and diffusion-weighted imaging (DWI) acquisitions were obtained. Insular cortical thickness, volume and fractional anisotropy (FA) values were assessed. Asymmetry indices were then constructed. Neonatal Behavioral Assessment Scale (NBAS) test was performed on IUGR neonates at 42 weeks.

Results

Late-onset SGA fetuses had significantly thinner insular cortical thickness and smaller insular cortical volume as compared with controls. SGA also presented a more pronounced left asymmetry in the posterior cortex and significantly lower FA values in the left insula. Insular measurements in the SGA group were significantly correlated with neurobehavior as assessed by NBAS scores.

Conclusions

Insular cortical morphometry was significantly different in late-onset SGA fetuses and correlated with poorer neurobehavioral performance. This data support the impact of growth restriction in brain development and the potential value of cortical assessment as a biomarker of neurodevelopment in fetuses at risk.

Key words: Fetal brain imaging, insula, insular cortex, neurobehavior, SGA, IUGR.

INTRODUCTION

Intrauterine growth restriction (IUGR) is defined as the underachievement of the genetic growth potential, affecting 6-10% of all pregnancies[1]. IUGR is a major contributor of perinatal and long term morbidity[2-7], being the association with abnormal neurodevelopment in late childhood among the most consistently reported[7]. Studies in the neonatal period show lower neurobehavioral test scores[8] and studies later in infancy and during school age have consistently reported neurocognitive difficulties[6, 9]. Neurodevelopmental impairment in IUGR is associated with specific neurostructural changes on MRI studies[10, 11]. This may open opportunities of developing imaging biomarkers to identify those fetuses at risk of an impaired neurodevelopment.

Human cortical development is a central mechanism of consciousness, playing an important role in emotion, language and cognition[12, 13]. Neuroimaging technologies provide an opportunity to assess cortical development in utero by means of ultrasound (US) or conventional MRI sequences[14, 15]. It has been previously demonstrated that late-onset growth restriction is associated with brain reorganizational changes, showing alterations in their brain microstructure and metabolism[10, 16]. In previous studies, we reported that late-onset SGA showed significant differences in their gyrification pattern, brain volumetry and degree of cortical asymmetry assessed by fetal MRI[17]. These differences were particularly prominent in the insular area, showing deeper fissure measurements, smaller operculums and a more pronounced lobar insular right asymmetry in term SGA. However, it is still unknown whether the differences in cortical development indicate a higher risk of poorer neurological development.

In this study we explored the hypothesis that insular cortex differences in-utero are associated with changes in neonatal neurobehavior in late-onset SGA fetuses. We focused on insular cortex given previous reports suggesting more pronounced changes in this area[17] and considering the important implications of this brain region in human cognitive functions[18, 19]. We evaluated several morphometric and microstructural features of the insula in a cohort of 65 late-onset SGA fetuses as compared with 59 normally grown fetuses, and we analyzed the association with neonatal neurobehavioral scores.

MATERIAL AND METHODS

Subjects

This study is part of a larger prospective research program on IUGR involving fetal, neonatal and long term postnatal follow-up. The protocol of this study was approved by the institutional Ethics Committee (Institutional Review Board 2008/4422) and all participants gave written informed consent. Due to the exploratory nature of our study and since there was no previous data analyzing the association between brain insula with neurobehavior, we arbitrarily established a sample size of 50-70 per study group. Therefore, an initial sample of 143 singleton fetuses were included in our cohort, however around 15% of them had to be excluded due to insufficient image quality for delineation according to our standards, leaving a total of 124 fetuses in our cohort, classified in 65 late-onset SGA and 59 appropriate for gestational age (AGA) fetuses. Pregnancies were dated according to the first trimester crown-rump length measurement[20]. Late-onset SGA was defined by an estimated and postnatally confirmed birthweight <10th centile[1, 21], according to local standards[22] with normal umbilical Doppler (umbilical artery pulsatility index <95th centile)[23]. AGA were

defined as normal fetuses with an estimated and postnatally confirmed birthweight ≥10th centile, according to local standards[22]. Exclusion criteria included congenital malformations, chromosomal abnormalities, perinatal infections, chronic maternal pathology, contraindications for MRI and non-cephalic presentations.

Clinical and Ultrasound data

SGA patients were followed-up in our fetal growth restriction unit from diagnosis until delivery. The entire sample underwent serial Doppler US scans using a General Electric Voluson E8, 6-2MHz curved-array transducer (GE Medical Systems, Zipf, Austria). Fetal umbilical artery (UA) and middle cerebral artery (MCA) pulsatility index (PI) were measured in three or more consecutive waveforms, with the angle of insonation as close as possible to 0° in absence of fetal or maternal movements. Both measurements were used for the calculation of the cerebroplacental ratio (CPR), considering an abnormal CPR a value <5th centile[24]. Uterine arteries (UtA) PI were measured transabdominally and mean value was considered abnormal when >95th centile[25]. All fetuses in this study had at least one US scan within one week before delivery. Maternal, perinatal and neonatal data were prospectively recorded in all study patients.

Differences among IUGR fetuses according to severity parameters

Several prognostic factors have been identified as predictors of poor neonatal outcome among term growth restricted fetuses, including abnormal cerebroplacental ratio[26], uterine artery Doppler[4, 27] and birth weight below the 3rd centile[2]. For further assessment of the SGA population we subdivided the study group using these above mentioned prognostic factors into the following categories: (1) IUGR defined by birthweight <3rd centile and/or abnormal

CPR and/or abnormal UtA; (2) SGA defined by the remaining cases that did not fulfill these criteria, and (3) controls defined by birthweight ≥10th centile. The categorization was performed according to the last scan before delivery which was at most within a week from birth.

Fetal MRI imaging acquisition

MRI was performed at 37 weeks of gestational age on a clinical MR system using the Institut d'Investigacions Biomediques August Pi i Sunyer (IDIBAPS) image platform, operating at 3.0 Tesla (Siemens Magnetom Trio Tim syngo MR B15, Siemens, Germany) without fetal sedation[28]. A body coil with 8 elements was wrapped around the mother's abdomen. Routine fetal imaging took around 20 minutes and consisted on single-shot, fast spin echo T2-weighted sequences (TR 990ms, TE 137ms, slice thickness 3.5mm, no gap, field of view 260mm, voxel size 1.4x1.4x3.5mm, matrix 192x192, flip angle 180º, acquisition time 24 seconds) acquired in the three orthogonal planes. Subsequently, 12-directions DWI acquisition was obtained (TR 9300ms, TE 94ms, diffusion weighting b-value 1000s/mm², slice thickness 2.2mm, no gap, field of view 220mm, voxel size 2.2×2.2×2.2mm, matrix 100x100, flip angle 90º, acquisition time 2.30 minutes). If the quality of the images was suboptimal, sequences were repeated.

Structural MRI images were reviewed for the presence of anatomical abnormalities by an experienced neuroradiologist blinded to group membership.

Fetal imaging post processing

Offline analyses of all measurements were performed using the semiautomatic Analyze 9.0 software (Biomedical Imaging Resource, Mayo Clinic; Kansas, USA) by two experienced

examiners blinded to group membership. The cortical plate was identified by the intensity threshold defined as the T2-weighted hypointense rim delineating the brain surface[29].

1. Biometric Measurements:
    a. Insular cortical thickness (ICT) was measured bilaterally in the axial plane located immediately below the plane of the anterior commissure and the cavum of the septum pellucidi. Anterior, middle and posterior thickness of the insular cortex were manually delineated from its inner-to-external cortical border (Figure 1). Every measurement was performed three times and the mean of each one was used for further analysis. The anterior and posterior ICT were traced on the limiting portion with the frontal and temporal operculum respectively[30]. Middle ICT was measured equidistantly from the anterior and posterior measurements.
    b. Insular lobe depth (ID) was measured bilaterally in the same axial plane described above as reported elsewere[17] (Figure 1). ID was measured to correct the ICT for differences in head size obtaining a ratio (ICT/ID) for each measurement in order to perform the statistical analysis.

2. Volumetric measurements were delineated through cursor-guided free-hand traces on individual images of the insular cortex and brain volumes. The region-of-interest (ROI) traced on each image created an area that was multiplied by the slice thickness in order to produce a volume. ROI volumes from successive slices were then summed to yield the volume of the full extent from the desired ROI[31].
    a. Insular cortical volume (ICV): the whole insular cortex was traced bilaterally in the coronal plane. The anatomical boundaries chosen for delineation were:

-anteriorly the most rostral slice containing the insular cortex and,

-posteriorly the fusion of the superior and inferior circular insular sulci in the coronal plane[32].

On each coronal slice, the insular cortex was limited superiorly by the superior circular insular sulcus, and inferiorly by the inferior circular insular sulcus or the orbitoinsular sulcus[32, 33] (Figure 2).

b. Total brain volume (TBV) was delineated as reported elsewhere[17] (Figure 2). TBV was measured to correct the insular cortical volume for differences in head size.

3. Asymmetry indices (AI): an asymmetry coefficient for ICT and ICV size was calculated using the following formula AI= (Right–Left)/(Right+Left) where a negative value indicated a larger left-sided structure[34].

4. Fractional anisotropy: FA maps were analyzed using the ITK-SNAP 2.4 software. A ROI of 43mm^3 was traced at the level of the corresponding anterior, middle and posterior ICT measurements bilaterally in order to obtain FA values (Figure 3). Mean FA values and SD were used for further analysis.

Neurobehavioral performance

Postnatal follow up was offered to all late-onset SGA patients and neurobehavioral assessment was performed prospectively at 42-43 weeks using the NBAS test by 1 of 2 observers accredited by The Brazelton Institute (Harvard Medical School, Boston, MA)[35]. The examination consisted on 7 behavioral areas including habituation, motor, social-interactive, organization of state, regulation of state, autonomic nervous system and attention, as

reported elsewhere[8, 35]. The scores from the behavioral areas were converted into centiles according to normal curve references for our population[36], considering an abnormal result a score <5th centile.

Interobserver agreement

Intraclass correlation coefficients (ICC) and their 95% confidence intervals (CIs) were assessed in 10 fetuses between two independent and blinded to group membership examiners, with a significance level set at 5% ($p < 0.05$). We aimed for an optimum reliability of at least 0.75 and moderate reliability of 0.4. A two-way mixed model was chosen for analysis. The degree of agreement was also examined using the Bland–Altman test.

Statistical analysis of clinical and insular cortical data

Student´s t test for independent samples and Pearson´s X^2 tests were used to compare quantitative and qualitative data respectively. Multivariate analyses of covariance (MANCOVA) adjusted by gender, gestational age (GA) at MRI, maternal smoking and body mass index (BMI) were conducted to assess biometric, volumetric, FA and asymmetry differences between late-onset SGA and AGA. The association between measurements and NBAS test scores in growth restricted fetuses was assessed by a MANCOVA analysis taking into account the same covariates plus age at NBAS test. Furthermore, this association was tested performing an ordinal regression in which the amount of NBAS test's clusters <5th centile were considered as the dependent variable and insular cortical measurements as the independent variables. Same covariates were taken into account in this test. A *p value* <0.05 was set as significant. The software package SPSS 17.0 (SPSS, Chicago, IL, USA) was used for the statistical analyses.

RESULTS

Clinical characteristics in the study population

Maternal characteristics and GA at MRI did not differ between cases and controls (Table 1). As expected, late-onset SGA fetuses were delivered earlier with higher rates of labor induction, emergency cesarean section and longer stay in the neonatal intensive unit care (Table 2).

Interobserver agreement

Overall measurements showed a good interobserver reliability. The ICC was 0.94 (CIs: 0.78-0.99) and 0.74 (0.01-0.94) for the left and right insula, respectively. The Bland–Altman plot between paired measurements were −3.2 (95% limits of agreement 13 to −19.4) and 3.1 (26.6 to -20.4) for the left and right insula, respectively.

Differences between late-onset SGA and AGA

1. Insular cortical thickness analysis

Late-onset SGA fetuses showed thinner insular cortex in all measurements expressed as ratios: left-anterior ICT/ID (late-onset SGA: 0.044 ± 0.011 vs. AGA: 0.051 ± 0.013; p<0.01), left-middle ICT/ID (0.047 ± 0.01 vs. 0.054 ± 0.01; p<0.01) and left-posterior ICT/ID (0.048 ± 0.01 vs. 0.053 ± 0.01; p=0.02); right-anterior ICT/ID (0.038 ± 0.01 vs. 0.046 ± 0.01; p<0.01), right-middle ICT/ID (0.040 ± 0.01 vs. 0.048 ± 0.01; p<0.01) and right posterior ICT/ID (0.038 ± 0.01 vs. 0.046 ± 0.01; p<0.01) (Table 3).

2. Insular cortical volume analysis

Late-onset SGA had smaller left and right ICV (left: 0.904cm^3 ± 0.274 vs. 1.099cm^3 ± 0.283; p<0.01 and right: 0.860cm^3 ± 0.258 vs. 1.059cm^3 ± 0.287; p<0.01, respectively) (Table 4).

3. Asymmetry Indices analysis

Late-onset SGA fetuses showed a more pronounced left insular cortical AI in thickness and volume analyses compared to controls, with statistical significance differences in the left posterior insular cortex (AI: -0.115 vs. -0.078; p= 0.038).

4. FA analysis

Mean FA values of late-onset SGA showed a trend for lower values in the left insula, showing statistical significance in the left anterior insula (316.65 ± 123.45 vs. 457.94 ± 195.67; p=0.03).

Differences in the insular analysis according to clinical severity

According to the previously described definition, our sample was divided in 40 IUGR, 25 SGA and 59 controls. There was a significant linear tendency to more pronounced alterations in thickness and volume of the insular cortex in IUGR as compared with SGA and controls (Figure 4).

Insular cortical association with neurobehavioral outcome in late-onset SGA

We found significant associations between several insular measurements and NBAS test scores from specific clusters in late-onset SGA (Table 5). These findings were supported by the results from the ordinal regression analysis which showed a significant change of the global scoring distribution towards overall lower NBAS scores in late-onset SGA (model p

value=<0.01), with statistical significance in: left-anterior ICT (p=0.04), left-middle ICT (p=0.02), right-anterior ICT (p=0.03), right-middle ICT (p=0.04), anterior cortical thickness AI (p=0.03), middle cortical thickness AI (p=0.03), left insular lobe depth (p=0.04) and TBV (p=0.03).

DISCUSSION

In this study we provide evidence that late-onset SGA fetuses show significant differences in biometric, volumetric and FA values of the insular cortex, which are associated with the neonatal neurobehavioral outcome in this population.

Our results go in line with other authors who reported thinner cortex[13], decreased gray matter[13], and increased left cortical asymmetry[37] in IUGR newborns. Previous reports on neurodevelopmental outcome of late-onset SGA fetuses, have shown worse scores in attention, social, self-regulation, communication, problem-solving and memory function areas[8, 9, 38]. All of these functions are closely related to the insula and the limbic system functionality[18, 19]. Accordingly, we found significant associations between insular measurements and different areas from the NBAS test, linking thinner and smaller insulas with worse neurobehavioral outcomes in term SGA.

Even if we acknowledge that the cortical development is a complex process that involves extra-and intracranial factors that interact in the organization of lamination and synaptogenesis, from a pathophysiological standpoint, the potential mechanisms leading to prominent alterations in the insular cortex under fetal growth restriction are worth consideration. It has been reported that the hippocampus, which has a close phylogenetic origin with the insula[33], is particularly vulnerable to intrauterine hypoxic situations[13, 39]. Therefore, it could be speculated that the insular cortex could be more susceptible to a

relative sustained undernutrion and/or hypoxia as well, modifying its morphological changes and active synaptogenesis of third trimester. Indeed, lower FA values in our SGAs could be interpreted as a less organized cortex in this area. By the same token, significantly increased left cortical asymmetry could be the result of an altered maturational course in this condition. It remains to be explored whether these differences in growth restriction may be related to a greater susceptibility to develop neuropsychiatric disorders[40].

The result of this study showed that the presence of any of the prenatal severity parameters was associated with more pronounced differences in the insula. However, the subgroup of small fetuses without this severity signs also showed significant differences in several of the insular measures with respect to controls. These results are in line with recent findings suggesting that factors determining a poorer perinatal prognosis do not necessarily correlate with long term outcome[41], therefore this study provide further support to the need of improving the understanding of the pathophysiology of late-onset SGA.

IUGR affects up to 6-10% of all pregnancies, and consequently the relevance of this condition as a contributor to neurodevelopmental disorders in childhood can hardly be overestimated. In addition, increasing evidence suggests the existence of sub-clinical forms of growth restriction, which go undetected by current definitions based on estimated fetal weight percentiles[42]. Here we support the notion for the development of imaging biomarkers based on cortical analysis. Identifying fetuses at-risk for abnormal neurodevelopment in fetal medicine lays the basis to perform specific strategies to potentially improve both pre and postnatal management which have shown to improve neurobehavior and brain structure when compared to those receiving standard care[43]. Moreover, the implications of these results could be also applied to other conditions in fetal

medicine aiming to identify endophenotypes more susceptible to develop neurological disorders.

Our results should be interpreted in light of limitations. Measurements were performed by manual delineation. To counter this problem we used a previously reported methodology described for patients with neuropsychiatric disorders[32, 33] and we confirmed an acceptable interobserver agreement rate. Additionally, given the precision of the anatomical landmarks, a considerable amount of images were not susceptible to be processed, mostly due to motion artifacts, which seemed a fair trade off for the robustness of the results. We acknowledge that functional outcome is based on neonatal neurobehavioral scores and not in a long-term cognitive evaluation. However, increasing evidence supports the link between neonatal neurobehavioral skills with later neurocognitive development[44]. Moreover the NBAS test was performed only in SGA and these results were compared to reference values from our population. We think this comparison is feasible since cases represent a homogeneous sample which is highly representative of the condition of interest with similar demographic characteristics to controls. Some of the strengths of the study should be highlighted. Patients were prospectively followed up until delivery. The use of a two-dimensional approach with HASTE images assured a reproducible method to analyze specific ROIs from the insular cortex. Moreover, the use of a multifocal approach brought robustness to the individual results. Finally, insular measurements were corrected for the potential bias of having smaller insulas in smaller brains in order to have more reliable results.

To conclude, this study provides evidence that late-onset SGA fetuses present differences in insular cortical development which is further related to their neurobehavioral performance. Further research involving long-term follow-up is warranted to evaluate the morphometric

analysis of the fetal insula as an imaging biomarker in the prediction of abnormal neurodevelopment in fetuses with growth restriction and other fetal conditions.

Acknowledgments

This work was supported by grants from The Cerebra Foundation for the Brain Injured Child (Carmarthen, Wales, UK), the Thrasher Research Fund (Salt Lake City, USA), Obra Social "la Caixa" (Barcelona, Spain), Fundación Dexeus (Barcelona, Spain) and Banca Cívica de Caja Navarra (Proyecto TETD). G.E.U was supported by CONICYT (PFCHA/<Doctorado al Extranjero 4ª Convocatoria><72120071>), Chile. M.S.C. was supported by Instituto de Salud Carlos III Rio Hortega (CM10/00222), Spain. Dra. Gabriela Egaña-Ugrinovic thanks Carles Falcón from the Neuroimage Laboratory and the IDIBAPS platform for the technical support declaring no compensation reward.

REFERENCES

1. Gardosi J. Intrauterine growth restriction: new standards for assessing adverse outcome. Best Pract Res Clin Obstet Gynaecol 2009;23:741-9.
2. Savchev S, Figueras F, Cruz-Martinez R, Illa M, Botet F, Gratacos E. Estimated weight centile as a predictor of perinatal outcome in small-for-gestational-age pregnancies with normal fetal and maternal Doppler indices. Ultrasound Obstet Gynecol;39:299-303.
3. Doctor BA, O'Riordan MA, Kirchner HL, Shah D, Hack M. Perinatal correlates and neonatal outcomes of small for gestational age infants born at term gestation. Am J Obstet Gynecol 2001;185:652-9.
4. Severi FM, Bocchi C, Visentin A, Falco P, Cobellis L, Florio P, Zagonari S, Pilu G. Uterine and fetal cerebral Doppler predict the outcome of third-trimester small-for-gestational age fetuses with normal umbilical artery Doppler. Ultrasound Obstet Gynecol 2002;19:225-8.
5. Lindqvist PG, Molin J. Does antenatal identification of small-for-gestational age fetuses significantly improve their outcome? Ultrasound Obstet Gynecol 2005;25:258-64.
6. Ley D, Tideman E, Laurin J, Bjerre I, Marsal K. Abnormal fetal aortic velocity waveform and intellectual function at 7 years of age. Ultrasound Obstet Gynecol 1996;8:160-5.
7. Arcangeli T, Thilaganathan B, Hooper R, Khan KS, Bhide A. Neurodevelopmental delay in small babies at term: a systematic review. Ultrasound Obstet Gynecol;40:267-75.

8. Figueras F, Oros D, Cruz-Martinez R, Padilla N, Hernandez-Andrade E, Botet F, Costas-Moragas C, Gratacos E. Neurobehavior in term, small-for-gestational age infants with normal placental function. Pediatrics 2009;124:e934-41.
9. Eixarch E, Meler E, Iraola A, Illa M, Crispi F, Hernandez-andrade E, Gratacos E, Figueras F. Neurodevelopmental outcome in 2-year-old infants who were small-for-gestational age term fetuses with cerebral blood flow redistribution. Ultrasound Obstet Gynecol 2008;32:894-9.
10. Batalle D, Eixarch E, Figueras F, Muñoz-Moreno E, Bargallo N, Illa M, Acosta-rojas R, Amat-Roldan I, Gratacos E. Altered small-world topology of structural brain networks in infants with intrauterine growth restriction and its association with later neurodevelopmental outcome. Neuroimage;60:1352-66.
11. Eikenes L, Martinussen MP, LunD LK, Lohaugen GC, Indredavik MS, Jacobsen GW, Skranes J, Brubakk AM, Haberg AK. Being born small for gestational age reduces white matter integrity in adulthood: a prospective cohort study. Pediatr Res;72:649-54.
12. Huppi PS. Cortical development in the fetus and the newborn: advanced MR techniques. Top Magn Reson Imaging;22:33-8.
13. Dubois J, Benders M, Borradori-Tolsa C, Cachia A, Lazeyras F, Ha-Vinh Leuchter R, Sizonenko SV, Warfield SK, Mangin JF, Hüppi PS. Primary cortical folding in the human newborn: an early marker of later functional development. Brain 2008;131:2028-41.
14. Pistorius LR, Hellmann PM, Visser GH, Malinger G, Prayer D. Fetal neuroimaging: ultrasound, MRI, or both? Obstet Gynecol Surv 2008;63:733-45.
15. Prayer D, Kasprian G, Krampl E, Ulm B, Witzani L, Prayer L, Brugger PC. MRI of normal fetal brain development. Eur J Radiol 2006;57:199-216.
16. Sanz-Cortes M, Figueras F, Bonet-Carne E, Padilla N, Tenorio V, Bargallo N, Amat-Roldan I, Gratacos E. Fetal brain MRI texture analysis identifies different microstructural patterns in adequate and small for gestational age fetuses at term. Fetal Diagn Ther;33:122-9.
17. Egaña-Ugrinovic G, Sanz-Cortes M, Figueras F, Bargallo N, Gratacos E. Differences in cortical development assessed by fetal MRI in late-onset intrauterine growth restriction. Am J Obstet Gynecol.
18. Augustine JR. Circuitry and functional aspects of the insular lobe in primates including humans. Brain Res Brain Res Rev 1996;22:229-44.
19. Nieuwenhuys R. The insular cortex: a review. Prog Brain Res;195:123-63.
20. Robinson HP, Fleming JE. A critical evaluation of sonar "crown-rump length" measurements. Br J Obstet Gynaecol 1975;82:702-10.
21. Chauhan SP, Gupta LM, Hendrix NW, Berghella V. Intrauterine growth restriction: comparison of American College of Obstetricians and Gynecologists practice bulletin with other national guidelines. Am J Obstet Gynecol 2009;200:409 e1-6.
22. Figueras F, Meler E, Iraola A, Eixarch E, Coll O, Figueras J, Francis A, Gratacos E, Gardosi J. Customized birthweight standards for a Spanish population. Eur J Obstet Gynecol Reprod Biol 2008;136:20-4.
23. Arduini D, Rizzo G. Normal values of Pulsatility Index from fetal vessels: a cross-sectional study on 1556 healthy fetuses. J Perinat Med 1990;18:165-72.
24. Baschat AA, Gembruch U. The cerebroplacental Doppler ratio revisited. Ultrasound Obstet Gynecol 2003;21:124-7.

25. Gomez O, Figueras F, Fernandez S, Bennasar M, Martínez JM, Puerto B, Gratacos E. Reference ranges for uterine artery mean pulsatility index at 11-41 weeks of gestation. Ultrasound Obstet Gynecol 2008;32:128-32.
26. Bahado-Singh RO, Kovanci E, Jeffres A, Oz U, Deren O, Copel J, Mari G. The Doppler cerebroplacental ratio and perinatal outcome in intrauterine growth restriction. Am J Obstet Gynecol 1999;180:750-6.
27. Hofstaetter C, Dubiel M, Gudmundsson S, Marsal K. Uterine artery color Doppler assisted velocimetry and perinatal outcome. Acta Obstet Gynecol Scand 1996;75:612-9.
28. Tremblay E, Therasse E, Thomassin-Naggara I, Trop I. Quality initiatives: guidelines for use of medical imaging during pregnancy and lactation. Radiographics;32:897-911.
29. Righini A, Parazzini C, Doneda C, Avagliano L, Arrigoni F, Rustico M, Consonni D, Re TJ, Bulfamante G, Triulzi F. Early formative stage of human focal cortical gyration anomalies: fetal MRI. AJR Am J Roentgenol;198:439-47.
30. Chen CY, Zimmerman RA, Faro S, Parrish B, Wang Z, Bilaniuk LT, Chou TY. MR of the cerebral operculum: topographic identification and measurement of interopercular distances in healthy infants and children. AJNR Am J Neuroradiol 1995;16:1677-87.
31. Cohen JD, Mock JR, Nichols T, Zadina J, Corey DM, Lemen L, Bellugi U, Galaburda A, Reiss A, Foundas AL. Morphometry of human insular cortex and insular volume reduction in Williams syndrome. J Psychiatr Res;44:81-9.
32. Takahashi T, Suzuki M, Hagino H, Zhou SY, Kawasaki Y, Nohara S, Nakamura K, Yamashita I, Seto H, Kurachi M. Bilateral volume reduction of the insular cortex in patients with schizophrenia: a volumetric MRI Study. Psychiatry Res 2004;132:187-96.
33. Crespo-Facorro B, Kim J, Andreasen NC, O'Leary DS, Bockholt HJ, Magnotta V. Insular cortex abnormalities in schizophrenia: a structural magnetic resonance imaging study of first-episode patients. Schizophr Res 2000;46:35-43.
34. Dubois J, Benders M, Cachia A, Lazeyras F, Ha-Vinh Leuchter R, Sizonenko SV, Borradori-Tolsa C, Mangin JF, Hüppi PS. Mapping the early cortical folding process in the preterm newborn brain. Cereb Cortex 2008;18:1444-54.
35. Brazelton TB NJ. Neonatal Behavioral Assessment Scale. 3rd ed. London: MacKeith Press, 1995.
36. Costas Moragas C, Fornieles Deu A, Botet Mussons F, Boatella Costa E, de Caceres Zurita ML. [Psychometric evaluation of the Brazelton Scale in a sample of Spanish newborns]. Psicothema 2007;19:140-9.
37. Dubois J, Benders M, Lazeyras F, Borradori-Tolsa C, Leuchter RH, Mangin JF, Hüppi PS. Structural asymmetries of perisylvian regions in the preterm newborn. Neuroimage;52:32-42.
38. Geva R, Eshel R, Leitner Y, Fattal-Valevski A, Harel S. Memory functions of children born with asymmetric intrauterine growth restriction. Brain Res 2006;1117:186-94.
39. Lodygensky GA, Seghier ML, Warfield SK, Tolsa CB, Sizonenko S, Lazeyras F, Hüppi PS. Intrauterine growth restriction affects the preterm infant's hippocampus. Pediatr Res 2008;63:438-43.
40. Huppi PS. Neuroimaging of brain development--discovering the origins of neuropsychiatric disorders? Pediatr Res 2008;64:325.

41. Savchev S, Sanz-Cortes M, Cruz-Martinez R, Arranz A, Botet F, Gratacos E, Figueras F. Neurodevelopmental outcome of full-term small-for-gestational-age infants with normal placental function. Ultrasound Obstet Gynecol.
42. Mula R, Savchev S, Parra M, Arranz A, Botet F, Costas-Moragas C, Gratacos E, Figueras F. Increased fetal brain perfusion and neonatal neurobehavioral performance in normally grown fetuses. Fetal Diagn Ther;33:182-8.
43. Als H, Duffy FH, McAnulty G, Butler SC, Lightbody L, Kosta S, Weisenfeld NI, Robertson R, Parad RB, Ringer SA, Blickman JG, Zurakowski D, Warfield Sk. NIDCAP improves brain function and structure in preterm infants with severe intrauterine growth restriction. J Perinatol;32:797-803.
44. Canals J, Hernandez-Martinez C, Esparo G, Fernandez-Ballart J. Neonatal Behavioral Assessment Scale as a predictor of cognitive development and IQ in full-term infants: a 6-year longitudinal study. Acta Paediatr;100:1331-7.

FIGURE LEGENDS

Figure 1. Insular cortical thickness and insular depth assessed using Analyze software.

Legend: A) Anterior, middle and posterior insular cortical thickness delineations are depicted by yellow lines. **B)** Left insular depth is represented by a yellow line, perpendicularly to the interhemispheric fissure which is depicted in red. Examples are presented in axial T2-weighted MR images of a 37 weeks of gestational age fetus.

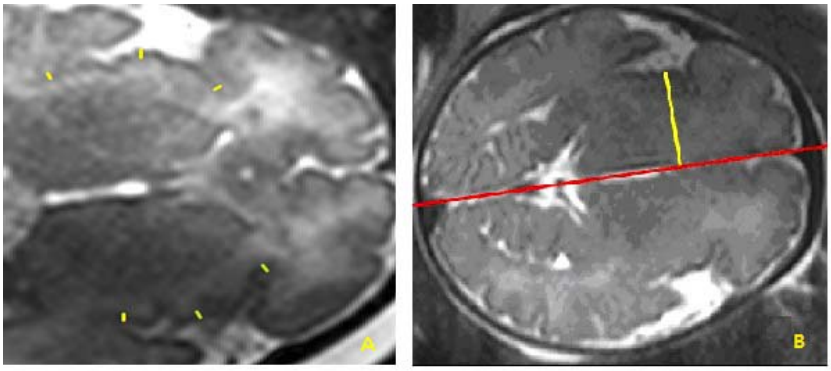

Figure 2. Insular cortical and TBV assessment by semi-automatic delineation.

Legend: ROI are identified as the red area sampled by the Analyze software. **A)** Insular cortical volume and **B)** TBV using axial T2-weighted MR images in a 37 weeks of gestational age fetus.

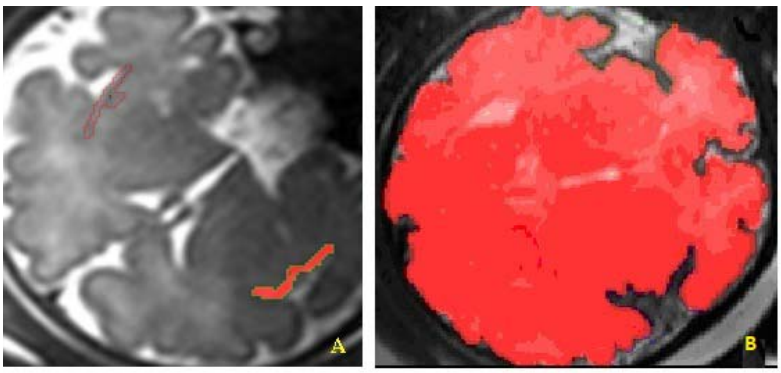

Figure 3. FA map and ROI delineation of the insular cortex.

Legend: FA map showing the delineation of the anterior, middle and posterior insular cortex bilaterally used to obtain the FA values of these ROIs. Example is presented using axial MR images in 37 weeks of GA fetus.

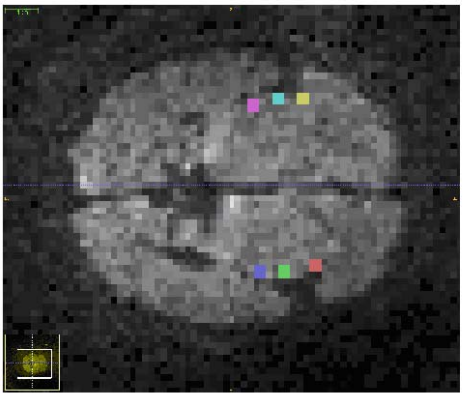

Figure 4. Insular cortical thickness (A) and volume (B) according to prenatal severity signs.

Legend: Polynomial contrast analysis showing differences between IUGR (late-onset SGA showing the presence of severity parameters defined as CPR <5th centile, IP UtA Doppler >95th centile, and/or birthweight <3rd centile), SGA (late-onset SGA without severity parameters) and AGA. Bars depict the mean within each group. **A)** *p<0.01 and †p<0.05. Linear tendency for insular cortical thickness/insular depth in IUGR, SGA and AGA. AL, ML and PL: anterior, middle and posterior left thickness; AR, MR and PR: anterior, middle and posterior insular cortical left thickness. **B)** * and † p<0.05. Linear tendency for insular cortical volume bilaterally in IUGR, SGA and AGA.

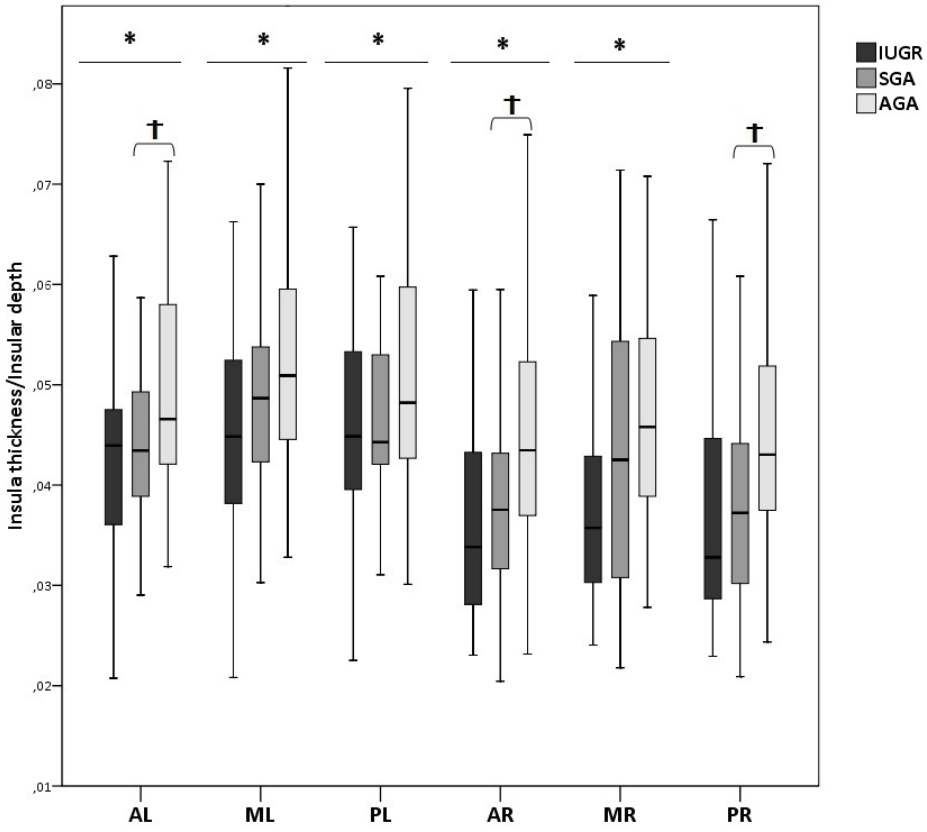

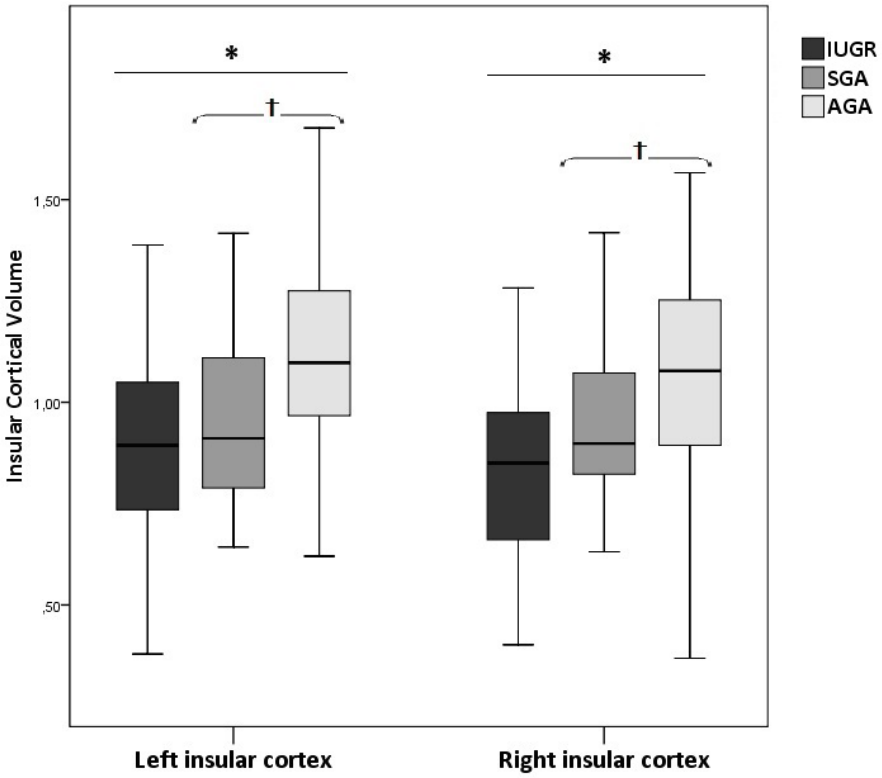

TABLES

Table 1. Maternal characteristics of the study groups.

	SGA (N = 65)	AGA (N = 59)	*P**
Maternal age (y)	32.1 ± 5.9	32.3 ± 4.2	0.82
Maternal smoking	16.9%	5.1%	**0.03**
Maternal BMI (kg/m2)	22.2 ± 3.6	23.1 ± 3.7	0.20
Primiparity	53.2%	46.8%	0.65
White ethnicity	54.4%	45.6%	0.46
GA at MRI (w)	37.5± 0.8	37.6 ± 0.9	0.06

Results are expressed as mean ± SD or percentage as appropriate. *Student´s t-test for independent samples or Pearson´s X^2 test. BMI: Body mass index. GA: gestational age. MRI: Magnetic Resonance Imaging. y= years; kg=kilograms; m^2= square meter; w=weeks.

Table 2. Perinatal outcome of the study groups.

	SGA (N = 65)	AGA (N = 59)	*P**
GA at birth (w)	38.7 ± 1.0	40.0 ± 1.1	**<0.01**
Birthweight (g)	2479 ± 279	3436 ± 299	**<0.01**
Birthweight centile	3.9 ± 6.07	53.3 ± 23.8	**<0.01**
Male gender	53.5%	46.5%	0.70
Labor induction	72.3%	20.3%	**<0.01**
Emergency cesarean section	26.1%	6.7%	**<0.01**
Neonatal acidosis†	15.4%	5.0%	0.07
Apgar score <7 at 5 minutes	3.1%	0%	0.08
NICU stay length (d)	0.3	0	**0.04**
GA at NBAS	42.9 ± 2.9	43.2 ± 2.0	0.50
Adaptation days from delivery to NBAS test	29.7 ± 17.8	23.4 ± 13.3	0.06

Results are expressed as mean ± SD or percentage as appropriate. *Student´s t-test for independent samples or Pearson´s X^2 test. GA: gestational age. Neonatal acidosis†: umbilical artery pH<7.15 and base excess > 12 mEq/L. NICU: Neonatal Intensive care unit. w=weeks; g=grams; NBAS= Neonatal Behavioral Assessment Scale.

Table 3. Insular cortical thickness corrected by insular depth in the study groups.

Insular cortical thickness/insular depth	SGA (N = 65)	AGA (N = 59)	*P**
Left anterior ICT/ left ID	0.044 ± 0.011	0.051 ± 0.014	**<0.01**
Left middle ICT/ left ID	0.047 ± 0.011	0.054 ± 0.013	**<0.01**
Left posterior ICT/ left ID	0.048 ± 0.011	0.053 ± 0.014	**0.02**
Right anterior ICT/ right ID	0.038 ± 0.011	0.046 ± 0.013	**<0.01**
Right middle ICT/ right ID	0.040 ± 0.011	0.048 ± 0.014	**<0.01**
Right posterior ICT/ right ID	0.038 ± 0.012	0.046 ± 0.013	**<0.01**

Results are expressed as mean ± *SD*.* GLM adjusted for gender, GA at MRI, maternal smoking and BMI. ICT: insular cortical thickness; ID: insular depth.

Table 4. Insular cortical volumes in the study groups.

	SGA (N = 65)	AGA (N = 59)	*P**
Left insular volume (cm3)	0.904 ± 0.274	1.099 ± 0.283	**<0.01**
Right insular volume (cm3)	0.860 ± 0.258	1.059 ± 0.287	**<0.01**

Results are expressed as mean ± SD.* GLM adjusted for gender, GA at MRI, TBV, maternal smoking and BMI.

Table 5. Insular cortical morphometry and its association with neurobehavioral outcome in late-onset SGA.

Insular measurement		NBAS Cluster	*P**
Left insular cortical thickness			
	Anterior	Organization of state	**0.04**
		Autonomic nervous system	**0.04**
		Social-interactive	**0.03**
	Middle	Regulation of state	**0.03**
		Attention	**0.04**
	Posterior	Autonomic nervous system	**0.04**
Right insular cortical thickness			
	Middle	Regulation of state	**0.02**
	Posterior	Autonomic nervous system	**0.04**
Insular lobe depth			
	Right	Regulation of state	**0.04**
Cortical thickness AI			
	Posterior	Autonomic nervous system	**0.02**
	Middle	Regulation of state	**0.03**

* GLM considering the NBAS test's clusters <5th centile as the dependent variable and insular cortical measurements as the independent variables adjusted for gender, GA at MRI, GA at NBAS, maternal smoking and BMI.

5.3 STUDY 3

Corpus callosum differences assessed by fetal MRI in late-onset intrauterine growth restriction and its association with neurobehavior

Egaña-Ugrinovic G, Sanz-Cortés M, Couve-Pérez C, Figueras F, Gratacós E

Prenatal Diagnosis. 2014

State: accepted for publication.

Impact factor: 2.683

Quartile: 1st

CORPUS CALLOSUM DIFFERENCES ASSESSED BY FETAL MRI IN LATE-ONSET INTRAUTERINE GROWTH RESTRICTION AND ITS ASSOCIATION WITH NEUROBEHAVIOR

Gabriela EGAÑA-UGRINOVIC, MD[1]; Magdalena SANZ-CORTÉS, PhD[1]; Constanza COUVE-PEREZ, MD[1]; Francesc FIGUERAS, PhD[1]; Eduard GRATACÓS, PhD[1].

[1] Maternal-Fetal Medicine Department, Institut Clínic de Ginecologia, Obstetrícia i Neonatologia (ICGON); Fetal and Perinatal Medicine Research Group, Institut d'Investigacions Biomediques August Pi i Sunyer (IDIBAPS) and Centro de Investigación Biomédica en Red de Enfermedades Raras (CIBERER). Hospital Clínic, Universitat de Barcelona, Barcelona, Spain.

Corresponding author:

Eduard Gratacós

Maternal-Fetal Medicine Department

Hospital Clínic – Maternitat

Sabino de Arana 1, 08028, Barcelona, Spain

Telephone: +34 93 227 9333 Fax: +34 93 227 5612

Email: gratacos@clinic.ub.es

Abstract word count: 184 Text word count: 2824

Tables: 4 Figures: 3

This article has been accepted for publication and undergone full peer review but has not been through the copyediting, typesetting, pagination and proofreading process, which may lead to differences between this version and the Version of Record. Please cite this article as doi: 10.1002/pd.4381

Funding

This work was supported by grants from The Cerebra Foundation for the Brain Injured Child (Carmarthen, Wales, UK), the Thrasher Research Fund (Salt Lake City, USA), Obra Social "la Caixa" (Barcelona, Spain), Fundación Dexeus (Barcelona, Spain) and Banca Cívica de Caja Navarra (Proyecto TETD). G.E.U was supported by CONICYT (PFCHA/<Doctorado al Extranjero 4ª Convocatoria><72120071>), Chile. M.S.C. was supported by Instituto de Salud Carlos III Rio Hortega (CM10/00222), Spain.

Disclosure

None of the authors have a conflict of interest

No prior or duplicate publication or submission are intended

Bulleted Statement

- What's already known about this topic?
  - It has been reported that early and severe IUGR fetuses showed reduced corpus callosum growth by ultrasound assessment
  - Abnormal corpus callosum has been related to worse verbal IQ and verbal fluency
- What does this study add?
  - To our knowledge, this is the first report of corpus callosum assessment in a milder and more frequent form of fetal growth restriction which is then correlated with neurobehavior.
  - Brain reorganization due to chronic placental insufficiency may affect white matter development in term IUGR fetuses.

ABSTRACT

Objective

To evaluate corpus callosum (CC) development by Magnetic Resonance Imaging (MRI) in late-onset intrauterine growth restricted (IUGR) fetuses compared to appropriate for gestational age (AGA) and its association with neurobehavioral outcome.

Method

117 late-onset IUGR and 73 control fetuses were imaged using a 3T MRI scanner at term, obtaining T2 half-Fourier acquisition single-shot turbo spin-echo (HASTE) anatomical slices. CC length, thickness, total area and the areas after a subdivision in 7 portions were assessed. Neonatal Behavioral Assessment Scale (NBAS) test was performed on IUGR newborns at 42 ± 1 weeks.

Results

IUGR fetuses showed significantly smaller CC (Total CC Area IUGR: 1.3996 ± 0.26 vs. AGA: 1.664 ± 0.31; $p<0.01$) and smaller subdivision areas as compared with controls. The differences were slightly more pronounced in fetuses with very low birth weight and abnormal brain or uterine Doppler. CC measurements were significantly associated with neurobehavioral outcome in IUGR cases.

Conclusions

CC development was significantly altered in late-onset IUGR fetuses and correlated with worse neurobehavioral performance. CC could be further explored as a potential imaging biomarker to predict abnormal neurodevelopment in pregnancies at risk.

Key words: Fetal brain imaging, corpus callosum, neurobehavior, SGA, IUGR.

INTRODUCTION

Intrauterine growth restriction (IUGR) affects 5-10% of all newborns and has well-recognized perinatal and long-term consequences[1-3]. Abundant evidence supports an increased prevalence of abnormal neurodevelopment in this condition[4-6]. Around 20-40% of IUGR children will experience cognitive challenges and learning disabilities during school life[3, 5]. Impaired neurodevelopment is not exclusive of early severe IUGR, but it affects a significant proportion of children with milder, late-onset forms[6-9], which represent the majority of instances of fetal growth restriction. Neurostructural imaging studies on term IUGR have demonstrated changes on gyrification[9], cortical morphometry, connectivity[8] and metabolism[7]. Characterization of the neurostructural brain changes occuring in IUGR is critical for defining the brain phenotypes associated with different clinical forms of IUGR, and for the development of clinically useful imaging biomarkers.

The majority of research MRI techniques used to report brain changes under IUGR are of limited applicability. Aside from complex image processing settings, they entail long acquisition times that are commonly affected by fetal movements. Thus, there is a need to identify simpler biomarkers of abnormal neurodevelopment. In this study we explored the value of the corpus callosum (CC) as a biomarker of abnormal neurodevelopment. From a neuroimaging perspective, the CC is a well-defined brain structure that can be easily identified in standard MRI sequences, or midsagittal views in standard neurosonography. The CC is a thick plate of WM fibers that represents the main pathway of association between the two cerebral hemispheres[10]. As such, it is considered a surrogate of white matter (WM) growth, and has been proposed as a sensitive indicator of normal brain development and maturation[11]. Preliminary studies in early IUGR fetuses have suggested

that CC development could be altered[12]. However, no studies involving late-onset IUGR have been reported on this matter.

In this study we evaluated CC morphometry by MRI assessment in 117 late-onset IUGR fetuses as compared to 73 controls. In addition, we tested the hypothesis that fetal CC biometries are associated with neonatal neurobehavioral performance in IUGR newborns.

MATERIAL AND METHODS

Subjects

This study is part of a larger prospective research program on IUGR involving fetal, neonatal and long term postnatal follow-up. The specific protocol of this study was approved by the institutional Ethics Committee (Institutional Review Board 2008/4422) and all participants gave written informed consent. The study design contemplated recruitment of 120 cases and 80 controls.

Pregnancies were dated according to the first trimester crown-rump length measurement[13]. Late-onset IUGR was defined by an estimated and postnatally confirmed fetal weight <10th centile[14], according to local growth charts[15] with normal umbilical Doppler (umbilical artery pulsatility index <95th centile)[16]. AGA subjects were defined as normal term fetuses with an estimated and postnatally confirmed fetal weight ≥10th centile[14] according to local growth charts[15]. Exclusion criteria included congenital malformations, chromosomal abnormalities, perinatal infections, chronic maternal pathology, contraindications for MRI and non-cephalic presentations.

Clinical and Ultrasound data

IUGR patients were followed-up in our fetal growth restriction unit from diagnosis until delivery. The entire sample underwent serial Doppler ultrasound scans using a General Electric Voluson E8, 6-2MHz curved-array transducer (GE Medical Systems, Zipf, Austria). Fetal umbilical artery (UA) and middle cerebral artery (MCA) pulsatility index (PI) were measured as described elsewere[9]. Both measurements were used for the calculation of the cerebroplacental ratio (CPR). Abnormal CPR was defined as a value <5th centile for gestational age according to previously published reference values[17]. Uterine arteries (UtA) PI were measured transabdominally and mean value was considered abnormal when >95th centile[18]. All fetuses in this study had at least one scan preformed within one week before delivery.

To explore if there was an association between CC measurements and the severity of growth restriction, for the purposes of this study group IUGR was subdivided into[9]: (1) IUGR^{+} defined by birth weight <3rd centile and/or abnormal CPR and/or abnormal UtA and (2) IUGR^{-} when none of these criteria was present. Maternal, perinatal and neonatal data were prospectively recorded in all study patients.

Fetal MRI imaging acquisition

MRI was performed at 37 weeks of gestational age (GA) on a clinical MR system using the IDIBAPS image platform, operating at 3.0 Tesla (Siemens Magnetom Trio Tim syngo MR B15, Siemens, Germany) without fetal sedation and following the American College of Radiology guidelines[19]. A surface coil around the maternal abdomen was centered over the fetal head. Routine fetal imaging took around 20 minutes and consisted on single-shot, fast spin echo T2-weighted sequences (TR 990ms, TE 137ms, slice thickness 3.5mm, no gap, field of view

260mm, voxel size 1.4 x 1.4 x 3.5mm, matrix 192 x 192, flip angle 180º, acquisition time 24 seconds) acquired in the three orthogonal planes. If the quality of the images was suboptimal, sequences were repeated. Structural MRI images were reviewed for the presence of anatomical abnormalities by an experienced neuroradiologist blinded to group membership.

Offline analysis

Imaging post processing and measurements were performed using the semiautomatic Analyze 9.0 software (Biomedical Imaging Resource, Mayo Clinic; Kansas, USA) by two experienced examiners blinded to group membership. CC was identified in the mid-sagittal plane as a slightly curved horizontal T2-weighted hypointense structure[20]. The slice chosen for CC assessment had to accomplish strict quality criteria defined as: the identification of the cavum septi pellucidi, thalamus, midbrain, cerebellar vermis and cisterna magna[21, 22] (Figure 1). Furthermore, a clear visualization of the body, splenium, genu, and rostrum of the CC had to be accomplished.

Linear measurements

a. CC length was measured from the most anterior part of the genu to the most posterior part of the splenium tracing a straight rostrocaudal line between the two points, known as the outer-to-outer CC lenght[20] (Figure 1). This measurement was measured three times and the mean value was used for further analysis.
b. CC thickness was measured in its anterior, middle and posterior portions corresponding to the genu, body and splenium thickness respectively[23, 24]. The thickness of the genu and splenium was measured at the same level where the line

for CC length was traced. CC body thickness was measured equidistantly from the anterior and posterior measurements[23] (Figure 1).

Area measurements

a. Total CC area was delineated through cursor-guided free-hand traces. It was limited superiorly by the cingulate gyrus which is identified as a hyperintense curved shaped line and inferiorly, by the cavum septi pellucidi and cavum vergae[23, 25] (Figure 2).
b. CC was subdivided in seven areas described by Witelson et al[23] (Figure 2) in order to measure the rostrum, genu, rostral body, anterior midbody, posterior midbody, isthmus and splenium areas (Figure 2).

Cephalic Index

In order to correct for differences in head size, cephalic index (CI) was considered by measuring the biparietal and occipitofrontal diameters (BPD and OFD respectively. BPD and OFD were measured as reported elsewhere[9]. To calculate the CI we used a previously reported formula: CI= BPD/OFD*100)[26].

Neurobehavioral performance

Postnatal follow up was offered to all IUGR patients and neurobehavioral assessment was performed prospectively at 42-43 weeks using the NBAS test by 1 of 2 observers accredited by The Brazelton Institute (Harvard Medical School, Boston, MA)[27]. The examination consisted on 7 behavioral areas including habituation, motor, social-interactive, organization of state, regulation of state, autonomic nervous system and attention, as reported elsewhere[27, 28]. The scores from the behavioral areas were converted into centiles

according to normal curve references for our population, considering an abnormal result a score <5th centile for the corresponding cluster[29].

Interobserver reliability

To establish both biometric and volumetric measurement reliability, all measurements from 20 fetuses were assessed independently by two experienced examiners blinded to group membership. Reliability between measurements from both observers was assessed by the intraclass correlation coefficient (ICC) and their 95% confidence intervals (CI). A two-way mixed model was chosen for agreement analysis. An ICC of 1 indicates perfect reproducibility between measurements, while a value of 0 is interpreted as reproducibility that is no better or worse than that expected by chance. We considered an ICC value between 0.5 and 0.7 as adequate and more than 0.7 as excellent agreement[30].

Statistical analysis of clinical and CC data

Due to the exploratory nature of this study and since there was no previous data analyzing the association between CC morphometry with neurobehavior, we arbitrarily established a sample size of 120-80 per study group. Student´s t test for independent samples and Pearson´s X^2 tests were used to compare quantitative and qualitative data respectively. Multivariate analyses of covariance (MANCOVA) adjusted by gender, maternal smoking and body mass index (BMI) were conducted to assess CC differences between late-onset IUGR and AGA and also to perform a polynomial contrast in order to evaluate the linear trend of the different clinical severity subgroups. The association between measurements and NBAS test scores in IUGR was assessed by an ordinal regression taking into account the same covariates plus age at NBAS test. The amount of NBAS test's clusters <5th centile were

considered as the dependent variable and CC measurements as the independent variables. A *p* value <0.05 was set as significant. The software package SPSS 17.0 (SPSS, Chicago, IL, USA) and MedCalc 8.0 (Broekstraat, Belgium) were used for the statistical analyses.

RESULTS

Clinical characteristics in the study population

Three (3%) IUGR and seven (9%) AGA fetuses had to be excluded due to insufficient image quality for delineation according to the quality standards defined in this study, leaving a total of 117 late-onset IUGR and 73 control fetuses. Among IUGR fetuses, 77 were defined as $IUGR^{+}$ and 38 as $IUGR^{-}$ according to the criteria defined above. Maternal characteristics and time of MRI scan did not differ between cases and controls (Table 1). As expected, IUGR fetuses were delivered earlier with higher rates of labor induction, emergency cesarean section and longer stay in the neonatal intensive unit care (Table 2).

Interobserver reliability

Overall biometric and volumetric measurements showed acceptable to good interobserver reliability. Regarding linear measurements analysis, the ICC was for length 0.942 (95% CI 0.852 to 0.978); 0.577 (95% CI -0.47 to 0.834) for genu thickness; 0.642 (95% CI 0.081 to 0.864) for middle thickness; and 0.403 (95% CI -0.332 to 0.755) for splenium thickness. The ICC for total area was 0.86 (95% CI 0.398 to 0.954); and for CC subdivisions was 0.69 (95% CI -0.20 to 0.892) for rostrum; 0.893 (95% CI 0.733 to 0.957) for genu; 0.887 (95% CI 0.715 to 0.955) for rostral body; 0.596 (95% CI -0.22 to 0.84) for anterior midbody; 0.771 (95% CI 0.437 to 0.908) for posterior midbody; 0.648 (95% CI 0.138 to 0.859) for isthmus; and 0.679 (95% CI -0.162 to 0.896) for splenium.

CC morphometric analysis

Regarding linear measurements of the CC, late-onset IUGR fetuses showed a trend for shorter CC length/CI (IUGR: 0.49 ± 0.05 vs. AGA: 0.51 ± 0.04; *p*=0.2) and thinner splenium/CI (0.037 ± 0.010 vs. 0.04 ± 0.009; *p*=0.05) (Table 3).

In terms of area measurements, late-onset IUGR presented globally smaller CC expressed as the ratio CC area/CI (1.3996 ± 0.26 vs. 1.664 ± 0.31; p<0.01). Likewise, late IUGRs showed smaller areas in all subdivisions, reaching statistical significance in genu/CI, rostral body/CI, anterior midbody/CI, posterior midbody area/CI, isthmus/CI and splenium/CI (Table3).

In general, CC length and area were similarly reduced in $IUGR^{+}$ and $IUGR^{-}$, as compared with controls, but there was a linear trend indicating a relationship with the severity criteria defined in this study (Figure 3).

Association between morphometric CC analyses with neurobehavioral outcome in late-onset IUGR

The NBAS test was performed at 42.5 ± 2.8 GA weeks in the IUGR population and the time from birth until the neurobehavior test was 28.8 ± 16.8 days. The results from the ordinal regression analysis between the CC measurements and the neurobehavioral test showed a significant change of the global scoring distribution towards overall lower NBAS scores in IUGR at the presence of smaller measurements of the CC (Table 4). Specifically, smaller total area (*p*=0.03), rostrum (*p*=0.02), genu (*p*=0.03), rostral body (*p*=0.02), anterior midbody (*p*=0.03) and splenium (*p*=0.03) had a significant negative effect on the number of abnormal NBAS clusters.

COMMENT

In this study late-onset IUGR fetuses presented differences in CC linear and area measurements. Furthermore, several CC measurements were correlated with abnormal neurobehavioral scores in fetuses with IUGR. These findings confirm previous reports supporting the notion that brain reorganization may affect WM development in term growth restriction[12, 31] and suggest the potential use of CC as a clinically applicable biomarker of brain reorganization in late-onset IUGR.

Previous studies in early and severe IUGR infants have shown decreased WM volume in the cerebellum[31]. Moreover, one-year-old IUGR infants present abnormal brain networks, which might suggest brain reorganization of the WM connectivity[8]. Referring particularly to the CC, our results go in line with a previous study reporting a reduced growth rate of this structure assessed by ultrasound in early-onset IUGR fetuses[12]. The authors proposed that their findings may reflect altered maturation of the WM microstructure in IUGR. In another study, a smaller posterior portion of the CC was also described in preterm children, with a significant association with worse verbal IQ and verbal fluency[32]. To our knowledge this morphometric analysis of the CC development might supports the notion that brain reorganization could affect WM development in term IUGR as well; although a multifocal approach study, involving connectivity of the corpus callosum, could further support to this hypothesis..

The CC achieves its normal shape around 18 weeks of gestation, but its maturational process extends from pregnancy until the end of the adolescence[32]. CC growth in late pregnancy is predominantly an area rather than a length increase . Thickening occurs in response to axonal growth and pruning[10], following an anterior-posterior directionality and reaching uniform measurements at term[33]. Interestingly, our findings in late-onset IUGR

fetuses were mainly related to smaller areas in the majority of CC subdivisions evaluated, rather than reduced linear measurements of the CC, which supports a late effect. The impact of in utero conditions on CC development is supported by postmortem studies showing an intrinsic vulnerability to chronic hypoxia of immature oligodendrocytes and callosal fibers located closer to the germinal matrix[34, 35]. Moreover, experimental models have shown myelination deficits in the CC of rats exposed to hypoxia, resulting in smaller CC[36]. Finally, a close relation has been described between an integral CC development and a proper brain cortical development[33, 37]. This association is in line with the results of this study and previous studies on late-onset IUGR fetuses reporting differences in the pattern of brain sulcation[9].

From a clinical perspective, this study provides further evidence of the existence of brain reorganization in late-onset IUGR. Growth restriction is a well-known risk factor to present cognitive challenges, learning disabilities and neuropsychiatric disorders[3, 4, 38, 39]. It has been proposed that subtle structural abnormalities associated to these impairments are detectable long before the appearance of functional symptoms[38]. The CC presents the advantage of being a well-defined structure which can also be explored by a standard neurosonographic ultrasound scan. Remarkably, CC developmental abnormalities have been associated to different cognitive disorders[10]. The value of CC assessment deserved further attention to explore its use as a potential imaging biomarker in order to identify higher-risk pregnancies of abnormal neurodevelopment in several prenatal conditions, suchas growth restriction[4], congenital heart disease[40] or congenital cytomegalovirus infection[41] among others . Prenatal detection would allow targeted strategies that have shown to improve neurodevelopmental outcome, functional brain connectivity and brain structure in infants at risk[42]. As in previous studies[1, 9], we classified IUGR according to the presence or absence of

signs of adverse perinatal outcome. Although, term IUGR fetuses with the presence of severity signs showed more accentuated shorter and smaller CC areas, the less severe form of growth restriction also presented CC differences as compared to controls. These findings are in line with previous studies[1, 7, 43], suggesting that late onset IUGR with normal brain Doppler, also defined as small for gestational age, are not "constitutionally" small fetuses, but probably suffer a form of restriction that remains to be better characterized.

We acknowledge some limitations in this study. Measurements were performed by manual delineation. To counter this problem we used a previously reported methodology which has been widely used by other authors in MRI assessment of the CC[23]. Another limitation of this study was the precision of the anatomical landmarks required to delineate the CC, therefore some images were not susceptible to be processed mostly due to motion artifacts. Furthermore, we acknowledge that the results on neurodevelopment were based on a neonatal neurobehavioral test and long term studies of neurocognitive function will respond to this hypothesis. However, increasing evidence supports the link between neonatal neurobehavioral skills with later neurocognitive development[44]. The study has methodological strengths, as for example we used well-defined anatomical landmarks and a previously reported CC segmentation[21, 23]. Moreover, in order to have more reliable results, CC measurements were corrected for the potential bias of having smaller CC in smaller brains. The CC segmentation here used, presents the advantage of an easy transfer to an ultrasound approach. Finally, cases represented a homogeneous sample which is highly representative of the condition of interest and all patients were prospectively followed up until delivery.

To our knowledge this is the first study on CC development in late-onset IUGR fetuses describing morphometric differences which are further related to their neurobehavioral

performance. Further research involving long-term follow-up is warranted to evaluate the potential used of the CC as an imaging biomarker in the prediction of abnormal neurodevelopment in fetuses with IUGR and other fetal conditions.

Acknowledgments

Dra. Gabriela Egaña thanks the Neuroimage Laboratory and the IDIBAPS platform for the technical support.

REFERENCES

1. SAVCHEV S, FIGUERAS F, CRUZ-MARTINEZ R, ILLA M, BOTET F, GRATACOS E. Estimated weight centile as a predictor of perinatal outcome in small-for-gestational-age pregnancies with normal fetal and maternal Doppler indices. Ultrasound Obstet Gynecol;39:299-303.
2. ARCANGELI T, THILAGANATHAN B, HOOPER R, KHAN KS, BHIDE A. Neurodevelopmental delay in small babies at term: a systematic review. Ultrasound Obstet Gynecol;40:267-75.
3. LEITNER Y, FATTAL-VALEVSKI A, GEVA R, et al. Neurodevelopmental outcome of children with intrauterine growth retardation: a longitudinal, 10-year prospective study. J Child Neurol 2007;22:580-7.
4. SAVCHEV S, SANZ-CORTES M, CRUZ-MARTINEZ R, et al. Neurodevelopmental outcome of full-term small-for-gestational-age infants with normal placental function. Ultrasound Obstet Gynecol.
5. EIXARCH E, MELER E, IRAOLA A, et al. Neurodevelopmental outcome in 2-year-old infants who were small-for-gestational age term fetuses with cerebral blood flow redistribution. Ultrasound Obstet Gynecol 2008;32:894-9.
6. DUBOIS J, BENDERS M, BORRADORI-TOLSA C, et al. Primary cortical folding in the human newborn: an early marker of later functional development. Brain 2008;131:2028-41.
7. SANZ-CORTES M, FIGUERAS F, BARGALLO N, PADILLA N, AMAT-ROLDAN I, GRATACOS E. Abnormal brain microstructure and metabolism in small-for-gestational-age term fetuses with normal umbilical artery Doppler. Ultrasound Obstet Gynecol;36:159-65.
8. BATALLE D, EIXARCH E, FIGUERAS F, et al. Altered small-world topology of structural brain networks in infants with intrauterine growth restriction and its association with later neurodevelopmental outcome. Neuroimage;60:1352-66.
9. EGANA-UGRINOVIC G, SANZ-CORTES M, FIGUERAS F, BARGALLO N, GRATACOS E. Differences in cortical development assessed by fetal MRI in late-onset intrauterine growth restriction. Am J Obstet Gynecol.
10. PAUL LK. Developmental malformation of the corpus callosum: a review of typical callosal development and examples of developmental disorders with callosal involvement. J Neurodev Disord;3:3-27.
11. GOODYEAR PW, BANNISTER CM, RUSSELL S, RIMMER S. Outcome in prenatally diagnosed fetal agenesis of the corpus callosum. Fetal Diagn Ther 2001;16:139-45.
12. GOLDSTEIN I, TAMIR A, REECE AE, WEINER Z. Corpus callosum growth in normal and growth-restricted fetuses. Prenat Diagn;31:1115-9.
13. ROBINSON HP, FLEMING JE. A critical evaluation of sonar "crown-rump length" measurements. Br J Obstet Gynaecol 1975;82:702-10.
14. CHAUHAN SP, GUPTA LM, HENDRIX NW, BERGHELLA V. Intrauterine growth restriction: comparison of American College of Obstetricians and Gynecologists practice bulletin with other national guidelines. Am J Obstet Gynecol 2009;200:409 e1-6.
15. FIGUERAS F, MELER E, IRAOLA A, et al. Customized birthweight standards for a Spanish population. Eur J Obstet Gynecol Reprod Biol 2008;136:20-4.
16. ARDUINI D, RIZZO G. Normal values of Pulsatility Index from fetal vessels: a cross-sectional study on 1556 healthy fetuses. J Perinat Med 1990;18:165-72.
17. BASCHAT AA, GEMBRUCH U. The cerebroplacental Doppler ratio revisited. Ultrasound Obstet Gynecol 2003;21:124-7.
18. GOMEZ O, FIGUERAS F, FERNANDEZ S, et al. Reference ranges for uterine artery mean

pulsatility index at 11-41 weeks of gestation. Ultrasound Obstet Gynecol 2008;32:128-32.
19. TREMBLAY E, THERASSE E, THOMASSIN-NAGGARA I, TROP I. Quality initiatives: guidelines for use of medical imaging during pregnancy and lactation. Radiographics;32:897-911.
20. HARRELD JH, BHORE R, CHASON DP, TWICKLER DM. Corpus callosum length by gestational age as evaluated by fetal MR imaging. AJNR Am J Neuroradiol;32:490-4.
21. ACHIRON R, ACHIRON A. Development of the human fetal corpus callosum: a high-resolution, cross-sectional sonographic study. Ultrasound Obstet Gynecol 2001;18:343-7.
22. STANCAK A, COHEN ER, SEIDLER RD, DUONG TQ, KIM SG. The size of corpus callosum correlates with functional activation of medial motor cortical areas in bimanual and unimanual movements. Cereb Cortex 2003;13:475-85.
23. WITELSON SF. Hand and sex differences in the isthmus and genu of the human corpus callosum. A postmortem morphological study. Brain 1989;112 (Pt 3):799-835.
24. LERMAN-SAGIE T, BEN-SIRA L, ACHIRON R, et al. Thick fetal corpus callosum: an ominous sign? Ultrasound Obstet Gynecol 2009;34:55-61.
25. BOGER-MEGIDDO I, SHAW DW, FRIEDMAN SD, et al. Corpus callosum morphometrics in young children with autism spectrum disorder. J Autism Dev Disord 2006;36:733-9.
26. LIM KI, DELISLE MF, AUSTIN SJ, WILSON RD. Cephalic index is not a useful sonographic marker for trisomy 21 and trisomy 18. Fetal Diagn Ther 2004;19:491-5.
27. BRAZELTON TB NJ. Neonatal Behavioral Assessment Scale. 3rd ed. London: MacKeith Press, 1995.
28. FIGUERAS F, OROS D, CRUZ-MARTINEZ R, et al. Neurobehavior in term, small-for-gestational age infants with normal placental function. Pediatrics 2009;124:e934-41.
29. COSTAS MORAGAS C, FORNIELES DEU A, BOTET MUSSONS F, BOATELLA COSTA E, DE CACERES ZURITA ML. [Psychometric evaluation of the Brazelton Scale in a sample of Spanish newborns]. Psicothema 2007;19:140-9.
30. DEL RIO M, MARTINEZ JM, FIGUERAS F, et al. Doppler assessment of fetal aortic isthmus blood flow in two different sonographic planes during the second half of gestation. Ultrasound Obstet Gynecol 2005;26:170-4.
31. PADILLA N, FALCON C, SANZ-CORTES M, et al. Differential effects of intrauterine growth restriction on brain structure and development in preterm infants: a magnetic resonance imaging study. Brain Res;1382:98-108.
32. NOSARTI C, RUSHE TM, WOODRUFF PW, STEWART AL, RIFKIN L, MURRAY RM. Corpus callosum size and very preterm birth: relationship to neuropsychological outcome. Brain 2004;127:2080-9.
33. MOSES P, COURCHESNE E, STILES J, TRAUNER D, EGAAS B, EDWARDS E. Regional size reduction in the human corpus callosum following pre- and perinatal brain injury. Cereb Cortex 2000;10:1200-10.
34. VASUNG L, JOVANOV-MILOSEVIC N, PLETIKOS M, MORI S, JUDAS M, KOSTOVIC I. Prominent periventricular fiber system related to ganglionic eminence and striatum in the human fetal cerebrum. Brain Struct Funct;215:237-53.
35. BACK SA, LUO NL, BORENSTEIN NS, LEVINE JM, VOLPE JJ, KINNEY HC. Late oligodendrocyte progenitors coincide with the developmental window of vulnerability for human perinatal white matter injury. J Neurosci 2001;21:1302-12.
36. LANGMEIER M, POKORNY J, MARES J, TROJAN S. Changes of the neuronal structure produced by prolonged hypobaric hypoxia in infant rats. Biomed Biochim Acta

1989;48:S204-7.
37. WARREN DJ, CONNOLLY DJ, GRIFFITHS PD. Assessment of sulcation of the fetal brain in cases of isolated agenesis of the corpus callosum using in utero MR imaging. AJNR Am J Neuroradiol;31:1085-90.
38. HUPPI PS. Neuroimaging of brain development--discovering the origins of neuropsychiatric disorders? Pediatr Res 2008;64:325.
39. HAGLUND NG, KALLEN KB. Risk factors for autism and Asperger syndrome. Perinatal factors and migration. Autism;15:163-83.
40. OWEN M, SHEVELL M, DONOFRIO M, et al. Brain Volume and Neurobehavior in Newborns with Complex Congenital Heart Defects. J Pediatr.
41. FOULON I, NAESSENS A, FOULON W, CASTEELS A, GORDTS F. A 10-year prospective study of sensorineural hearing loss in children with congenital cytomegalovirus infection. J Pediatr 2008;153:84-8.
42. ALS H, DUFFY FH, MCANULTY G, et al. NIDCAP improves brain function and structure in preterm infants with severe intrauterine growth restriction. J Perinatol;32:797-803.
43. CRISPI F, FIGUERAS F, CRUZ-LEMINI M, BARTRONS J, BIJNENS B, GRATACOS E. Cardiovascular programming in children born small for gestational age and relationship with prenatal signs of severity. Am J Obstet Gynecol;207:121 e1-9.
44. CANALS J, HERNANDEZ-MARTINEZ C, ESPARO G, FERNANDEZ-BALLART J. Neonatal Behavioral Assessment Scale as a predictor of cognitive development and IQ in full-term infants: a 6-year longitudinal study. Acta Paediatr;100:1331-7.

Table 1. Maternal characteristics of the study groups.

	IUGR (N = 117)	AGA (N = 73)	P*
Maternal age (y)	31.8 ± 5.6	32.2 ± 4.2	0.55
Maternal smoking	23.3%	5.5%	**<0.01**
Maternal BMI (kg/m2)	22.2 ± 3.9	22.9 ± 3.6	0.19
Primiparity	75.7%	67.1%	0.22
Caucasian ethnicity	76.7%	71.2%	0.40

Results are expressed as mean ± SD or percentage as appropriate. *Student´s t-test for independent samples or Pearson´s X^2 test. BMI: Body mass index. y= years; kg=kilograms; m^2= square meter.

Table 2. Perinatal outcome of the study groups.

	IUGR (N = 117)	AGA (N = 73)	P*
GA at birth (w)	38.7 ± 1.1	40.0 ± 1.1	**<0.01**
Birth weight (g)	2426 ± 301	3429 ± 310	**<0.01**
Birth centile	2.69 ± 2.77	51.8 ± 24,35	**<0.01**
Male gender	57.8%	54.8%	0.69
Labor induction	77.2%	23.5%	**<0.01**
Emergency cesarean section	27.2%	5.5%	**<0.01**
Neonatal acidosis†	10.6%	6.6%	0.39
Apgar score <7 at 5 minutes	2.6%	0%	0.07
NICU stay length (d)	0.2	0	**0.04**

Results are expressed as mean ± SD or percentage as appropriate. *Student´s t-test for independent samples or Pearson´s X^2 test. GA: gestational age. Neonatal acidosis†: umbilical artery pH<7.15 and base excess > 12 mEq/L. NICU: Neonatal Intensive care unit. w=weeks; g=grams; d=days.

Table 3. CC measurements in the study groups.

	IUGR (N = 117)	AGA (N = 73)	P*
Lenght/CI	0.49 ± 0.05	0.51 ± 0.04	0.22
Anterior thickness / CI	0.027 ± 0.008	0.029 ± 0.009	0.25
Middle thickness / CI	0.018 ± 0.004	0.019 ± 0.005	0.35
Posterior thickness / CI	0.037 ± 0.011	0.040 ± 0.009	0.20
Total area / CI	1.40 ± 0.26	1.66 ± 0.31	**<0.01**
Rostrum area / CI	0.094 ± 0.057	0.117 ± 0.068	0.20
Genu area / CI	0.160 ± 0.067	0.21 ± 0.084	**<0.01**
Rostral body area / CI	0.315 ± 0.06	0.382 ± 0.076	**<0.01**
Anterior midbody area / CI	0.172 ± 0.038	0.201 ± 0.042	**0.02**
Posterior midbody area / CI	0.164 ± 0.036	0.189 ± 0.044	**0.04**
Isthmus area / CI	0.14 ± 0.031	0.169 ± 0.04	**<0.01**
Splenium area / CI	0.358 ± 0.09	0.396 ± 0.109	**0.03**

Results are expressed as mean ± SD.* GLM adjusted for gender, maternal smoking and BMI. CI: cephalic index.

Table 4. CC measurements and its association with neurobehavioral outcome in late-onset IUGR.

CC measurement	Coefficient value	P*
Length	-0.14	0.52
Anterior thickness	-0.19	0.84
Middle thickness	-3.49	0.05
Posterior thickness	0.34	0.65
Total area	-0.48	**0.03**
Rostrum area	-0.59	**0.02**
Genu area	0.54	**0.03**
Rostral body area	-0.56	**0.02**
Anterior midbody area	-0.77	**0.04**
Posterior midbody area	-0.01	0.99
Isthmus area	-0.70	0.16
Splenium area	-0.52	**0.03**

*Ordinal regression adjusted for gender, GA at MRI, GA at NBAS, maternal smoking and BMI, where the NBAS test's clusters <5th centile were considered as the dependent variable and CC measurements as the independent variables. A negative coefficient value indicated that at the presence of smaller CC measurements the amount of NBAS test's clusters <5th centile increased.

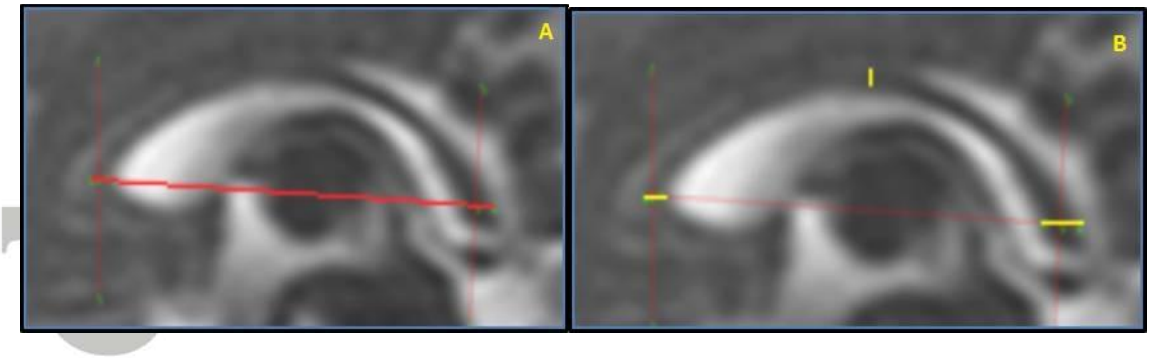

Legend: (A) Thicker red line indicates the CC length measured from its outer to outer limits. (B) Yellow lines indicate the genu, middle and splenium thicknesses from left to right. Illustrations are performed in a T2-weighted MR image of 37 weeks of gestational age fetus.

Figure 1. Illustration of CC linear measurements assessed by the Analyze software.

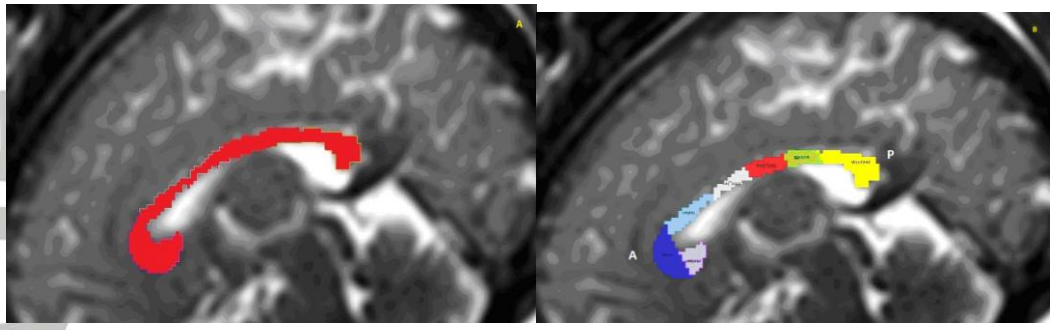

Legend: (A) Total CC area (B) and areas from CC subdivision corresponding to the rostrum (purple), genu (blue), rostral body (light blue), anterior midbody (white), posterior midbody (red), isthmus (green) and splenium (yellow). Illustration is performed in a T2-weighted MR image of 37 weeks of gestational age fetus.

Figure 2. Illustration of CC areas assessed by semi-automatic delineation.

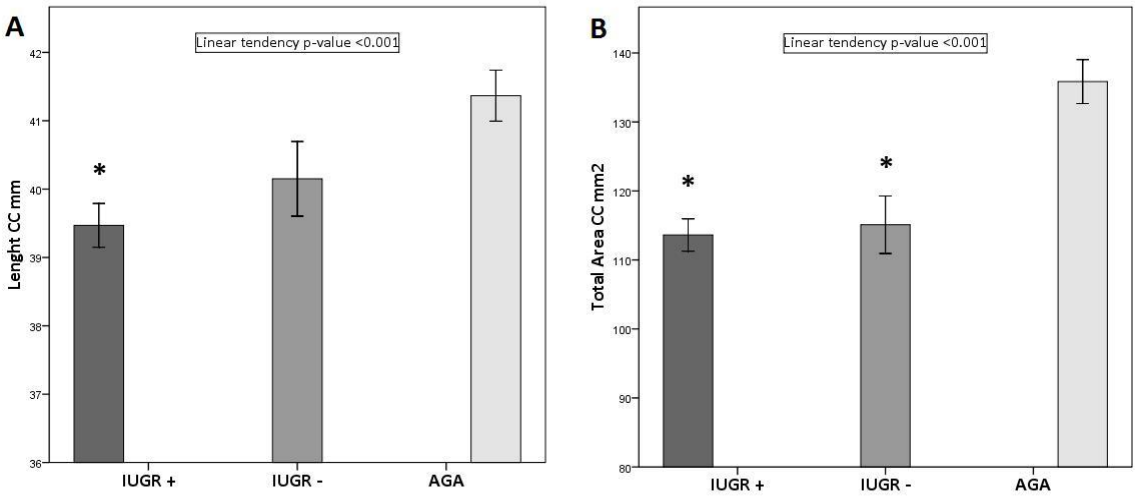

Legend: Linear tendency by polynomial contrast analysis showing differences between IUGR+ (IUGR with signs of clinical severity defined as CPR <5th centile, UtA Doppler before birth >95th centile, or a birthweight <3rd centile), IUGR- (IUGR without clinical severity sings) and AGA. Bars depict the mean ± SD. *p<0.05 compared with AGA.

Figure 3. Differences among IUGR fetuses according to clinical severity criteria in CC length and total area.

5.4 STUDY 4

Neurosonographic assessment of the corpus callosum as a potential biomarker of abnormal neurodevelopment in late-onset fetal growth restriction

Egaña-Ugrinovic G, Savchev S, Bazán-Arcos C, Puerto B, Gratacos E, Sanz-Cortés M.

Fetal Diagnosis and Therap., 2014

State: Submitted

Impact factor: 1.902

Quartile: 2nd

NEUROSONOGRAPHIC ASSESSMENT OF THE CORPUS CALLOSUM AS IMAGING BIOMARKER OF ABNORMAL NEURODEVELOPMENT IN LATE-ONSET FETAL GROWTH RESTRICTION

Gabriela Egaña-Ugrinovic, MD; Stefan Savchev, MD; Carolina Bazán-Arcos, MD; Bienvenido Puerto, MD; Eduard Gratacós, MD, Magdalena Sanz-Cortés, MD.

Fetal i+D Fetal Medicine Research Center, BCNatal - Barcelona Center for Maternal-Fetal and Neonatal Medicine (Hospital Clínic and Hospital Sant Joan de Deu), Institut d'Investigacions Biomediques August Pi i Sunyer (IDIBAPS), Centre for Biomedical Research on Rare Diseases (CIBER-ER), and University of Barcelona, Barcelona, Spain.

Corresponding author:

Eduard Gratacós

BCNatal - Barcelona Center for Maternal-Fetal and Neonatal Medicine, Hospital Clínic and Hospital Sant Joan de Deu

Sabino de Arana, 1

08028 Barcelona, Spain

Telephone: +34 93 227 9333

Fax: +34 93 227 5612

Email: gratacos@clinic.ub.es

Abstract word count: 217 **Text word count:** 2675

Short version of the title:

Neurosonographic assessment of the corpus callosum in late IUGR

Disclosure

None of the authors have a conflict of interest

Funding

This work was supported by grants from The Cerebra Foundation for the Brain Injured Child (Carmarthen, Wales, UK), Obra Social “la Caixa” (Barcelona, Spain), and Fundación Dexeus (Barcelona, Spain). G.E.U was supported by CONICYT (PFCHA/<Doctorado al Extranjero 4ª Convocatoria><72120071>), Chile. M.S.C. was supported by Instituto de Salud Carlos III Rio Hortega (CM10/00222), Spain.

No reprints will be available.

ABSTRACT

Objective

To explore corpus callosum (CC) developmental differences by ultrasound in late-onset small fetuses compared with adequate for gestational age (AGA) controls.

Study design

94 small (estimated fetal weight <10th centile) and 71 AGA fetuses were included. Small fetuses were further subdivided into fetal growth restriction (IUGR, n=64) and small for gestational age (SGA, n=30) based on poor perinatal outcome factors, i.e. birth weight <3rd centile and/or abnormal cerebroplacental ratio and/or uterine artery Doppler. The entire cohort was scanned to assess CC by transvaginal neurosonography obtaining axial, coronal and midsagittal images. CC length, thickness, total area and the areas after a subdivision in 7 portions were evaluated by semiautomatic software. Furthermore, weekly average growth of the CC in each study group was calculated and compared.

Results

Small fetuses showed significantly shorter (small fetuses: 0.49 vs. AGA: 0.52; p<0.01) and smaller CC (1.83 vs. 2.03; p <0.01) with smaller splenium (0.47 vs. 0.55; p<0.01) compared to controls. CC growth rate was also reduced when compared to controls. Changes were more prominent in small fetuses with abnormal cerebroplacental Doppler suggesting fetal growth restriction.

Conclusions

Neurosonographic assessment of CC showed significantly altered callosal development, suggesting in-utero brain reorganization in small fetuses. This data support the potential value of CC assessment by US to monitor brain development in fetuses at risk.

Key words: corpus callosum, neurosonography, SGA, IUGR.

INTRODUCTION

Intrauterine growth restriction (IUGR) is a frequent condition affecting 6-10% of all pregnancies and is a major contributor of perinatal and long term morbidity [1-3]. Currently, the clinical surrogate marker for fetal growth restriction is fetal smallness, as defined by an ultrasound estimated fetal weight below the 10^{th} centile [4]. The majority of small fetuses are identified in late gestation [5]. At this pregnancy stage, the distinction between IUGR associated with placental insufficiency from other forms of fetal smallness, normally termed small for gestational age (SGA), can be challenging [6]. Abnormal neurodevelopment is among the most relevant consequences associated with fetal smallness [7-9]. Several studies have described brain reorganizational changes and neurodevelopment deficits [10-12]. Defining phenotype(s) of brain reorganization under IUGR could be an opportunity to develop image biomarkers for the identification of small fetuses at risk and the various clinical forms under the common diagnosis of fetal smallness.

The corpus callosum (CC) is an interesting imaging biomarker candidate to assess fetal neurodevelopment [13-15]. CC is the major commissure connecting both cerebral hemispheres, and it represents an important white matter structure. Previous reports on preterm infants, children diagnosed with autism spectrum disorders, attention-deficit hyperactivity and language disorders showed alterations in CC microstructure [13,14]. Furthermore, we have previously shown that CC development assessed by MRI is altered in term SGA fetuses and is associated with neonatal neurobehavior [16]. CC can be reliably assessed by fetal neurosonography (NSG), which represents a cheaper and more readily available imaging technique than MRI [17]. In expert hands and using multiplanar approaches, brain ultrasound may provide an excellent visualization of the CC after 18

weeks [18,19]. However, the potential value of fetal NSG to assess CC morphometry as a biomarker of brain development in fetal smallness has not been explored.

The objective of this study was to test whether NSG can detect CC morphometric and growth differences in late-onset small fetuses when compared with controls. In addition, we evaluated whether the pattern of CC changes is different when small fetuses are sub-classified as IUGR or SGA according to known poor prognosis factors [6].

MATERIAL AND METHODS

Subjects

This study is part of a larger prospective research program on IUGR involving fetal, neonatal and long term postnatal follow-up. The specific protocol of this study was approved by the institutional Ethics Committee (Institutional Review Board 2008/4422) and all participants gave written informed consent. A total of 175 singleton fetuses were included in our cohort, classified in 98 late-onset small fetuses and 77 AGA fetuses. The sample size was not determined a priori by a statistical calculation relating to estimation accuracy, since there is no data about CC assessment by NSG in small fetuses compared to controls. Therefore the study design contemplated a recruitment of 70-90 fetuses in each study group. Pregnancies were dated according to the first trimester crown-rump length measurement [20]. Late-onset small fetuses were defined by an estimated and postnatally confirmed fetal weight $<10^{th}$ centile, with diagnosis established later than 32 weeks' gestation [4-6,21]. AGA fetuses were recruited among normal pregnancies attending third trimester routine pregnancy care and delivering at term at our institution. Patients were offered an extra ultrasound which was scheduled between 34 and 36 weeks. AGA was defined as an estimated and postnatally confirmed fetal weight $\geq 10^{th}$ centile [4], according to local growth charts [21]. Exclusion criteria included congenital malformations, chromosomal abnormalities, perinatal infections, chronic maternal pathology and non-cephalic presentations.

Clinical and Ultrasound data

Small fetuses were followed-up in our fetal growth restriction unit from diagnosis until delivery. Doppler ultrasound scans were performed using a General Electric Voluson E8, 6-

2MHz curved-array transducer (GE Medical Systems, Zipf, Austria) obtaining fetal umbilical artery and middle cerebral artery pulsatility index (PI) [22]. Both measurements were used for the calculation of the cerebroplacental ratio (CPR) as CPR= MCA PI/UA PI. Abnormal CPR was defined as a value <5th centile for gestational age according to previously published reference values [23]. Uterine arteries (UtA) PI were measured transabdominally and mean value was considered abnormal when >95th centile [24]. All fetuses in this study had at least one scan performed within one week before delivery. Maternal, perinatal and neonatal data were prospectively recorded in all study patients.

To explore if there was an association between CC measurements and the severity of growth restriction, small fetuses were subdivided into (1) Late-onset IUGR if predictors of a poorer perinatal outcome were present such as birth weight <3rd centile and/or abnormal CPR and/or abnormal UtA [6], and (2) SGA when none of those factors were present.

Neurosonography

A detailed NSG was performed in both cases and controls at least once in the NSG Department by two expert examiners (GE and SS) using a two dimensional transabdominal and transvaginal approach. The same equipment was used for all scans (Voluson 730 Expert scanner, equipped with a 5-9 MHz transvaginal transducer; GE Medical Systems, Zipf, Austria). All NSG were performed during the third trimester of pregnancy. In small fetuses, NSG exam was performed between 1 or 2 weeks after the initial diagnosis of an estimated fetal weight <10th centile. AGA fetuses were recruited from our general population matching the gestational age at NSG of small fetuses. Fetal brain exams were performed and standardized based on the ISUOG guidelines for fetal brain assessment [25,26]. CC was identified in the midsagittal plane as a slightly curved hypoechoic structure [27]. The slice

chosen for CC assessment had to accomplish strict quality criteria defined as the identification of the cavum septi pellucidi, thalamus, midbrain, cerebellar vermis and cisterna magna [27] (Figure 1). Furthermore, a clear visualization of the body, splenium, genu, and rostrum of the CC had to be present. Neurosonographic images were obtained prospectively and later analyzed offline.

Image processing

Imaging post-processing and measurements were performed using the semiautomatic Analyze 9.0 software (Biomedical Imaging Resource, Mayo Clinic; Kansas, USA) by two experienced examiners blinded to group membership.

Linear measurements

a. CC length was measured from the most anterior part of the genu to the most posterior part of the splenium tracing a straight rostrocaudal line between the two points, known as the outer-to-outer CC length [28] (Figure 1). This measurement was obtained three times and the mean value was used for further analysis.

b. CC thickness was measured in its anterior, middle and posterior portions corresponding to the genu, body and splenium thickness respectively [29,30]. The thickness of the genu and splenium was measured at the same level where the line for CC length was traced. CC body thickness was measured equidistantly from the anterior and posterior measurements (Figure 1). These measurements were obtained three times and the mean value was used for further analysis.

Area measurements

a. Total CC area was delineated through cursor-guided free-hand traces limited superiorly by the hyperechoic sulcus of the CC and the cingulate gyrus and inferiorly, by the cavum septi pellucidi and cavum vergae [27] (Figure 2).

b. CC was subdivided in seven areas described by Witelson *et al* [30] (Figure 2) in order to measure, from anterior to posterior, the rostrum, genu, rostral body, anterior midbody, posterior midbody, isthmus and splenium areas (Figure 2).

Normalization by cephalic Index

In order to correct for a smaller head size influencing the size of brain structures in small fetuses, cephalic index (CI) was used as a normalization factor. CI was calculated using biparietal (BPD) and occipitofrontal (OFD) diameters by applying a previously reported formula: CI= BPD/OFD*100 [31]. All CC measures in this study are reported and compared statistically as corrected values, defined as the following ratio: CC measurement/CI.

CC growth assessment

In order to assess CC growth rate differences between small fetuses and controls, we used a previously reported methodology [32] where the average growth rate per week was calculated by dividing the differences in CC length/CI, CC total area/CI and splenium/CI by the number of weeks along the study.

Interobserver reliability

Reliability between measurements from two observers blinded to group membership was assessed by the intraclass correlation coefficient (ICC) and their 95% confidence intervals (CI) in 20 fetuses. A two-way mixed model was chosen for agreement analysis. An ICC of 1

indicates perfect reproducibility between measurements, while a value of 0 is interpreted as reproducibility that is no better or worse than that expected by chance. We considered an ICC value between 0.5 and 0.7 as adequate and more than 0.7 as excellent agreement [33].

Statistical analysis of clinical and CC data

Student´s t test for independent samples and Pearson´s X^2 tests were used to compare quantitative and qualitative data respectively. Multivariate analyses of covariance (MANCOVA) adjusted by gestational age (GA) at NSG, maternal smoking and maternal body mass index were conducted to assess CC differences between small fetuses and controls. Student´s t test was preformed to evaluate growth velocity differences between the study groups. A polynomial contrast using MANCOVA was used in order to evaluate CC differences across clinical severity subgroups adjusting for the same potential confounding variables above mentioned. A p value <0.05 was set as significant. The software package SPSS 17.0 (SPSS, Chicago, IL, USA) was used for the statistical analyses.

RESULTS

Clinical characteristics in the study population

Maternal characteristics did not differ between cases and controls (Table 1). No structural abnormalities were found in the study groups. As expected, small fetuses were delivered earlier with higher rates of labor induction, emergency cesarean section and longer stay in the neonatal intensive unit care (Table 2). Five percent of the images had to be discarded because of insufficient quality to perform image post-processing, leaving a total of 165 fetuses scanned, classified in 94 small fetuses and 71 controls.

Corpus callosum morphometry

Overall, small fetuses showed a significantly reduced CC length, and total CC area. Likewise, all the subdivisions of the CC had smaller areas, with significant differences in the rostral body, anterior midbody and the splenium (Table 3). After adjusting for potential confounding covariates, CC length (p=0.03), total CC area (p=0.03) and splenium (p<0.01) remained significantly different between the two groups.

CC morphometric comparison was then performed dividing small fetuses into IUGR and SGA, as defined above. There was a significant linear trend across the study groups for shorter CC length (p=0.01), smaller total CC area (p=0.04) and smaller spleniums (p=0.02) (Figure 3). However, as observed in Figure 3, SGA fetuses had in general smaller corrected values as compared with controls.

Corpus callosum growth comparison between small fetuses and AGA

Average total CC area growth was lower in small fetuses compared to AGA (0.025/week vs. 0.035/week; *p*=0.04). Splenium growth (0.010/week vs. 0.027/week; *p*=0.02) was also lower in small fetuses.

Interobserver reliability

Overall biometric and area measurements showed acceptable to good interobserver reliability. Regarding linear measurements analysis, the ICC for length was 0.9 (95% CI 0.85 to 0.99); genu thickness 0.58 (95% CI -0.47 to 0.83); middle thickness 0.64 (95% CI 0.08 to 0.86) and splenium thickness 0.40 (95% CI -0.33 to 0.76). The ICC for total area was 0.86 (95% CI 0.40 to 0.95) and for CC area subdivisions was for rostrum 0.69 (95% CI -0.20 to 0.89); genu 0.89 (95% CI 0.73 to 0.96); rostral body 0.89 (95% CI 0.72 to 0.96); anterior midbody 0.60 (95% CI -0.22 to 0.84); posterior midbody 0.77 (95% CI 0.44 to 0.91); isthmus 0.65 (95% CI 0.14 to 0.86) and for splenium 0.68 (95% CI -0.16 to 0.90).

COMMENT

We showed how small fetuses present differences in CC linear and area measurements and had lower callosal growth rate assessed by NSG. These findings support the notion that brain reorganization may affect white matter development in growth restricted fetuses [34-36], and also that NSG can be a valid tool to detect such differences.

Although several studies have highlighted how late-onset small fetuses present significant microstructural and metabolic brain differences when compared with their AGA counterparts [12,34,37,38], there is no experience assessing this structure in small fetuses using NSG. Previous reports have highlighted the importance of CC growth in different conditions associated to neurodevelopmental impairments such as in preterm-born adolescents that show specific microstructural callosal abnormalities [14] that correlated with neurodevelopmental impairments [15]. Similarly, children with developmental language disorders and attention-deficit hyperactive disorders present smaller splenium areas [13]. Results from early-onset IUGR fetuses show that there is a reduced growth rate of this structure assessed by ultrasound, suggesting an altered white matter microstructure maturation [36]. Supporting this knowledge and in line with the results from this study, late-onset small fetuses showed global and specific callosal differences that were revealed by brain MRI [16]. Interestingly and coinciding with our results, posterior portions of the CC were particularly affected.

White matter maturation occurs mainly during the third trimester and persists during the first years of life; these circumstances make its development particularly vulnerable to adverse in-utero conditions and hypoxia [35]. Reports from rats show that exposure to hypoxia resulted in smaller CC [39], which was related to myelination deficits. Furthermore,

postmortem studies from neonates that suffered perinatal asphyxia showed a reduced number of callosal fibers and immature oligodendrocytes [40,41]. During gestation, thickening of CC occurs in response to axonal growth and pruning [13] following an anterior-to-posterior directionality and reaching uniform measurements at term [42]. CC growth in late pregnancy is predominantly at the expense of an area, particularly in the posterior aspect, rather than an increase in length. [13] Interestingly, our findings demonstrated more marked changes in posterior CC areas such as the splenium.

As in previous studies, we classified small fetuses according to the presence or absence of signs of adverse perinatal outcome [6]. Although, late-onset IUGR fetuses with the presence of severity signs showed more accentuated shorter and smaller CC areas, the SGA group had a trend for CC differences as compared to controls, which is line with results from previous studies [3,37,43]. Even if this study does not contribute to clarify the nature of SGA versus IUGR, our results suggest that fetuses currently defined as SGA might suffer forms of growth restriction that remain to be better characterized. Further pathophysiological studies are required to gain insight in this matter and clarify the variety of mechanisms involved in fetal smallness.

From a clinical perspective, given the high prevalence of late-onset small fetuses and its impact on neurodevelopment [1,2,5,7], early detection of those small fetuses at higher risk for a suboptimal neurodevelopment is a critical goal in order to trigger strategies such as delivery planning, breast-feeding promotion and early educational interventions, which have shown to improve the neurodevelopmental outcome in similar populations at risk [44,45]. Ultrasonographic assessment of the CC can be obtained with low inter-observer variation in experienced hands [18,19]. Indeed, the midsagittal plane of the fetal brain is an easily available view in standard NSG. Evaluation of CC can constitute a useful imaging

biomarker to assess brain development in IUGR and other conditions associated with abnormal neurodevelopment.

We acknowledge some limitations in this study. Although our sample size is similar to previous studies on the same field [34,36], larger studies are required to clarify the clinical heterogeneity found in late-onset small fetuses. Also, we acknowledge that postnatal neurodevelopmental outcome was not evaluated, which prevented us to assess how callosal differences may correlate with postnatal performance. Nevertheless previous neuroimaging studies have demonstrated how CC changes are associated to postnatal neurobehavior [14,37,46]. Future studies confirming such association when CC is measured by means of NSG should be conducted. One of the main strengths of this study is that it was performed on a well-defined cohort characterized prenatally. Also, well-defined anatomical landmarks were used to delineate the CC. Furthermore, the study evaluated relative changes, since all CC measurements were corrected by the CI to avoid a false influence of fetal head size differences.

In summary this study demonstrates that late-onset small fetuses present significant differences in their CC development and morphology. These findings support that NSG can be considered a valid tool to detect subtle brain differences in fetuses exposed to late-onset growth restriction. Further research involving long-term follow-up is warranted to evaluate the potential use of the CC as an imaging biomarker in the prediction of abnormal neurodevelopment in fetuses at risk.

TABLES

Table 1. Maternal characteristics of the study groups.

	Small fetuses (N = 94)	AGA (N = 71)	*P**
Maternal age (y)	31.4 ± 5.9	32.9 ± 4.0	0.08
Maternal smoking	19.6%	10.0%	0.09
Maternal BMI (kg/m2)	21.5 ± 3.2	22.5 ± 3.4	0.07
Primiparity	70.7%	70.0%	0.93
Caucasian ethnicity	67.4%	67.6%	0.34
GA at NSG (w)	35.7 ± 1.6	35.9 ± 1.3	0.17

Results are expressed as mean ± SD or percentage as appropriate. *Student´s t-test for independent samples or Pearson´s X^2 test. BMI: Body mass index. GA: gestational age. NSG: neurosonography. y= years; kg=kilograms; m^2= square meter; w=weeks.

Table 2. Perinatal outcome of the study groups.

	Small fetuses (N = 94)	AGA (N = 71)	*P**
GA at birth (w)	38.0 ± 2.6	40.0 ± 1.2	**<0.01**
Birth weight (g)	2292 ± 547	3402 ± 380	**<0.01**
Birth centile	3.14	49.54	**<0.01**
Male gender	58.7%	55.1%	0.65
Labor induction	54.9 %	21.7%	**<0.01**
Emergency cesarean section	20.7%	8.7%	**0.04**
Neonatal acidosis†	10.6%	6.6%	0.39
Apgar score <7 at 5 minutes	0%	0%	0
NICU stay length (d)	2.1	0	**0.02**

Results are expressed as mean ± SD or percentage as appropriate. *Student´s t-test for independent samples or Pearson´s X^2 test. GA: gestational age. Neonatal acidosis†: umbilical artery pH<7.15 and base excess > 12 mEq/L. NICU: Neonatal Intensive care unit. w=weeks; g=grams; d=days.

Table 3. CC measurements in the study groups.

	Small fetuses (N = 94)	AGA (N = 71)	*P**
Lenght/CI	0.493 ± 0.042	0.516 ± 0.052	**<0.01**
Anterior thickness / CI	0.061 ± 0.013	0.064 ± 0.014	0.25
Middle thickness / CI	0.041 ± 0.007	0.043 ± 0.007	0.06
Posterior thickness / CI	0.066 ± 0.016	0.068 ± 0.015	0.42
Total area / CI	1.828 ± 0.432	2.034 ± 0.441	**<0.01**
Rostrum area / CI	0.135 ± 0.054	0.186 ± 0.250	0.06
Genu area / CI	0.283 ± 0.119	0.314 ± 0.110	0.09
Rostral body area / CI	0.341 ± 0.076	0.367 ± 0.073	**0.03**
Anterior midbody area / CI	0.224 ± 0.056	0.243 ± 0.051	**0.03**
Posterior midbody area / CI	0.219 ± 0.06	0.235 ± 0.046	0.05
Isthmus area / CI	0.206 ± 0.074	0.215 ± 0.055	0.40
Splenium area / CI	0.473 ± 0.125	0.554 ± 0.185	**<0.01**

*Student's t test for independent samples. Results are expressed as mean ± SD. CI: cephalic index.

FIGURES

Figure 1. Midsagittal view of the CC showing linear measurements.

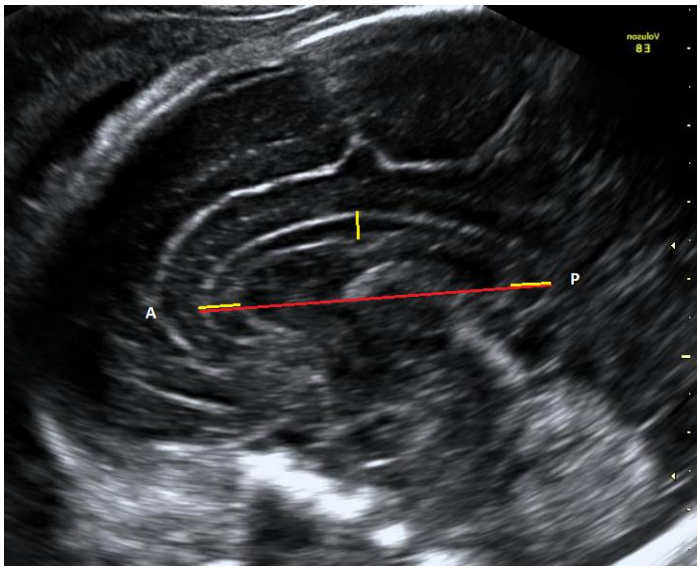

CC length measurement is shown with a red line. Yellow lines indicate the genu, middle and splenium thicknesses of the corpus callosum from anterior (A) to posterior (P). Illustration is performed in a 37 weeks of gestational age fetus.

Figure 2. Midsagittal view of the CC showing area measurements.
A)

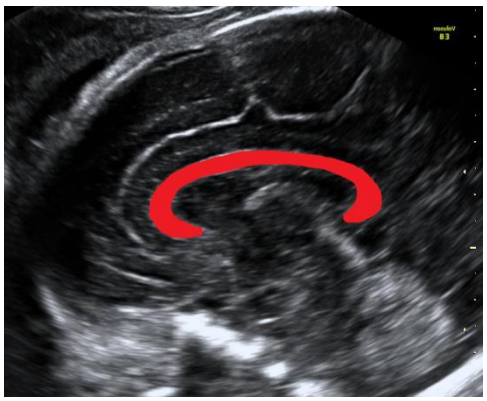

B)

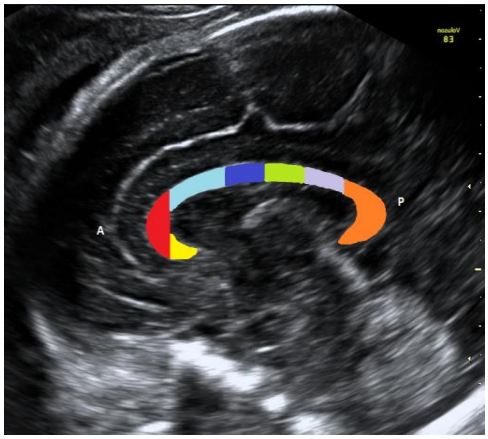

A) Total CC area assessment and **B)** areas from CC subdivisions corresponding from anterior (A) to posterior (P) to: rostrum, genu, rostral body, anterior midbody, posterior midbody, isthmus and splenium. Illustration is performed from a NSG scan in 37 weeks of gestational age fetus.

Figure 3. Differences in corrected CC biometries among AGA and small fetuses, divided as IUGR and SGA.

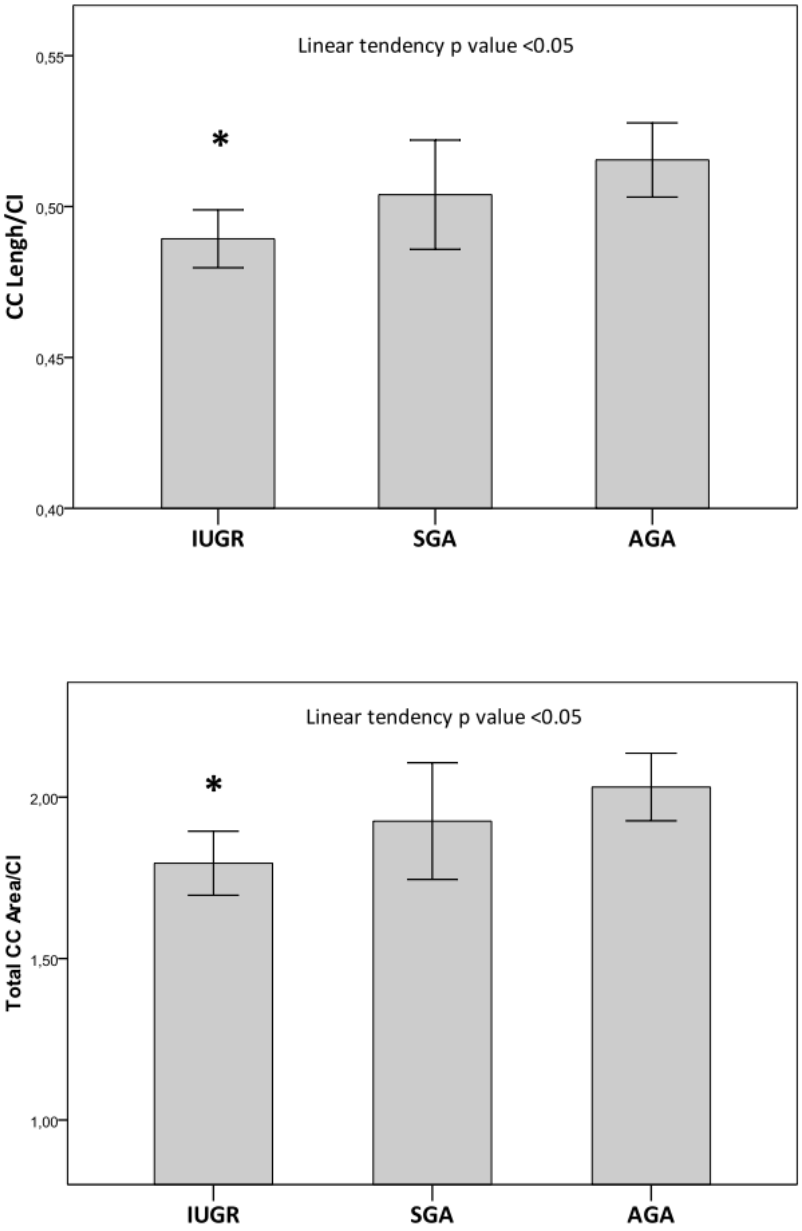

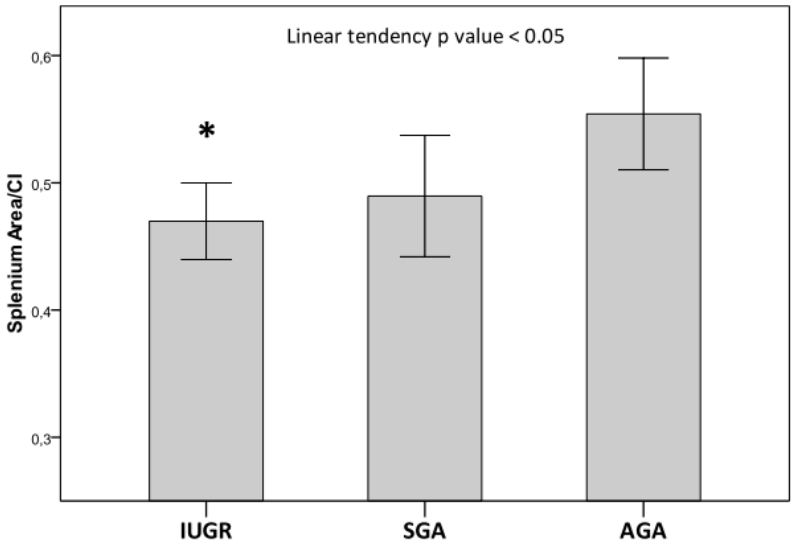

Linear tendency by polynomial contrast analysis showing differences between late-onset IUGR fetuses subclassified into IUGR and SGA, compared to adequate for gestational age (AGA) pairs. IUGR fetuses were defined as those with birth weight <3rd centile and/or CPR <5th centile and/or UtA Doppler >95th centile; and SGA were those without clinical severity signs. *p<0.05 compared with AGA. Results were adjusted by gestational age at NSG, maternal body mass index and smoking.

REFERENCES

1 Gardosi J: Clinical strategies for improving the detection of fetal growth restriction. Clin Perinatol;38:21-31, v.

2 Leitner Y, Fattal-Valevski A, Geva R, Eshel R, Toledano-Alhadef H, Rotstein M, Bassan H, Radianu B, Bitchonsky O, Jaffa AJ, Harel S: Neurodevelopmental outcome of children with intrauterine growth retardation: A longitudinal, 10-year prospective study. J Child Neurol 2007;22:580-587.

3 Savchev S, Figueras F, Cruz-Martinez R, Illa M, Botet F, Gratacos E: Estimated weight centile as a predictor of perinatal outcome in small-for-gestational-age pregnancies with normal fetal and maternal doppler indices. Ultrasound Obstet Gynecol;39:299-303.

4 Chauhan SP, Gupta LM, Hendrix NW, Berghella V: Intrauterine growth restriction: Comparison of american college of obstetricians and gynecologists practice bulletin with other national guidelines. Am J Obstet Gynecol 2009;200:409 e401-406.

5 Savchev S, Figueras F, Sanz-Cortes M, Cruz-Lemini M, Triunfo S, Botet F, Gratacos E: Evaluation of an optimal gestational age cut-off for the definition of early- and late-onset fetal growth restriction. Fetal Diagn Ther

6 Figueras F, Gratacos E: Update on the diagnosis and classification of fetal growth restriction and proposal of a stage-based management protocol. Fetal Diagn Ther

7 Savchev S, Sanz-Cortes M, Cruz-Martinez R, Arranz A, Botet F, Gratacos E, Figueras F: Neurodevelopmental outcome of full-term small-for-gestational-age infants with normal placental function. Ultrasound Obstet Gynecol

8 Geva R, Eshel R, Leitner Y, Valevski AF, Harel S: Neuropsychological outcome of children with intrauterine growth restriction: A 9-year prospective study. Pediatrics 2006;118:91-100.

9 Walker DM, Marlow N: Neurocognitive outcome following fetal growth restriction. Arch Dis Child Fetal Neonatal Ed 2008;93:F322-325.

10 Padilla N, Falcon C, Sanz-Cortes M, Figueras F, Bargallo N, Crispi F, Eixarch E, Arranz A, Botet F, Gratacos E: Differential effects of intrauterine growth restriction on brain structure and development in preterm infants: A magnetic resonance imaging study. Brain Res;1382:98-108.

11 Dubois J, Benders M, Borradori-Tolsa C, Cachia A, Lazeyras F, Ha-Vinh Leuchter R, Sizonenko SV, Warfield SK, Mangin JF, Huppi PS: Primary cortical folding in the human newborn: An early marker of later functional development. Brain 2008;131:2028-2041.

12 Batalle D, Eixarch E, Figueras F, Munoz-Moreno E, Bargallo N, Illa M, Acosta-Rojas R, Amat-Roldan I, Gratacos E: Altered small-world topology of structural brain networks in infants with intrauterine growth restriction and its association with later neurodevelopmental outcome. Neuroimage;60:1352-1366.

13 Paul LK: Developmental malformation of the corpus callosum: A review of typical callosal development and examples of developmental disorders with callosal involvement. J Neurodev Disord;3:3-27.

14 Counsell SJ, Edwards AD, Chew AT, Anjari M, Dyet LE, Srinivasan L, Boardman JP, Allsop JM, Hajnal JV, Rutherford MA, Cowan FM: Specific relations between neurodevelopmental abilities and white matter microstructure in children born preterm. Brain 2008;131:3201-3208.

15 Nosarti C, Rushe TM, Woodruff PW, Stewart AL, Rifkin L, Murray RM: Corpus callosum size and very preterm birth: Relationship to neuropsychological outcome. Brain

2004;127:2080-2089.
16 Egana-Ugrinovic G, Sanz-Cortes M, Couve-Perez C, Figueras F, Gratacos E: Corpus callosum differences assessed by fetal mri in late-onset intrauterine growth restriction and its association with neurobehavior. Prenat Diagn
17 Hagmann CF, Robertson NJ, Leung WC, Chong KW, Chitty LS: Foetal brain imaging: Ultrasound or mri. A comparison between magnetic resonance imaging and a dedicated multidisciplinary neurosonographic opinion. Acta Paediatr 2008;97:414-419.
18 Miguelote RF, Vides B, Santos RF, Matias A, Sousa N: Feasibility and reproducibility of transvaginal, transabdominal, and 3d volume reconstruction sonography for measurement of the corpus callosum at different gestational ages. Fetal Diagn Ther;31:19-25.
19 Malinger G, Zakut H: Transvaginal visualization of the corpus callosum. Am J Obstet Gynecol 1994;171:1677.
20 Robinson HP, Fleming JE: A critical evaluation of sonar "Crown-rump length" Measurements. Br J Obstet Gynaecol 1975;82:702-710.
21 Figueras F, Meler E, Iraola A, Eixarch E, Coll O, Figueras J, Francis A, Gratacos E, Gardosi J: Customized birthweight standards for a spanish population. Eur J Obstet Gynecol Reprod Biol 2008;136:20-24.
22 Arduini D, Rizzo G: Normal values of pulsatility index from fetal vessels: A cross-sectional study on 1556 healthy fetuses. J Perinat Med 1990;18:165-172.
23 Baschat AA, Gembruch U: The cerebroplacental doppler ratio revisited. Ultrasound Obstet Gynecol 2003;21:124-127.
24 Gomez O, Figueras F, Fernandez S, Bennasar M, Martinez JM, Puerto B, Gratacos E: Reference ranges for uterine artery mean pulsatility index at 11-41 weeks of gestation. Ultrasound Obstet Gynecol 2008;32:128-132.
25 Sonographic examination of the fetal central nervous system: Guidelines for performing the 'basic examination' and the 'fetal neurosonogram'. Ultrasound Obstet Gynecol 2007;29:109-116.
26 Youssef A, Ghi T, Pilu G: How to image the fetal corpus callosum. Ultrasound Obstet Gynecol;42:718-720.
27 Pashaj S, Merz E, Wellek S: Biometry of the fetal corpus callosum by three-dimensional ultrasound. Ultrasound Obstet Gynecol;42:691-698.
28 Harreld JH, Bhore R, Chason DP, Twickler DM: Corpus callosum length by gestational age as evaluated by fetal mr imaging. AJNR Am J Neuroradiol;32:490-494.
29 Lerman-Sagie T, Ben-Sira L, Achiron R, Schreiber L, Hermann G, Lev D, Kidron D, Malinger G: Thick fetal corpus callosum: An ominous sign? Ultrasound Obstet Gynecol 2009;34:55-61.
30 Witelson SF: Hand and sex differences in the isthmus and genu of the human corpus callosum. A postmortem morphological study. Brain 1989;112 (Pt 3):799-835.
31 Lim KI, Delisle MF, Austin SJ, Wilson RD: Cephalic index is not a useful sonographic marker for trisomy 21 and trisomy 18. Fetal Diagn Ther 2004;19:491-495.
32 Anderson NG, Laurent I, Cook N, Woodward L, Inder TE: Growth rate of corpus callosum in very premature infants. AJNR Am J Neuroradiol 2005;26:2685-2690.
33 Del Rio M, Martinez JM, Figueras F, Bennasar M, Palacio M, Gomez O, Coll O, Puerto B, Cararach V: Doppler assessment of fetal aortic isthmus blood flow in two different sonographic planes during the second half of gestation. Ultrasound Obstet Gynecol 2005;26:170-174.
34 Sanz-Cortes M, Figueras F, Bonet-Carne E, Padilla N, Tenorio V, Bargallo N, Amat-

Roldan I, Gratacos E: Fetal brain mri texture analysis identifies different microstructural patterns in adequate and small for gestational age fetuses at term. Fetal Diagn Ther;33:122-129.
35 Dubois J, Dehaene-Lambertz G, Kulikova S, Poupon C, Huppi PS, Hertz-Pannier L: The early development of brain white matter: A review of imaging studies in fetuses, newborns and infants. Neuroscience
36 Goldstein I, Tamir A, Reece AE, Weiner Z: Corpus callosum growth in normal and growth-restricted fetuses. Prenat Diagn;31:1115-1119.
37 Egana-Ugrinovic G, Sanz-Cortes M, Figueras F, Bargallo N, Gratacos E: Differences in cortical development assessed by fetal mri in late-onset intrauterine growth restriction. Am J Obstet Gynecol
38 Sanz-Cortes M, Figueras F, Bargallo N, Padilla N, Amat-Roldan I, Gratacos E: Abnormal brain microstructure and metabolism in small-for-gestational-age term fetuses with normal umbilical artery doppler. Ultrasound Obstet Gynecol;36:159-165.
39 Langmeier M, Pokorny J, Mares J, Trojan S: Changes of the neuronal structure produced by prolonged hypobaric hypoxia in infant rats. Biomed Biochim Acta 1989;48:S204-207.
40 Back SA, Luo NL, Borenstein NS, Levine JM, Volpe JJ, Kinney HC: Late oligodendrocyte progenitors coincide with the developmental window of vulnerability for human perinatal white matter injury. J Neurosci 2001;21:1302-1312.
41 Vasung L, Jovanov-Milosevic N, Pletikos M, Mori S, Judas M, Kostovic I: Prominent periventricular fiber system related to ganglionic eminence and striatum in the human fetal cerebrum. Brain Struct Funct;215:237-253.
42 Moses P, Courchesne E, Stiles J, Trauner D, Egaas B, Edwards E: Regional size reduction in the human corpus callosum following pre- and perinatal brain injury. Cereb Cortex 2000;10:1200-1210.
43 Crispi F, Figueras F, Cruz-Lemini M, Bartrons J, Bijnens B, Gratacos E: Cardiovascular programming in children born small for gestational age and relationship with prenatal signs of severity. Am J Obstet Gynecol;207:121 e121-129.
44 Isaacs EB, Fischl BR, Quinn BT, Chong WK, Gadian DG, Lucas A: Impact of breast milk on intelligence quotient, brain size, and white matter development. Pediatr Res;67:357-362.
45 Maulik PK, Darmstadt GL: Community-based interventions to optimize early childhood development in low resource settings. J Perinatol 2009;29:531-542.
46 Caldu X, Narberhaus A, Junque C, Gimenez M, Vendrell P, Bargallo N, Segarra D, Botet F: Corpus callosum size and neuropsychologic impairment in adolescents who were born preterm. J Child Neurol 2006;21:406-410.

5.5 STUDY 5

Correlation between brain microstructure assessed by fetal MRI and neurodevelopmental outcome at 2 years in term small for gestational age born infants

Egaña-Ugrinovic G, Sanz-Cortés M, Bazán-Arcos C, Couve-Pérez C, Gratacós E.

Am J Obstet Gynecol. 2014

State: submitted

Impact factor: 3.877

Quartile: 1st

CORRELATION BETWEEN STRUCTURAL BRAIN ABNORMALITIES ASSESSED BY FETAL MRI AND NEURODEVELOPMENTAL OUTCOME AT 2 YEARS IN INFANTS BORN SMALL FOR GESTATIONAL AGE.

Gabriela Egaña-Ugrinovic, MD; Carolina Bazán Arcos, MD; Constanza Couve-Pérez, MD; Eduard Gratacós, PhD; Magdalena Sanz-Cortés, PhD.

BCNatal - Barcelona Center for Maternal-Fetal and Neonatal Medicine (Hospital Clínic and Hospital Sant Joan de Deu), Institut d'Investigacions Biomediques August Pi i Sunyer (IDIBAPS), Centre for Biomedical Research on Rare Diseases (CIBER-ER), and University of Barcelona, Barcelona, Spain.

Corresponding author:

Eduard Gratacós

BCNatal | Barcelona Center for Maternal Fetal and Neonatal Medicine

Hospital Clínic and Hospital Sant Joan de Deu

Sabino de Arana, 1

08028 Barcelona, Spain

Telephone: +34 93 227 9333

Fax: +34 93 227 5612

Email: gratacos@clinic.ub.es

Abstract word count: 248 Text word count: 2714

Disclosure: The authors report no conflict of interest

Previous or intended publications:

1) Differences in cortical development assessed by fetal MRI in late-onset intrauterine growth restriction. Egaña-Ugrinovic G, Sanz-Cortes M, Figueras F, Bargalló N, Gratacós E. Am J Obstet Gynecol. 2013 Aug; 209(2):126.e1-8.
2) Corpus callosum differences assessed by fetal MRI in late-onset intrauterine growth restriction and its association with neurobehavior. Egaña-Ugrinovic G, Sanz-Cortés M, Couve-Pérez C, Figueras F, Gratacós E. Prenat Diagn. 2014 Apr 7. doi: 10.1002/pd.4381. [Epub ahead of print]

Acknowledgments: This work was supported by grants from The Cerebra Foundation for the Brain Injured Child (Carmarthen, Wales, UK), the Thrasher Research Fund (Salt Lake City, USA), Obra Social "la Caixa" (Barcelona, Spain), and Banca Cívica de Caja Navarra (Proyecto TETD). G.E.U was supported by CONICYT (PFCHA/<Doctorado al Extranjero 4ª Convocatoria><72120071>), Chile. M.S.C. was supported by Instituto de Salud Carlos III Rio Hortega (CM10/00222), Spain.

Condensation: We evaluated a theoretical predictive model for neurodevelopmental outcome at 2 years using fetal brain MRI assessment in small-born infants and controls.

Short version of the article: Correlation between brain structure and neurodevelopment in SGA.

No reprints will be available

ABSTRACT:

Objective: To predict neurodevelopmental outcome in a cohort of small born infants and controls at 2 years of age based on the differences of cortical development and corpus callosum assessed by fetal MRI at term. Secondarily, we aimed to obtain a characterization of brain differences that were present in small fetuses studying cortical development and corpus callosum morphometry by means of term fetal MRI.

Study design: We recruited 60 small fetuses and 42 controls that underwent a fetal brain MRI at 37 weeks of gestational age. Fetal cortical development and corpus callosum morphometry were evaluated. At 2 years, neurodevelopmental outcome was assessed by means of Bayley scale for infant and toddler development (Bayley-III). Results were considered abnormal if one or more of its domains presented a score <1 SD. To assess the association between brain measurements and neurodevelopment, correlation analyses were performed. Finally, we assessed which of the cortical development and corpus callosum variables better characterized differences in small fetuses using principal component analysis and these were used to construct a composite score for abnormal neurodevelopment. The predictive value of this composite score was assessed using a logistic regression.

Results: Small fetuses showed deeper fissures, thinner cortex and smaller corpus callosum; they also presented worse scores in the Bayley-III test. There was a negative correlation between cortical and callosum measurements with neurodevelopment. Callosal posterior midbody area, corpus callosum length and right lateral fissure depth were selected and combined in our composite score, which significantly predicted an abnormal Bayley III test re-sult,(p=0.026), outperforming other parameters such as clinical group (*p*=0.026).

Conclusions: Infant neurodevelopment can be predicted from term fetal MRI by assessing cortical development and corpus callosum. Although larger studies are warranted to confirm our findings, these results may open the possibility to detect those fetuses at risk for an abnormal neurodevelopment.

Key words: brain development, cortical development, corpus callosum, neurodevelopment, SGA, IUGR.

INTRODUCTION

Intrauterine growth restriction (IUGR) remains one of the main challenges in maternity care due to its frequency affecting between 5-8% of all live birth. Increasing evidence over the last 20 years has consistently demonstrated how being born small has important implications for long-term health quality[1-4], including neurodevelopmental deficits among the most reported consequences[4-7]. Although the anatomical bases of these outcomes are still poorly understood, it has been proposed that structural abnormalities might be present long before the appearance of functional symptoms[8-10]. Previous studies in preterm and severe IUGR have shown an association between specific brain structures assessed postnatally and functional outcome[8, 11-13]; the most consistent findings are in relation to cortical development and corpus callosum abnormalities[8, 11, 12, 14]. Both structures have been also explored in adult life and proposed as potential pathophysiological basis of certain neurocognitive and neuropsychiatric disorders[15-19].

Although neurostructural differences have been characterized in IUGR[5, 20-22] and that smallness is a well-known independent risk factor for the development of neurodevelopmental impairements[4, 5, 7, 22], there is no evidence that we can predict such outcome from prenatal life. Interestingly, it seems that not all IUGR are equally affected[22-24]. Thus, there is a need to search for brain imaging biomarkers to better identify those babies who will have an abnormal neurocognitive profile and accordingly, to allocate neurostimulation resources to a more limited population. We have recently shown how changes in brain morphometry are already present at term in small fetuses, and how these differences are associated to their neonatal neurobehavior[14, 24, 25].

The objective of this study was to identify an early brain phenotype that can predict functional outcome. For this purpose we first evaluated fetal brain developmental

differences assessed by brain magnetic resonance imaging (MRI) in term small fetuses and their 2-year neurodevelopmental outcome by means of the Bayley-III test compared to controls. After these results were obtained, we tested the predictive value of prenatal cortical and corpus callosum morphometry to identify those infants at risk for an abnormal neurodevelopment.

METHODS

Subjects

This study is part of a larger prospective research program on IUGR involving fetal, neonatal and long term postnatal follow-up carried out at BCNatal (Spain). The specific protocol of this study was approved by the institutional Ethics Committee (Institutional Review Board 2008/4422) and all participants gave written informed consent. We assembled a cohort between January 2009 and December 2011 of consecutive, singleton full-term babies who were suspected prenatally of being small fetuses defined by an estimated and postnatally confirmed fetal weight <10th centile, according to local standards[26, 27]. Only those small fetuses with normal UA pulsatility index were included (<95th centile)[28]. Appropriate-for-gestational age (AGA) subjects were defined as normal term fetuses with an estimated and postnatally confirmed fetal weight above the 10th centile, according to local standards[26, 27]. Pregnancies were dated according to the first-trimester crown–rump length measurement[29]. Exclusion criteria included congenital malformations, chromosomal abnormalities, perinatal infections, chronic maternal pathology, contraindications for MRI and non-cephalic presentations.

Clinical and Ultrasound data

Small for gestational age patients were followed-up in our fetal growth restriction unit from diagnosis until delivery. Baseline maternal characteristics and obstetric history were recorded in the hospital database upon study admittance. Data on ultrasound evaluations, subsequent complications of pregnancy, postpartum follow-up and perinatal progress were also collected prospectively.

The entire sample underwent Doppler US scans using a General Electric Voluson E8, 6-2MHz curved-array transducer (GE Medical Systems, Zipf, Austria). Fetal umbilical artery (UA) and middle cerebral artery (MCA) pulsatility index (PI) were measured as described elsewere[28]. Both measurements were used for the calculation of the cerebroplacental ratio (CPR) as CPR= MCA PI/UA PI. Abnormal CPR was defined as a value <5th centile for gestational age according to previously published reference values[30]. Uterine arteries (UtA) PI were measured transabdominally and mean value was considered abnormal when >95th centile[31]. All fetuses in this study had at least one US scan within one week before delivery and from fetal brain MRI.

Fetal MRI acquisition and offline analysis

MRI was performed at 37 weeks of gestational age on a clinical MR system using the Institut d'Investigacions Biomediques August Pi i Sunyer (IDIBAPS) image platform, operating at 3.0 Tesla (Siemens Magnetom Trio Tim syngo MR B15, Siemens, Germany) without fetal sedation[32]. A body coil with 8 elements was wrapped around the mother's abdomen. Routine fetal imaging took around 20 minutes and consisted on single-shot, fast spin echo T2-weighted sequences (TR 990ms, TE 137ms, slice thickness 3.5mm, no gap, field of view 260mm, voxel size 1.4x1.4x3.5mm, matrix 192x192, flip angle 180º, acquisition time 24 seconds) acquired in the three orthogonal planes. If the quality of the images was suboptimal, sequences were repeated. Structural MRI images were reviewed for the presence of anatomical abnormalities by an experienced neuroradiologist blinded to group membership.

Offline analyses of cortical development and corpus callosum morphometry measurements were performed using the semiautomatic Analyze 9.0 software (Biomedical Imaging

Resource, Mayo Clinic; Kansas, USA). The methodologies used to delineate these structures are reported elsewhere[14, 20, 24]. All cortical development parameters were corrected by the biparietal diameter (BPD) expressed as ratios (cortical development parameter/BPD) and the corpus callosum measurements by the cephalic index (CI) expressed as ratios (corpus callosum measurement/CI).

Neurodevelopmental assessment

Developmental function was evaluated at 2 years using the Bayley Scales of Infant and Toddler Development, 3rd Edition (Bayley-III), which is a revision of the prior edition (Bayley, 1993)[33]. The Bayley-III is an instrument that assesses infant development across five domains, including cognitive, language and motor competencies. Parent reported questionnaires are incorporated into the Bayley-III in order to assess social-emotional and adaptive behaviors. All evaluations were performed by one of three trained psychologists, blinded to the study group and perinatal outcomes. According to the test manual, abnormal result for each domain was defined as a Bayley-III score below 1 SD (<85). We considered a pathological neurodevelopmental outcome at the presence of at least one abnormal domain.

Statistical analysis

Student's-t test for independent samples and Pearson´s X^2 were used to compare quantitative and qualitative data, respectively. Multiple Analysis of Covariance (MANCOVA) adjusting by body mass index, gender and gestational age at the MRI was performed to assess cortical and corpus callosum developmental differences between small fetuses and AGA. MANCOVA also was conducted to assess neurodevelopment differences between

small-born and AGA infants, adjusting by the following confounding variables: gender; socioeconomic class defined as routine occupations, long-term unemployment, or never employed (UK National Statistics Socio-Economic Classification); months at the Bayley-III test and breastfeeding (at least 6 months after delivery).

The entire sample was divided into two groups according to whether or not they had an abnormal Bayley-III to assess its association with cortical development and corpus callosum measurements by means of a multivariate analysis. Then, taking into account the entire cohort, correlations analyses between brain structures and Bayley-III outcome were performed to assess the directionality of the associations. The predictive value of cortical development and corpus callosum morphometry on neurodevelopment was tested by means of logistic regressions in the entire cohort, adjusting by the same set of covariates describe above. In order to construct a predictive algorithm to detect those cases that will present an abnormal neurodevelopment at 2 years, a composite score was created. For this purpose, and in order to select which variables would better represent the abnormal neurodevelopment, a dimensionality reduction was performed using a principal components analysis (PCA). Finally, we conducted a stepwise logistic regression to evaluate the predictive capacity of this composite score.

The Statistical Package for the Social Sciences (SPSS 17.0, SPSS Inc., Chicago, IL, USA) was used for the statistical analysis.

RESULTS

A total of 110 fetuses fulfilled the inclusion criteria. Of these, 8 births were lost during follow-up, having no means of contact for neurocognitive evaluation leaving a total of 60 small fetuses and 42 controls. Maternal characteristics and gestational age at MRI did not differ between cases and controls (Table 1). As expected, term small fetuses were delivered earlier with higher rates of labor induction, emergency cesarean section and longer stay in the neonatal intensive unit care (Table 2).

A. Differences between small fetuses and AGA

1) Cortical development and corpus callosum assessment

Term small fetuses had overall deeper fissures measurements, reaching statistical significance in the left insula, right insula and left cingulate fissure. They also presented thinner insular cortical thicknesses and smaller insular cortical volumes. Regarding the corpus callosum measurements, small fetuses showed smaller corpus callosum total areas and smaller areas from its subdivision with statistical significance in the genu, rostral body, anterior midbody, posterior midbody, isthmus and splenium areas.

2) Neurodevelopmental outcome

It was assessed at 23.5 ± 1.2 and 23.9 ± 1.0 months in small fetuses and controls, respectively. Small-born infants showed lower score in all domains from the Bayley-III test (Figure 1). Differences in the cognitive, language and motor domains remained significant after adjusting for potential confounders variables.

B. Cortical development and corpus callosum predictive value of an abnormal neurodevelopmental outcome

1) Abnormal vs. normal Bayley-III test

We segregated the entire sample into two groups defined as having an abnormal Bayley-III test or not. Those infants with an abnormal Bayley-III presented shallower fissures, thinner insular cortical thicknesses and smaller corpus callosum areas. These differences reached statistical significance in the right parietoccipital fissure ($p=0.04$), total corpus callosum area ($p=0.01$), rostral body ($p<0.01$), anterior midbody ($p=0.01$), posterior midbody ($p<0.01$), isthmus ($p=0.02$) and callosal length ($p=0.01$).

2) Correlations analyses

Taking into account the entire cohort, we found a negative linear correlation between cortical and corpus callosum measurements with neurodevelopmental outcome, indicating that smaller measures were associated to worse Bayley-III scores, reaching statistical significance in the biparietal diameter (Pearson -0.329; $p<0.01$), fronto-occipital diameter (Pearson -0.372; $p<0.01$), insular asymmetry (Pearson 0.306; $p=0.01$), total corpus callosum area (Pearson -0,250; $p=0.02$), rostral body area (Pearson -0.298; $p<0.01$), anterior midbody area (Pearson -0.232; $p=0.03$), posterior midbody area (Pearson -0.333; $p<0.01$) and isthmus area (Pearson -0.235; $p=0.03$).

3) Linear regression and principal component analysis

The regression analysis suggested a significant predictive value of abnormal neurodevelopment for several cortical development features (biparietal diameter, fronto-occipital diameter, left insular depth, right lateral fissure depth, and the anterior and middle

insular cortical thicknesses) and corpus callosum measurements (posterior midbody area and callosal length). These measurements were further tested by a principal component analysis in order to select the best predictive parameters and we found that a combination of the posterior midbody area, corpus callosum length and right lateral fissure depth provided the best classification model of having an abnormal Bayley-III test (Figure 2). A composite score (ranging from 0 to 1) was constructed using a combination of these variables according to the following formula obtained by logistic regression: Composite score=e-(Y)/ (1 + e-(Y)), where Y= 1.183 + (Posterior midbody/CI * corpus callosum length/CI * Right lateral fissure/BPD * -41.264). The composite score achieved a higher predictiveness as compared with any of the individual parameters previously analyzed (p=0.026). The ROC curve of the model resulted in an area under the curve of 78% (95% confidence interval: 62-93%) (Figure 3).

DISCUSSION

This study reports for the first time the impact of fetal brain development in functional outcome in a cohort of term small-born infants and controls. We show that shallower fissures and smaller corpus callosum can predict an abnormal neurodevelopment defined by an abnormal Bayley-III test at 2 years. These findings support the notion that brain development at term might represent an early phenotype of later functional development[8].

A different pattern of cortical development with deeper fissures and thinner cortex in small fetuses goes in line with previous studies, which have shown how brain reprogramming affects not only severe IUGR[8] but term small fetuses as well, through brain microstructure[34], metabolism[21] and connectomic analyses[35], and regarding the smaller corpus callosum found in this population, it has been described how preterm babies present similar alterations in its microstructure[11, 12]. Moreover, small-born infants showed worse neurodevelopmental outcome, mainly in the cognitive, language and motor domains, which has been recently reported[5, 22]. Different studies on severe IUGR newborns have shown an association between their brain developmental profile and early functional outcome[8, 36, 37]. So, we thought that it was plausible that brain structure at term could be predictive of neurological deficits that may appear later on in life. Indeed, a close relation can be established between the competencies altered in small-born infants and the insular cortex and corpus callosum functionality[38-40]. We acknowledge that the execution of these domains might involve the activation of different brain areas; nevertheless, the insula and the corpus callosum have been specifically involved as sensory and motor integration regions responsible for human emotion, language and cognition[38, 40]. Indeed, a thinner cortical thickness may be responsible for lower IQ scores measured in severe IUGR born children[7]. Moreover, insular abnormalities have been implicated in a large number of dysfunctions such as aphasia,

mood disorders and autism[38, 39], and corpus callosum alterations have been found in children with language and attention-deficit hyperactive disorder[40].

From a pathophysiological standpoint, it is likely that the alterations found in these brain regions might be related to their time table of development and a special vulnerability to chronic hypoxic/undernourished environment[8, 41]. It is well-known that by the end of pregnancy there is an active cortical development, synaptogenesis and pruning, which are critical for the adult-like appearance of the brain before birth[8, 40]. Sulci and gyri formation not only depend on genetic background, but also depend on external factors like the tension from white matter fibers as pregnancy progresses[42]. In a normal scenario, an integral corpus callosum development facilitates normal fetal brain gyrification[43]. However, it seems that chronic hypoxic conditions can affect this delicate relation, both inducing cortical brain reprogramming[8, 20, 24] and altering immature oligodendrocytes from corpus callosum fibers located closer to the germinal matrix[44, 45]. Our study suggests that term brain development alterations could constitute the first step in the cascade of functional impairment underlying neurodevelopmental pathologies[9]. This notion is particularly interesting as fetal brain imaging could give us the opportunity to identify biomarkers of abnormal functional outcome in pregnancies at risks even before symptomatology is present.

Although IUGR has been defined as an independent risk factor for neuropsychiatric conditions[7], not all small fetuses will develop neurological impairments. This selectivity in the long-term consequences of smallness has not been address yet. Probably, the identification of subgroups with true growth restriction will become of greater interest with the development of new definitions for IUGR. For the moment, a closer prenatal follow-up of fetal wellness, and maybe brain development monitoring of these fetuses, could be justified to improve parental counseling. Early educational intervention have been

documented to improve cognitive performance and, in some cases, to reduce antisocial behavior at a young age[46]. The finding of poorer motor development in the small-born infants may suggest that motor training and general developmental programs, in which parents learn how to promote infant development, may be promising ways to promote these competencies in infants at high risk of developmental motor disorders[47, 48].

Although we couldn't consistently demonstrate a correlation between structure and function particularly in the small-born population, probably due to the limited sample size, our results from the logistic regression and principal component analysis selected specific features of brain development above than belonging to a particular clinical group. Therefore, neurodevelopmental outcome at 2 years might be more dependent to the antenatal brain phenotype than being small or not, which opens the door to larger studies. Another limitation of this study arises in relation to the challenging segmentation of the fetal brain. Fetal MRI exhibit motion artifacts and limited contrast between different tissues that are more difficult to overcome than in adult brains, due to the difference in size of the structures of interest and the age-dependent maturation of the different brain tissues[49]. To overcome this problem, we used strict anatomical landmarks and only subjects with no motion artifacts images were included in the analyses. Also the MRI scan was performed close to term to favor an engagement of the fetal head in the maternal pelvis. Between the strength of this study are the prospective methodology used and the well-defined clinical groups, accounting for a homogeneous sample, which is highly representative of the condition of interest.

In conclusion, we found a significant correlation between fetal brain development at term and the neurodevelopmental outcome at 2 years. Moreover, we evaluated a theoretical predictive model using several brain structures to detect those fetuses at risk for an

abnormal neurodevelopment. These results support the value of brain reorganizational changes as potential image biomarkers to predict those infants at risk for an abnormal neurodevelopment.

TABLES

Table 1. Maternal characteristics of the study groups.

	SGA (N = 60)	**AGA (N = 42)**	**P***
Maternal age (y)	31.8 ± 5.6	32.2 ± 4.2	0.59
Caucasian ethnicity (%)	76.7%	71.2%	0.40
Primiparity (%)	75.7%	67.1%	0.22
Maternal high education (%)	44.1%	71.8%	**<0.01**
Maternal smoking (%)	23.3%	5.5%	**<0.01**
Maternal BMI (kg/m2)	22.2 ± 3.9	22.9 ± 3.6	0.19
GA at MRI (w)	37.5± 0.8	37.6 ± 0.9	0.06
Breastfeeding (%)	55.9%	71.4%	0.21

Results are expressed as mean ± SD or percentage as appropriate. *Student´s t-test for independent samples or Pearson´s X2 test. BMI: Body mass index. y= years; kg=kilograms; m2= square meter; m=months.

Table 2. Perinatal outcome of the study groups.

	SGA (N =60)	AGA (N = 42)	P*
GA at birth (w)	38.7 ± 1.1	40.0 ± 1.1	**<0.01**
Birth weight (g)	2426 ± 301	3429 ± 310	**<0.01**
Birth weight centile	3.1 ± 4.9	52.2 ± 24.0	**<0.01**
Male gender (%)	57.8%	54.8%	0.69
Labor induction (%)	77.2%	23.5%	**<0.01**
Emergency cesarean section (%)	27.2%	5.5%	**<0.01**
Neonatal acidosis† (%)	10.6%	6.6%	0.39
Apgar score <7 at 5 minutes (%)	2.6%	0%	0.07
NICU stay length (d)	0.2	0	**0.04**
Head circumference (cm)	42.5 ± 2.8	43.2 ± 2.3	0.10
Months at Bayley-III	23.5 ± 1.2	23.9 ± 1.0	**0.04**

Results are expressed as mean ± SD or percentage as appropriate. *Student´s t-test for independent samples or Pearson´s X2 test. GA: gestational age. Neonatal acidosis†: umbilical artery pH<7.15 and base excess > 12 mEq/L. NICU: Neonatal Intensive care unit. w=weeks; g=grams; cm=centimeters; Bayley-III= Bayley Scales of Infant and Toddler Development.

FIGURES

Figure 1. Score distribution for each neurodevelopmental domain assessed by Bayley-III in the study group.

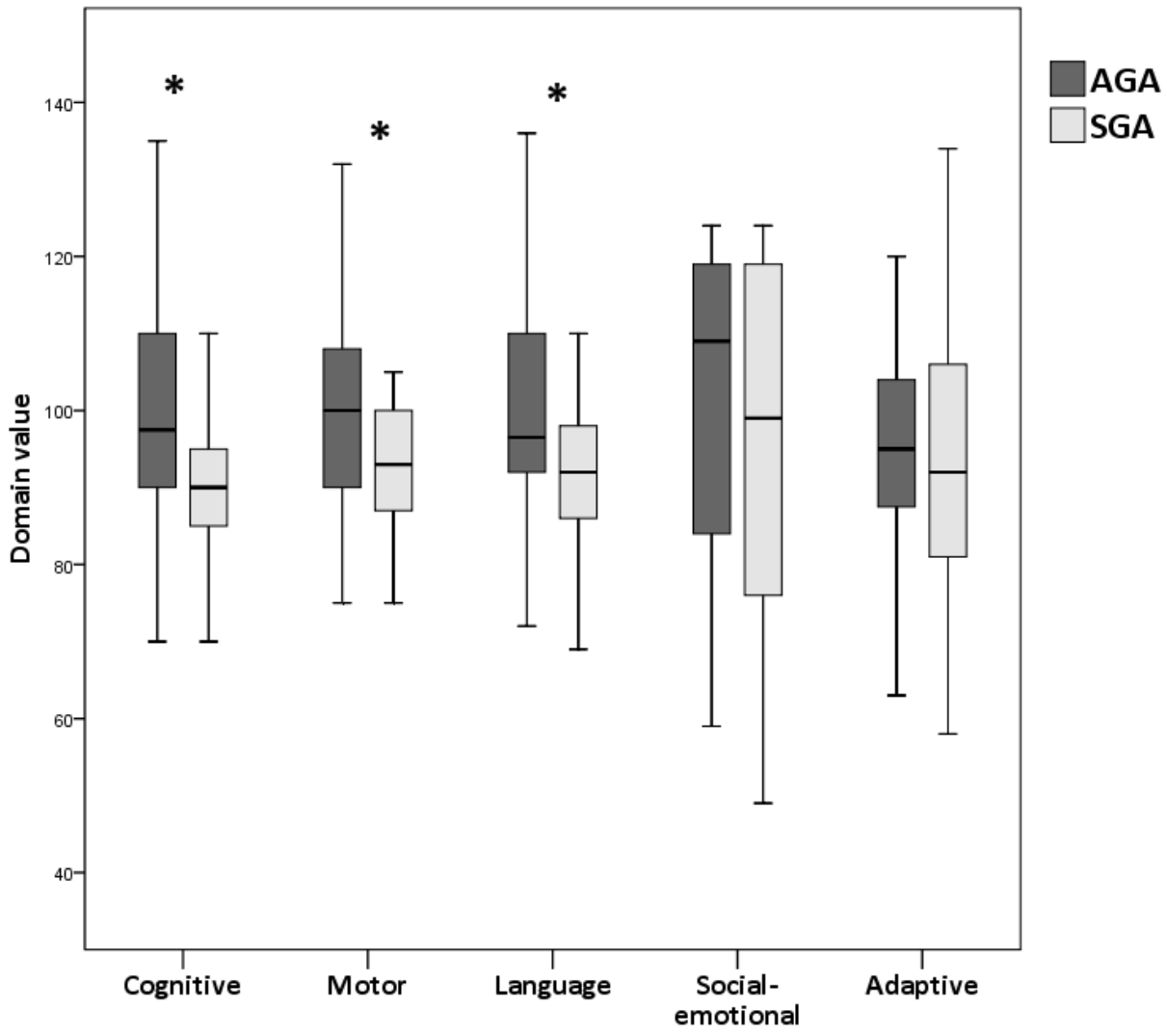

Figure 2. Composite score between normal and abnormal Bayley-III

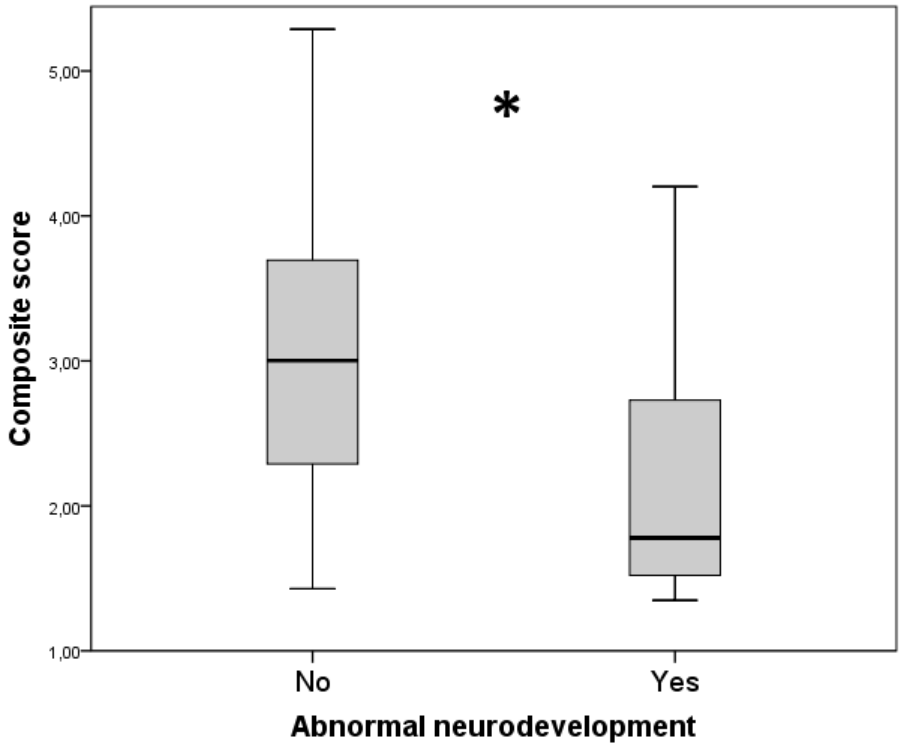

* p<0.01. Composite score obtained by logistic regression. The score contains a combination of posterior midbody area, corpus callosum length and right lateral fissure depth.

Figure 3. ROC curve from the composite score to predict an abnormal Bayley-III

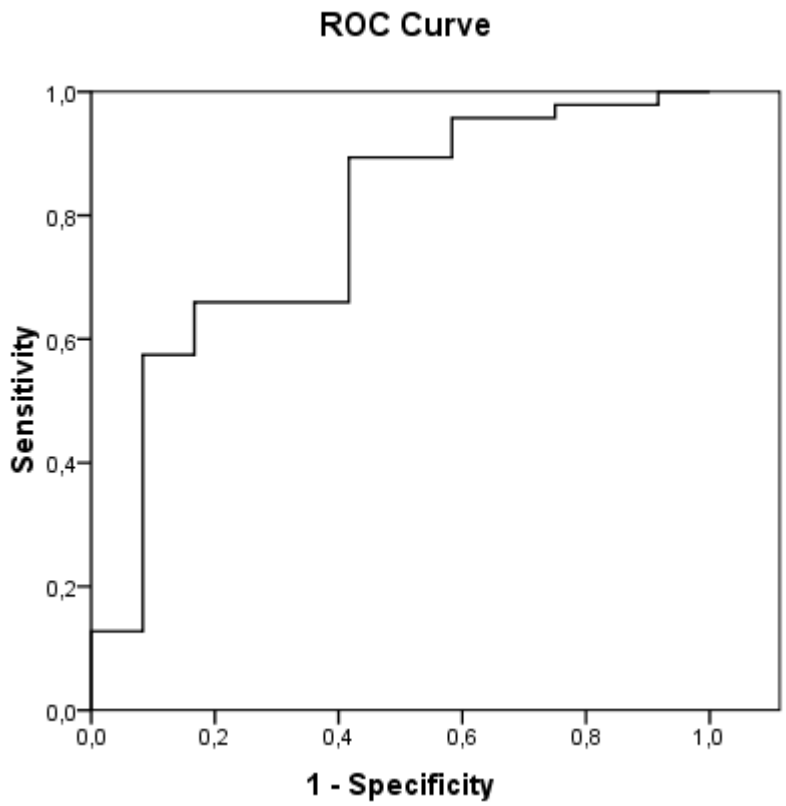

ROC curve of the composite score to predict an abnormal neurodevelopment assessed by the Bayley-III test showing an area under the curve of 78% (95% confidence interval: 62-93%).

REFERENCES

1. FIGUERAS F, EIXARCH E, GRATACOS E, GARDOSI J. Predictiveness of antenatal umbilical artery Doppler for adverse pregnancy outcome in small-for-gestational-age babies according to customised birthweight centiles: population-based study. BJOG 2008;115:590-4.
2. FIGUERAS F, GRATACOS E. Update on the Diagnosis and Classification of Fetal Growth Restriction and Proposal of a Stage-Based Management Protocol. Fetal Diagn Ther.
3. CRISPI F, FIGUERAS F, CRUZ-LEMINI M, BARTRONS J, BIJNENS B, GRATACOS E. Cardiovascular programming in children born small for gestational age and relationship with prenatal signs of severity. Am J Obstet Gynecol;207:121 e1-9.
4. LEY D, TIDEMAN E, LAURIN J, BJERRE I, MARSAL K. Abnormal fetal aortic velocity waveform and intellectual function at 7 years of age. Ultrasound Obstet Gynecol 1996;8:160-5.
5. ARCANGELI T, THILAGANATHAN B, HOOPER R, KHAN KS, BHIDE A. Neurodevelopmental delay in small babies at term: a systematic review. Ultrasound Obstet Gynecol;40:267-75.
6. FIGUERAS F, OROS D, CRUZ-MARTINEZ R, et al. Neurobehavior in term, small-for-gestational age infants with normal placental function. Pediatrics 2009;124:e934-41.
7. GEVA R, ESHEL R, LEITNER Y, VALEVSKI AF, HAREL S. Neuropsychological outcome of children with intrauterine growth restriction: a 9-year prospective study. Pediatrics 2006;118:91-100.
8. DUBOIS J, BENDERS M, BORRADORI-TOLSA C, et al. Primary cortical folding in the human newborn: an early marker of later functional development. Brain 2008;131:2028-41.
9. HUPPI PS. Neuroimaging of brain development--discovering the origins of neuropsychiatric disorders? Pediatr Res 2008;64:325.
10. BARKER DJ. The origins of the developmental origins theory. J Intern Med 2007;261:412-7.
11. COUNSELL SJ, EDWARDS AD, CHEW AT, et al. Specific relations between neurodevelopmental abilities and white matter microstructure in children born preterm. Brain 2008;131:3201-8.
12. NOSARTI C, RUSHE TM, WOODRUFF PW, STEWART AL, RIFKIN L, MURRAY RM. Corpus callosum size and very preterm birth: relationship to neuropsychological outcome. Brain 2004;127:2080-9.
13. BOGER-MEGIDDO I, SHAW DW, FRIEDMAN SD, et al. Corpus callosum morphometrics in young children with autism spectrum disorder. J Autism Dev Disord 2006;36:733-9.
14. EGANA-UGRINOVIC G, SANZ-CORTES M, COUVE-PEREZ C, FIGUERAS F, GRATACOS E. Corpus callosum differences assessed by fetal MRI in late-onset intrauterine growth restriction and its association with neurobehavior. Prenat Diagn.
15. MAKRIS N, BIEDERMAN J, VALERA EM, et al. Cortical thinning of the attention and executive function networks in adults with attention-deficit/hyperactivity disorder. Cereb Cortex 2007;17:1364-75.
16. ROIZ-SANTIANEZ R, PEREZ-IGLESIAS R, QUINTERO C, et al. Insular cortex thinning in first episode schizophrenia patients. Psychiatry Res;182:216-22.
17. NORTHAM GB, LIEGEOIS F, TOURNIER JD, et al. Interhemispheric temporal lobe connectivity predicts language impairment in adolescents born preterm. Brain;135:3781-98.
18. CACHIA A, PAILLERE-MARTINOT ML, GALINOWSKI A, et al. Cortical folding abnormalities in schizophrenia patients with resistant auditory hallucinations. Neuroimage 2008;39:927-35.

19. NORDAHL CW, DIERKER D, MOSTAFAVI I, et al. Cortical folding abnormalities in autism revealed by surface-based morphometry. J Neurosci 2007;27:11725-35.
20. EGANA-UGRINOVIC G, SANZ-CORTES M, FIGUERAS F, BARGALLO N, GRATACOS E. Differences in cortical development assessed by fetal MRI in late-onset intrauterine growth restriction. Am J Obstet Gynecol.
21. SANZ-CORTES M, FIGUERAS F, BARGALLO N, PADILLA N, AMAT-ROLDAN I, GRATACOS E. Abnormal brain microstructure and metabolism in small-for-gestational-age term fetuses with normal umbilical artery Doppler. Ultrasound Obstet Gynecol;36:159-65.
22. SAVCHEV S, SANZ-CORTES M, CRUZ-MARTINEZ R, et al. Neurodevelopmental outcome of full-term small-for-gestational-age infants with normal placental function. Ultrasound Obstet Gynecol.
23. CRUZ-MARTINEZ R, FIGUERAS F, OROS D, et al. Cerebral blood perfusion and neurobehavioral performance in full-term small-for-gestational-age fetuses. Am J Obstet Gynecol 2009;201:474 e1-7.
24. EGANA-UGRINOVIC G, SANZ-CORTES M, FIGUERAS F, COUVE-PEREZ C, GRATACOS E. Fetal MRI Insular Cortical Morphometry and its Association with Neurobehavior in Late-Onset Small For Gestational Age Fetuses. Ultrasound Obstet Gynecol.
25. SANZ-CORTES M, RATTA GA, FIGUERAS F, et al. Automatic quantitative MRI texture analysis in small-for-gestational-age fetuses discriminates abnormal neonatal neurobehavior. PLoS One;8:e69595.
26. CHAUHAN SP, GUPTA LM, HENDRIX NW, BERGHELLA V. Intrauterine growth restriction: comparison of American College of Obstetricians and Gynecologists practice bulletin with other national guidelines. Am J Obstet Gynecol 2009;200:409 e1-6.
27. FIGUERAS F, MELER E, IRAOLA A, et al. Customized birthweight standards for a Spanish population. Eur J Obstet Gynecol Reprod Biol 2008;136:20-4.
28. ARDUINI D, RIZZO G. Normal values of Pulsatility Index from fetal vessels: a cross-sectional study on 1556 healthy fetuses. J Perinat Med 1990;18:165-72.
29. ROBINSON HP, FLEMING JE. A critical evaluation of sonar "crown-rump length" measurements. Br J Obstet Gynaecol 1975;82:702-10.
30. BASCHAT AA, GEMBRUCH U. The cerebroplacental Doppler ratio revisited. Ultrasound Obstet Gynecol 2003;21:124-7.
31. GOMEZ O, FIGUERAS F, FERNANDEZ S, et al. Reference ranges for uterine artery mean pulsatility index at 11-41 weeks of gestation. Ultrasound Obstet Gynecol 2008;32:128-32.
32. PATENAUDE Y, PUGASH D, LIM K, et al. The use of magnetic resonance imaging in the obstetric patient. J Obstet Gynaecol Can;36:349-55.
33. MILNE S, MCDONALD J, COMINO EJ. The use of the Bayley Scales of Infant and Toddler Development III with clinical populations: a preliminary exploration. Phys Occup Ther Pediatr;32:24-33.
34. SANZ-CORTES M, EGANA-UGRINOVIC G, ZUPAN R, FIGUERAS F, GRATACOS E. Brainstem and cerebellar differences and their association with neurobehavior in term small-for-gestational-age fetuses assessed by fetal MRI. Am J Obstet Gynecol.
35. BATALLE D, EIXARCH E, FIGUERAS F, et al. Altered small-world topology of structural brain networks in infants with intrauterine growth restriction and its association with later neurodevelopmental outcome. Neuroimage;60:1352-66.
36. TOLSA CB, ZIMINE S, WARFIELD SK, et al. Early alteration of structural and functional brain development in premature infants born with intrauterine growth restriction. Pediatr Res 2004;56:132-8.

37. KESLER SR, MENT LR, VOHR B, et al. Volumetric analysis of regional cerebral development in preterm children. Pediatr Neurol 2004;31:318-25.
38. NIEUWENHUYS R. The insular cortex: a review. Prog Brain Res;195:123-63.
39. AUGUSTINE JR. Circuitry and functional aspects of the insular lobe in primates including humans. Brain Res Brain Res Rev 1996;22:229-44.
40. PAUL LK. Developmental malformation of the corpus callosum: a review of typical callosal development and examples of developmental disorders with callosal involvement. J Neurodev Disord;3:3-27.
41. HERNANDEZ-ANDRADE E, FIGUEROA-DIESEL H, JANSSON T, RANGEL-NAVA H, GRATACOS E. Changes in regional fetal cerebral blood flow perfusion in relation to hemodynamic deterioration in severely growth-restricted fetuses. Ultrasound Obstet Gynecol 2008;32:71-6.
42. WARREN DJ, CONNOLLY DJ, GRIFFITHS PD. Assessment of sulcation of the fetal brain in cases of isolated agenesis of the corpus callosum using in utero MR imaging. AJNR Am J Neuroradiol;31:1085-90.
43. VOLPE P, PALADINI D, RESTA M, et al. Characteristics, associations and outcome of partial agenesis of the corpus callosum in the fetus. Ultrasound Obstet Gynecol 2006;27:509-16.
44. MOSES P, COURCHESNE E, STILES J, TRAUNER D, EGAAS B, EDWARDS E. Regional size reduction in the human corpus callosum following pre- and perinatal brain injury. Cereb Cortex 2000;10:1200-10.
45. BACK SA, LUO NL, BORENSTEIN NS, LEVINE JM, VOLPE JJ, KINNEY HC. Late oligodendrocyte progenitors coincide with the developmental window of vulnerability for human perinatal white matter injury. J Neurosci 2001;21:1302-12.
46. ALS H, DUFFY FH, MCANULTY G, et al. NIDCAP improves brain function and structure in preterm infants with severe intrauterine growth restriction. J Perinatol;32:797-803.
47. MORGAN C, NOVAK I, BADAWI N. Enriched environments and motor outcomes in cerebral palsy: systematic review and meta-analysis. Pediatrics;132:e735-46.
48. VAN HUS JW, JEUKENS-VISSER M, KOLDEWIJN K, et al. Comparing two motor assessment tools to evaluate neurobehavioral intervention effects in infants with very low birth weight at 1 year. Phys Ther;93:1475-83.
49. PRAYER D, KASPRIAN G, KRAMPL E, et al. MRI of normal fetal brain development. Eur J Radiol 2006;57:199-216.

6. RESULTS

6.1 STUDY 1: DIFFERENCES IN CORTICAL DEVELOPMENT ASSESSED BY FETAL MRI IN LATE-ONSET INTRAUTERINE GROWTH RESTRICTION

The results of this project have been published in an international journal and have been presented at the 22nd World Congress on Ultrasound in Obstetrics and Gynecology, 9-13 September 2012, Copenhagen, Denmark (Oral presentation short listed for the Young Investigator award).

This study evaluated the presence of cortical development differences between late-onset IUGR (N=52) and controls (N=50). Maternal characteristics and time of MRI scans did not differ between cases and controls. As expected, IUGR fetuses were delivered earlier with higher rates of labor induction, emergency cesarean section, neonatal acidosis and lower Apgar scores at 5 minutes of life (Table 1).

Table 1: Maternal and perinatal data in the study groups.

	IUGR (N = 52)	**AGA (N = 50)**	P*
Maternal data			
Maternal Age (y)	31.8 ± 6.2	32.2 ± 4.3	0.64
Maternal Smoking	15.4%	6%	0.13
Maternal Height (m)	1.58 ± 0.05	1.65 ± 0.06	<0.01
Maternal Weight (kg)	56.9 ± 10.1	63.2 ± 11.3	<0.01
Maternal BMI (kg/m^2)	22.7 ± 3.7	23.2 ± 3.9	0.49
Primiparity	65%	64%	0.88
Caucasian ethnicity	79%	68%	0.18
GA at MRI (w)	37.5 ± 0.8	37.7 ± 0.8	0.30

Perinatal data			
GA at birth (w)	38.8 ± 1.0	40.0 ± 1.0	<0.01
Birth weight (g)	2488 ± 247	3452 ± 311	<0.01
Birth weight centile	3.9 ± 6.6	55.2 ± 24.2	<0.01
Male gender	62%	52%	0.34
Labor Induction	77.1%	14.3%	<0.01
Emergency cesarean section	31%	6%	<0.01
Neonatal acidosis†	19.6%	5%	0.04
Apgar score <7 at 5 minutes	5.8%	0%	0.04
NICU stay length (d)	0.3	0	0.09

Results are expressed as mean ± SD or percentage as appropriate. *Student´s t-test for independent samples or Pearson´s X2 test. BMI: Body mass index. GA: gestational age. MRI: Magnetic Resonance Imaging. †Neonatal acidosis: umbilical artery pH<7.15 and base excess >12mEq/L. NICU: Neonatal Intensive care unit. y=years; m=meters; kg=kilograms; m^2= square meter; w=weeks; g=grams; d=days.

We found that late-onset IUGR fetuses showed a different pattern of brain development expressed by smaller BPD and deeper fissures measurements, with statistical significance in the right and left insula, and the left cingulate fissure as compared to controls (Table 2).

Table 2. Fissure depths in the study groups.

	IUGR (N = 52)	**AGA (N = 50)**	**P***
Left Insular Depth/BPD	0.293 ± 0.052	0.267 ± 0.029	**0.02**
Right Insular Depth/BPD	0.379 ± 0.066	0.318 ± 0.075	**<0.01**
Left Lateral Fissure/BPD	0.154 ± 0.042	0.151 ± 0.024	0.81
Right Lateral Fissure/BPD	0.151 ± 0.037	0.154 ± 0.042	0.82
Left Parietooccipital Fissure/BPD	0.139 ± 0.029	0.132 ± 0.036	0.18
Right Parietooccipital Fissure/BPD	0.138 ± 0.029	0.132 ± 0.036	0.22
Left Cingulate Fissure/BPD	0.096 ± 0.016	0.087 ± 0.019	**0.03**
Right Cingulate Fissure/BPD	0.093 ± 0.019	0.088 ± 0.018	0.19
Left Calcarine Fissure/BPD	0.180 ± 0.039	0.182 ± 0.040	0.56
Right Calcarine Fissure/BPD	0.179 ± 0.038	0.187 ± 0.041	0.14

Results are expressed as mean ± SD.* GLM adjusted for gender, gestational age at MRI and maternal body mass index. BPD: biparietal diameter.

Regarding the volumetric analysis, late-onset IUGR fetuses presented smaller total intracranial and brain volumes. They also showed smaller left opercular volumes (Figure 1).

Figure 1. Total brain volumes (A) and opercular volumes (B) in late-onset IUGR and AGA.

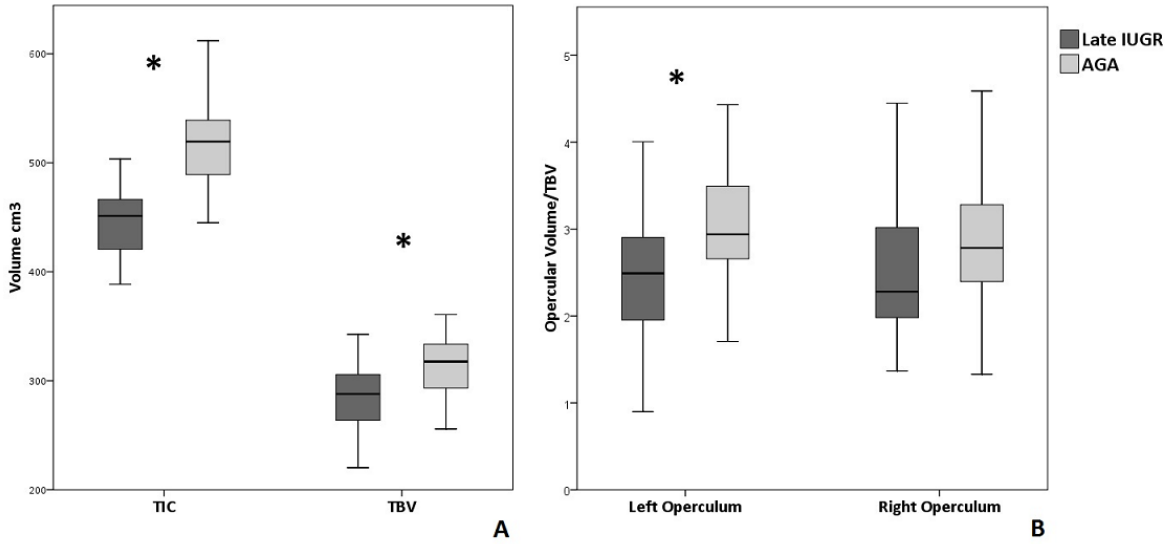

*p <0.05. (A) TIC: total intracranial volume and TBV: total brain volume; adjusting for gender, gestational age at MRI and maternal body mass index. (B) Opercular volumes adjusting for TBV, gender, gestational age at MRI and maternal BMI. AGA: adequate for gestational age.

IUGR fetuses showed a more pronounced right insular asymmetry compared to controls. We further explored the differences of cortical development among IUGR fetuses according to clinical severity, defined by the presence of any of the following factors associated to a poorer perinatal outcome (Figueras 2014): estimated fetal weight <3rd centile (Savchev 2012), abnormal cerebroplacental ratio (Bahado-Singh 1999) and abnormal uterine artery Doppler (Severi 2002). There was a significant linear tendency to more pronounced alterations in those growth restricted fetuses with clinical severity factors.

Figure 2. Differences among IUGR fetuses according to severity in globally significant cortical development parameters.

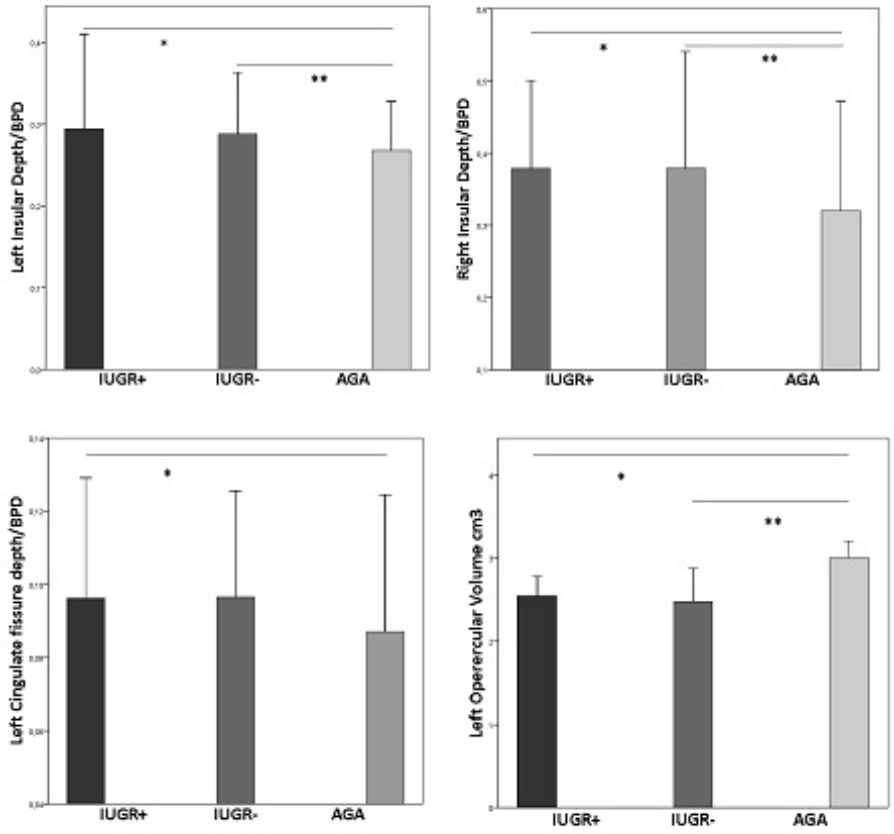

*and** p<0.05. Polynomial contrast analysis showing differences between IUGR+ (IUGR with factors associated to a poorer perinatal outcome), IUGR- (IUGR without these previously described factors) and AGA. Bars depict the mean within each group.

Finally, we performed a regression analysis in which the dependent variable was the diagnosis of late-onset IUGR and the independent variables were the cortical development parameters. The regression suggested that a combination of left and right insular depth corrected for BPD (LID/BPD and RID/BPD, respectively) and left parietoccipital fissure depth/BPD (LPOD/BPD) provided the best classification model of being late-onset IUGR. A composite score (ranging from 0 to 1) was constructed using a combination of these variables according to the following formula: Composite score= e-(Y)/ (1 + e-(Y)), where Y=

6.259 + [(LID/BPD * RID/BPD * -41.264) + (LPOD/BPD * -16.247)]. The composite score achieved a higher discrimination performance as compared with any of the individual parameters previously analyzed (Figure 3). The ROC curve of the model resulted in an area under the curve of 79% (95% confidence interval: 70-88%).

Figure 3. Classified model between late-onset IUGR and AGA fetuses.

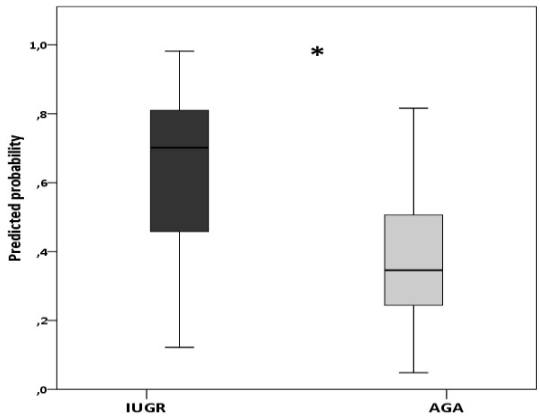

* p<0.01. Composite score obtained by logistic regression. The score contains a combination of left and right insular depth, and left parietoccipital fissure depth, all corrected by BPD.

Our findings support the hypothesis that late-onset IUGR fetuses present a different pattern of cortical development, with deeper fissures, smaller brain volumes and more pronounced right insular asymmetry. These alterations seem to follow a linear tendency according to the severity of growth restriction.

6.2 STUDY 2: FETAL MRI INSULAR CORTICAL MORPHOMETRY AND ITS ASSOCIATION WITH NEUROBEHAVIOR IN LATE-ONSET SMALL FOR GESTATIONAL AGE FETUSES.

The results of this project have been published in an international journal and have been presented at the 12th Fetal Medicine Foundation World Congress, 23-27 June 2013, Marbella, Spain (Oral presentation).

Maternal characteristics and gestational age at MRI did not differ between cases and controls. As expected, late-onset SGA fetuses were delivered earlier with higher rates of labor induction, emergency cesarean section and longer stay in the neonatal intensive unit care, as in our previous study.

We found that SGA fetuses showed thinner insular cortex in all measurements and smaller left and right insular cortical volumes (Table 1).

Table 1. Insular cortical thicknesses and volumes in the study groups.

	SGA (N = 65)	**AGA (N = 59)**	***P****
Insular cortical thickness/insular depth			
Left anterior ICT/ left ID	0.044 ± 0.011	0.051 ± 0.014	<0.01
Left middle ICT/ left ID	0.047 ± 0.011	0.054 ± 0.013	<0.01
Left posterior ICT/ left ID	0.048 ± 0.011	0.053 ± 0.014	0.02
Right anterior ICT/ right ID	0.038 ± 0.011	0.046 ± 0.013	<0.01
Right middle ICT/ right ID	0.040 ± 0.011	0.048 ± 0.014	<0.01
Right posterior ICT/ right ID	0.038 ± 0.012	0.046 ± 0.013	<0.01
Insular cortical volumes			
Left insular volume (cm3)	0.904 ± 0.274	1.099 ± 0.283	<0.01
Right insular volume (cm3)	0.860 ± 0.258	1.059 ± 0.287	<0.01

Results are expressed as mean ± *SD*.* GLM adjusted for gender, gestational at MRI, maternal smoking and body mass index. ICT: insular cortical thickness; ID: insular depth. Insular volumes were additionally adjusted for total brain volume.

Late-onset SGA fetuses also showed a more pronounced left insular cortical asymmetry in thickness and volume analyses compared to controls, with significant differences in the left posterior insular cortex (asymmetry index: -0.115 vs. -0.078; p= 0.038). They also showed a trend for lower fractional anisotropy values in the left insula, reaching statistical significance in the left anterior insula.

As in our previous study (Egana-Ugrinovic 2013), small fetuses were divided into two groups according to the presence of signs associated to a poorer perinatal (Figueras 2014). There was a significant linear tendency to more pronounced alterations in thickness and volume of the insular cortex in SGA with signs of poorer perinatal outcome as compared with cases without them and controls (Figure 1).

Figure 1. Insular cortical thicknesses (A) and volumes (B) according to prenatal severity signs.

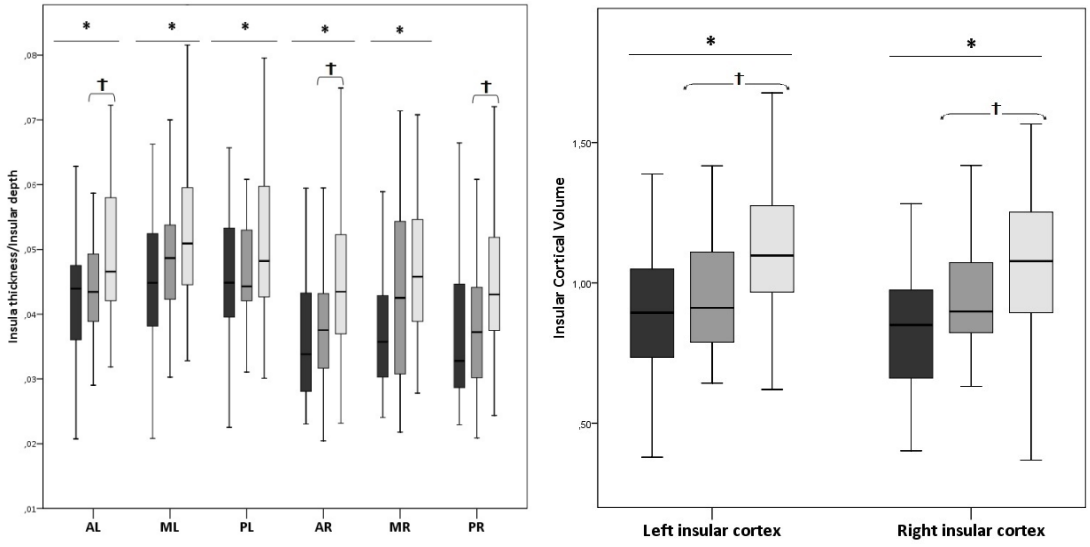

Polynomial contrast analysis showing differences between late-onset SGA showing the presence of severity signs (black box plot), late-onset SGA without these signs (grey box plot) and AGA (light grey box plot). Bars depict the mean within each group. A) *p<0.01 and †p<0.05. Linear tendency for insular cortical thickness/insular depth. AL, ML and PL: anterior, middle and posterior left thickness; AR, MR and PR: anterior, middle and posterior insular cortical left thickness. B) * and † p<0.05. Linear tendency for left and right insular cortical volume.

Finally we tested the association between insular morphometry and neurobehavior and we found that several insular measurements and NBAS test scores from specific clusters in late-onset SGA were associated (Table 2). These findings were supported by the ordinal regression analysis which showed a significant change of the global scoring towards overall lower NBAS scores in late-onset SGA (model p value=<0.01), with statistical significance in: left-anterior, left-middle, right-anterior and right-middle insular cortical thickness (p<0.05); anterior and middle cortical thickness asymmetry index (p=0.03); left insular lobe depth (p=0.04) and TBV (p=0.03).

Table 2. Insular cortical morphometry and its association with neurobehavioral outcome in late-onset SGA.

Insular measurement	**NBAS Cluster**	***P****
Left insular cortical thickness		
1. Anterior	Organization of state	0.04
	Autonomic nervous system	0.04
	Social-interactive	0.03
2. Middle	Regulation of state	0.03
	Attention	0.04
3. Posterior	Autonomic nervous system	0.04
Right insular cortical thickness		
1. Middle	Regulation of state	0.02
2. Posterior	Autonomic nervous system	0.04
Insular lobe depth		
1. Right	Regulation of state	0.04
Cortical thickness AI		
1. Posterior	Autonomic nervous system	0.02
2. Middle	Regulation of state	0.03

* GLM considering the NBAS test's clusters <5th centile as the dependent variable and insular measurements as the independent variables adjusted for gender, GA at MRI, GA at NBAS, maternal smoking and BMI.

Our findings confirm the study hypothesis that insular cortical morphometry was significantly different in late-onset SGA fetuses and correlated with poorer neurobehavioral performance in this population.

6.3 STUDY 3: CORPUS CALLOSUM DIFFERENCES ASSESSED BY FETAL MRI IN LATE-ONSET INTRAUTERINE GROWTH RESTRICTION AND ITS ASSOCIATION WITH NEUROBEHAVIOR.

The results of this project have been published in an international journal and have been presented at the 12th Fetal Medicine Foundation World Congress, 23-27 June 2013, Marbella, Spain (Oral presentation).

Three (3%) IUGR and seven (9%) AGA fetuses had to be excluded due to insufficient image quality for delineation, leaving a total of 117 late-onset IUGR and 73 control fetuses. Small fetuses presented smaller areas in the corpus callosum, particularly in the posterior portion. Again, we subdivided IUGR according to the presence of signs associated of a poorer perinatal outcome (Figueras 2014). In general, corpus callosum length and area were similarly reduced in IUGR with and without sings of poorer perinatal outcome, as compared with controls, but there was a linear trend suggesting a relationship with the severity criteria defined in this study (Figure 1).

Figure 1. Differences among IUGR fetuses according to clinical severity criteria in CC length and total area.

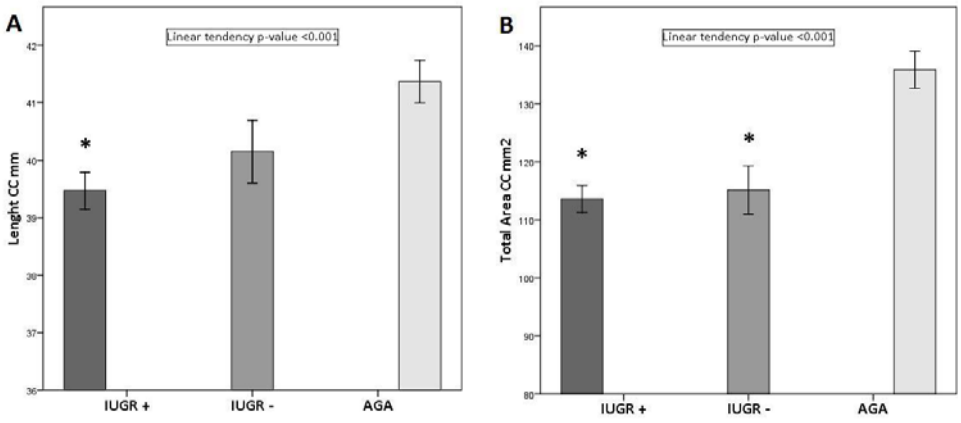

Linear tendency by polynomial contrast analysis showing differences between late-onset IUGR: IUGR+ are those IUGR with severity signs defined as cerebroplacental ratio <5th centile, UtA Doppler before birth >95th centile, or a birthweight <3rd centile), IUGR- (IUGR without severity sings) and AGA. Bars depict the mean ± SD. *p<0.05 compared with AGA.

The NBAS test was performed at 42-43 weeks in the IUGR population, with a mean of 28.8 ± 16.8 days after birth. The results from the ordinal regression analysis between the corpus callosum measurements and the neurobehavioral test showed a significant change of the global scoring towards lower NBAS scores in IUGR at the presence of smaller measurements of the corpus callosum. Specifically, smaller total area (p=0.03), rostrum (p=0.02), genu (p=0.03), rostral body (p=0.02), anterior midbody (p=0.03) and splenium (p=0.03) had a significant negative effect on the number of abnormal NBAS clusters (Table 1).

Table 1. Corpus callosum measurements and its association with neurobehavioral outcome in late-onset IUGR.

Corpus callosum measurement	Coefficient value	P*
Length	-0.14	0.52
Anterior thickness	-0.19	0.84
Middle thickness	-3.49	0.05
Posterior thickness	0.34	0.65
Total area	-0.48	0.03
Rostrum area	-0.59	0.02
Genu area	0.54	0.03
Rostral body area	-0.56	0.02
Anterior midbody area	-0.77	0.04
Posterior midbody area	-0.01	0.99
Isthmus area	-0.70	0.16
Splenium area	-0.52	0.03

*Ordinal regression adjusted for gender, gestational age at MRI, gestational age at NBAS, maternal smoking and body mass index, where the NBAS test's clusters <5th centile were considered as the dependent variable and corpus callosum measurements as the independent variables. A negative coefficient value indicated that at the presence of smaller corpus callosum measurements the amount of NBAS test's clusters <5th centile increased.

To our knowledge this is the first study on corpus callosum development in late-onset IUGR fetuses describing morphometric differences which are further related to their neurobehavioral performance.

6.4 STUDY 4: NEUROSONOGRAPHIC ASSESSMENT OF THE CORPUS CALLOSUM AS A POTENTIAL BIOMARKER OF ABNORMAL NEURODEVELOPMENT IN LATE-ONSET FETAL GROWTH RESTRICTION

The results of this project have been accepted for publication in an international journal and have been submitted as an abstract for the 24nd World Congress on Ultrasound in Obstetrics and Gynecology, 14-17 September 2014, Barcelona, Spain.

Maternal characteristics did not differ between cases and controls. As expected, small fetuses were delivered earlier with higher rates of labor induction, emergency cesarean section and longer stay in the neonatal intensive unit care, as in our previous studies. Five percent of the images had to be discarded because of insufficient quality to perform image post-processing, leaving a total of 165 fetuses scanned, classified in 94 small fetuses and 71 controls. No structural abnormalities were found in the study groups.

Small fetuses showed a reduced corpus callosum length, smaller total corpus callosum area and smaller areas in all the subdivisions (Table 1). After adjusting for potential confounding covariates, corpus callosum length, total corpus callosum and splenium area were significantly different between the two groups.

Table 1. Corpus callosum measurements in the study groups.

Corpus callosum measurement	Small fetuses (N = 94)	AGA (N = 71)	P*
Lenght/CI	0.493 ± 0.042	0.516 ± 0.052	<0.01
Anterior thickness / CI	0.061 ± 0.013	0.064 ± 0.014	0.25
Middle thickness / CI	0.041 ± 0.007	0.043 ± 0.007	0.06
Posterior thickness / CI	0.066 ± 0.016	0.068 ± 0.015	0.42
Total area / CI	1.828 ± 0.432	2.0344 ± 0.441	<0.01
Rostrum area / CI	0.135 ± 0.054	0.186 ± 0.250	0.06

Genu area / CI	0.283 ± 0.119	0.314 ± 0.110	0.09
Rostral body area / CI	0.341 ± 0.076	0.367 ± 0.073	0.03
Anterior midbody area / CI	0.224 ± 0.056	0.243 ± 0.051	0.03
Posterior midbody area / CI	0.219 ± 0.06	0.235 ± 0.046	0.05
Isthmus area / CI	0.206 ± 0.074	0.215 ± 0.055	0.40
Splenium area / CI	0.473 ± 0.125	0.554 ± 0.185	<0.01

*Student's t test for independent samples. Results are expressed as mean ± SD. CI: cephalic index.

To explore if there was an association between corpus callosum measurements and the severity of growth restriction, small fetuses were subdivided into (1) Late-onset IUGR if the previously reported predictors of a poorer perinatal outcome were present (Figueras 2014), and (2) SGA when none of those factors were present. We found that callosal differences were markedly present in late-onset IUGR fetuses, showing a significant linear trend for shorter and smaller corpus callosum, and smaller splenium area (Figure 1).

Figure 1. Differences in corrected corpus callosum biometries among AGA and small fetuses, divided as IUGR and SGA.

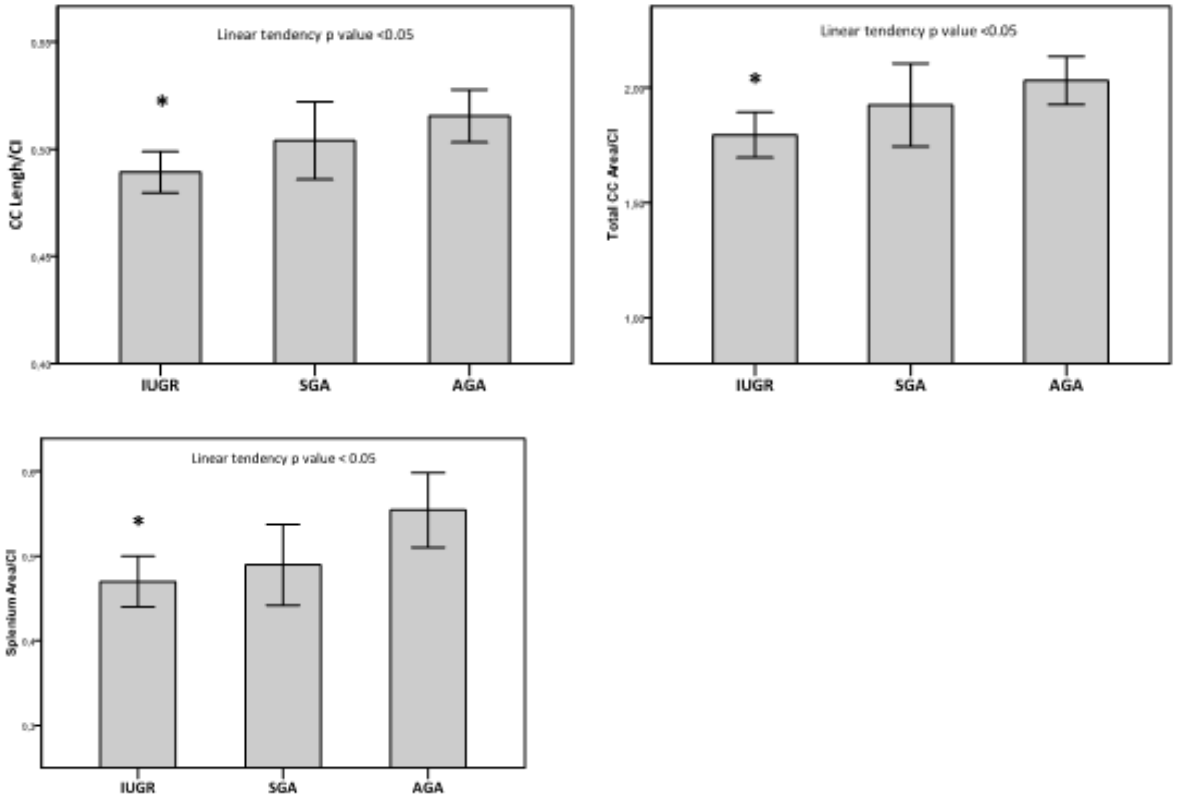

Linear tendency by polynomial contrast analysis showing differences between late-onset IUGR fetuses subclassified into IUGR and SGA, compared to AGA. IUGR fetuses were defined as those with birth weight <3rd centile and/or cerebroplacental ratio <5th centile and/or UtA PI >95th centile; and SGA when non of this factors were present. *p<0.05 compared with AGA. Results were adjusted by gestational age at NSG, maternal body mass index and smoking.

Regarding corpus callosum growth, significant differences were present between clinical groups. Average total corpus callosum area growth was lower in small fetuses compared to AGA (0.025/week vs. 0.034/week; *p*=0.04) as well as splenium growth (0.010/week vs. 0.027/week; *p*=0.02).

In summary this study shows that late-onset small fetuses present significant differences in their corpus callosum development and morphology. These findings support how NSG can be considered a valid tool to detect subtle brain differences in fetuses exposed to late-onset growth restriction. Further research involving long-term follow-up is warranted to evaluate the potential use of the corpus callosum assessment by NSG as an imaging biomarker of subtle anomalies of neurodevelopment in children at risk.

6.5 STUDY 5: CORRELATION BETWEEN BRAIN MICROSTRUCTURE ASSESSED BY FETAL MRI AND NEURODEVELOPMENTAL OUTCOME AT 2 YEARS IN TERM SMALL FOR GESTATIONAL AGE BORN INFANTS

The results of this project have been submitted to an international journal and as an abstract for the 24nd World Congress on Ultrasound in Obstetrics and Gynecology, 14-17 September 2014, Barcelona, Spain.

A total of 110 fetuses fulfilled the inclusion criteria. Of these, 8 births were lost during follow-up, having no means of contact for neurocognitive evaluation leaving a total of 60 small fetuses and 42 controls. Maternal characteristics did not differ between cases and controls and as expected, small fetuses were delivered earlier with higher rates of labor induction, emergency cesarean section and longer stay in the neonatal intensive unit care.

Differences between term small fetuses and AGA

1) Cortical development and corpus callosum assessment: small fetuses had overall deeper fissures measurements, reaching statistical significance in the left insula, right insula and left cingulate fissure. They also presented thinner insular cortical thicknesses and smaller insular cortical volumes. Regarding the corpus callosum measurements, small fetuses showed smaller corpus callosum total areas and smaller areas from its subdivision reaching statistical significance in the genu, rostral body, anterior midbody, posterior midbody, isthmus and splenium areas.

2) Neurodevelopmental outcome: Neurodevelopmental outcome was assessed at 23.5±1.2 and 23.9±1.0 months in small fetuses and controls, respectively. Small born infants showed lower score in all domains from the Bayley-III test (Figure 1). Differences in the

cognitive, language and motor domains remained significant after adjusting for potential confounders variables.

Figure 1. Score distribution for each neurodevelopmental domain assessed by Bayley-III in the study group.

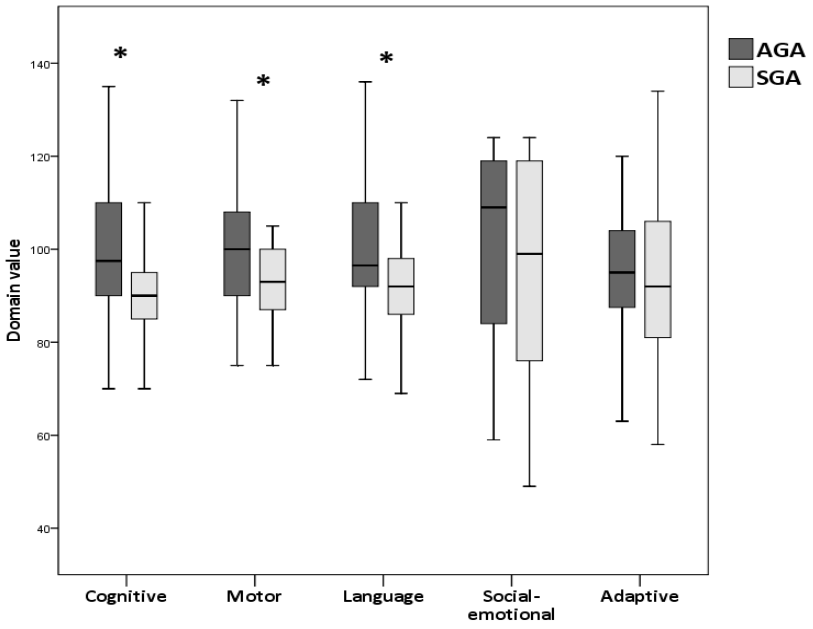

*p <0.05. GLM adjusting for gender, smoking, socio-economic class, month at Bayley-III and breastfeeding.

Correlation between CD and CC with abnormal neurodevelopmental outcome

1) Correlations analyses: taking into account the entire cohort, we found a negative linear correlation between cortical development and corpus callosum assessment with the neurodevelopmental outcome, indicating that smaller measurements were associated to worse Bayley-III scores, with statistical significance in the BPD (Pearson -0.329; p<0.01), fronto-occipital diameter (Pearson -0.372; p<0.01), insular asymmetry (Pearson 0.306; p=0.01), total corpus callosum area (Pearson -0,250; p=0.02), rostral body area (Pearson -0.298; p<0.01), anterior midbody area (Pearson -0.232; p=0.03), posterior midbody area (Pearson -0.333; p<0.01) and isthmus area (Pearson -0.235; p=0.03).

2) Linear regression analysis: we used a principal component analysis in order to select the most significant variables in the model. These variables were the posterior midbody

area, corpus callosum length and right lateral fissure depth. A composite score (ranging from 0 to 1) was constructed using a combination of them according to the following formula obtained by logistic regression: Composite score=e-(Y)/ (1 + e-(Y)), where Y= 1.183 + (Posterior midbody/CI * CC Length/CI * Right lateral fissure/BPD * -41.264). The composite score achieved a higher predictiveness as compared with any of the individual parameters (p=0.026) (Figure 3) and showed an area under the curve of 78% (95% confidence interval: 62-93%) for an abnormal Bayley-III (Figure 2).

Figure 2. Composite score and Bayley-III test.

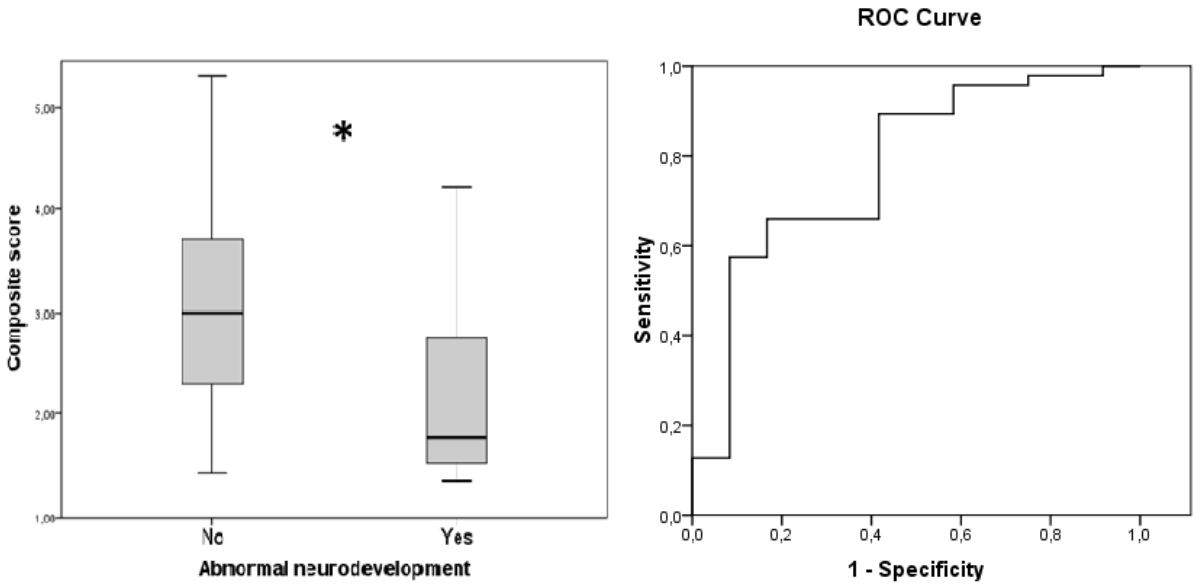

* p<0.01. Composite score obtained by logistic regression and its ROC curve for an abnormal Bayley-III test.

Our findings support the hypothesis that late-onset IUGR fetuses present a different pattern of cortical development with deeper fissures and smaller brain volumes, and a different corpus callosum morphometry with smaller areas. Moreover, full term IUGR fetuses have poorer neurodevelopmental outcome. We propose the use of a composite score using a combination of cortical development and corpus callosum parameters to predict abnormal neurodevelopment at 2 years.

7. DISCUSSION

Our first study provides evidence that late-onset IUGR fetuses present a different pattern of cortical development compared to normally grown fetuses, with deeper fissures, smaller brain volumes and a more pronounced right asymmetry. This data suggests that an abnormal brain maturation and reorganization could occur under chronic placental insufficiency conditions (Batalle 2012; Sanz-Cortes 2013; Makhoul 2004). These results are in line with reports from early IUGR neonates, where a disrupted cortical sulcation pattern was detected (Tolsa 2004; Dubois 2008). Furthermore, fetuses diagnosed with congenital heart defects whose brains are exposed to chronic/moderate hypoxia due to an impaired brain perfusion, present significant differences in cortical development and sulcation (Limperopoulos 2010; Clouchoux 2013).

Despite most areas were affected, the insula and cingulate fissure were the areas predominantly altered; both are responsible for interoceptive awareness and higher cognitive functions (Allen 1991). It could be inferred that they are predominantly affected due to their vulnerability to sustained undernutrion and/or hypoxia from a later maturation during pregnancy (Hernandez-Andrade 2008). On the other hand, the decreased brain volumes in IUGR might reflect reductions in brain cellularity, as described in experimental animal models of chronic hypoxia (Uno 1990).

It is also remarkable that term IUGR fetuses presented differences in the physiological brain asymmetry. This feature of normal brain development is thought to be responsible of lateralization of language and handedness, but abnormalities in normal brain asymmetry have been reported in different neurodevelopmental disorders such as autism, dyslexia and

schizophrenia among others. Therefore, it remains unknown whether the altered brain asymmetry in IUGR could be related to the prenatal origin of some of these neurocognitive disorders (Barker 2007; Dubois 2008; Huppi 2008).

The second study was designed in light of the results of the first study, where the perisylvian region showed to be one of the most affected areas of cortical development in term IUGR. Therefore, this study shows how late-onset IUGR fetuses present significant differences in thickness, volume and fractional anisotropy values of the insular cortex. Our results go in line with other authors who reported thinner cortex and decreased gray matter (Dubois 2008) in early and severe IUGR newborns. Previous reports on neurodevelopmental outcome of late-onset IUGR fetuses, have shown worse scores in attention, social, self-regulation, communication, problem-solving and memory function competencies among others (Geva 2006; Eixarch 2008; Figueras 2009). All of these functions are closely related to the insula and the limbic system functionality (Nieuwenhuys 2012; Augustine 1996). Accordingly, we found that thinner and smaller insulas were associated with worse neurobehavioral outcomes in IUGR.

From a pathophysiological standpoint, the potential mechanisms leading to prominent alterations in the insular cortex under IUGR conditions could be related to the fact that: 1) morphometric changes of the insula occur late in pregnancy, with an important deepening and stretching of the area under the surrounding brain lobes, and the fact that 2) during the third trimester an active synaptogenesis takes place, which could be particularly vulnerable to a chronic hypoxic environment. Supporting to some extent this hypothesis, lower fractional anisotropy values in our IUGR population could be interpreted as a sign of a less mature or organized cortex in this area.

Although our results are based on fetal brain MRI which has undeniable advantages when analyzing the fetal cortex, overall cortical development can be assessed by means of simpler techniques, particularly ultrasound, to identify the emergence of the brain fissures along the pregnancy (Pistorius 2010; Cohen-Sacher 2006). It seems feasible to assess the fetal cortex by means of a dedicated neurosonography in IUGR fetuses; this study seems warranted in the near future. To conclude, this study provides further evidence that late-onset IUGR fetuses present differences in their cortical development, particularly on the insular cortex which was further related a worse neurobehavioral performance.

The third study shows how late-onset IUGR fetuses presented differences in their corpus callosum morphometric MRI assessment. Furthermore, several callosal measurements were correlated with abnormal neurobehavioral scores in fetuses with IUGR. Our results go in line with previous studies reporting a reduced growth rate of the corpus callosum assessed by ultrasound in early-onset IUGR fetuses (Goldstein 2011) and smaller spleniums in preterm and growth restricted children (Nosarti 2004). Interestingly, our findings in late-onset IUGR fetuses were mainly related to smaller areas in the majority of corpus callosum subdivisions, rather than reduced linear measurements. This could be explained because callosal growth in the third trimester of pregnancy is predominantly based on an area increase rather than a length increase, and its thickening follows an anterior-to-posterior direction (Moses 2000).

Since the corpus callosum is one of the most representative white matter structures in the human brain, this study further supports the notion that brain reorganization affects white matter development as shown by connectivity analyses in one year old IUGR infants (Batalle 2012; Eikenes 2012). Remarkably, corpus callosum developmental abnormalities have been associated to different cognitive disorders (Paul 2011). Therefore, the value of corpus

callosum assessment deserved further attention to explore its use as a potential imaging biomarker in order to identify high-risk pregnancies of abnormal neurodevelopment, as reported in growth restriction (Savchev 2013), congenital heart disease (Owen 2014) and congenital cytomegalovirus infection (Foulon 2008).

To our knowledge this is the first study on corpus callosum development in late-onset IUGR fetuses describing morphometric differences which are further related to their neurobehavioral performance.

Based on the results obtained from our third study and the potential role of the corpus callosum as an imaging biomarker, we tested whether a detailed corpus callosum evaluation could be performed by a standard fetal brain ultrasound examination and if it could replicate our MRI findings. In **our fourth study** we found that late-onset small fetuses showed global and specific callosal differences, with a lower growth rate when assessed by neurosonography. Interestingly, and coinciding with our MRI results from the third study, posterior portions of the corpus callosum were particularly affected in small fetuses. Reports from rats show how the exposure to hypoxia resulted in smaller corpus callosum (Langmeier 1989), which was related to myelination deficits. Furthermore, postmortem studies from neonates that suffered perinatal asphyxia showed a reduced number of callosal fibers and immature oligodendrocytes (Vasung 2011; Back 2001). It seems that perinatal events can affect corpus callosum growth and can persist with clinical significance as shown in preterm-born adolescents who present smaller corpus callosum (Nosarti 2004). The potential role of the corpus callosum as an imaging biomarker is further supported by studies in subjects diagnosed with language disorders, autism and attention deficit hyperactivity disorders where smaller corpus callosums are found (Counsell 2008).

In summary this study provides further evidence that late-onset small fetuses present significant differences in their callosal development and morphology. Also, these findings support how neurosonography can be considered a valid tool to detect subtle brain differences in fetuses exposed to late-onset growth restriction.

In all these studies, we classified IUGR according to the presence or absence of signs of adverse perinatal outcome (Figueras 2014) in order to explore a relation between structural alterations and clinical severity. Although, small fetuses with the presence of severity signs, or so called IUGR, showed more accentuated differences in their cortical development and and corpus callosum morphology, those small fetuses without signs of adverse perinatal outcome also presented these differences when compared to controls. This is a relevant concept since small fetuses without the presence of these adverse perinatal outcome predictors are usually considered as "constitutionally small". Our findings are in line with other studies that found how this subpopulation presents metabolic differences and signs of cardiovascular remodeling, challenging the concept of being constitutionally small (Crispi 2010; Sanz-Cortes 2013; Savchev 2013). Our results support the need to better characterize those small fetuses at term that undergo true forms of placental insufficiency. As a consequence of this imprecise definition of real growth restriction and the difficulty in finding a common cause for all forms of IUGR, we used different terminology throughout the studies to define this population. As the term has evolved, we named them late-onset IUGR, term SGA or small fetuses. However, there is abundant evidence that SGA is a surrogate of fetal growth restriction (Figueras 2014) and that milder forms of IUGR will show signs of brain reprogramming as well, supported by the findings of our research.

Based on the results of the first four studies, we conducted **our fifth project** to test the predictive capacity of these brain microstructural differences detected in small fetuses for an abnormal neurodevelopment at two years of age. We found that small fetuses presented worse neurodevelopmental outcome. Furthermore, the prenatal brain assessment was associated to the results from the neurodevelopmental test. Some relevant pathophysiologic implications can be extracted from this association: an abnormal Bayley-III test was correlated to shallower fissures, thinner insular cortex and smaller corpus callosum areas.

Although previous studies have shown poorer neurodevelopmental outcome in term SGA (Arcangeli 2012; Savchev 2013), none of them have provided information about their brain developmental status before birth. Indeed, our previous experience showing how small fetuses show a different pattern in cortical development, with particular changes in the insular area and differences in their corpus callosum morphology, which were further associated to a worse neurobehavioral outcome in the neonatal period, give grounds on this microstructural/functional association (Egaña-Ugrinovic 2013; Egaña-Ugrinovic 2014; Sanz-Cortes 2013). Interestingly, we found that small-born babies had lower cognitive, motor and language competencies. All of these functions are closely related to the insula and callosal functionality. We acknowledge that the expression of these domains might involve the activation of different brain areas; nevertheless, the insula and the corpus callosum have been specifically involved in human emotion, language and cognition (Nieuwenhuys 2012; Paul 2011). Indeed, Geva *et al.* proposed that thinner cortex found in severe IUGR born children could be responsible for their lower IQ scores (Geva 2006). Therefore, our study

suggests that brain alterations at term could constitute the first step in the cascade of functional impairments underlying neurodevelopmental pathologies (Dubois 2008).

The importance of this work relies on the notion that late-onset IUGR is far more prevalent than the early-onset form. Consequently, late-onset IUGR represents a significant public health problem and its impact on the adverse neurodevelopment outcome of this population cannot be overestimated. The development of brain image biomarkers offers the possibility to detect structural abnormalities long before the appearance of functional symptoms (Huppi 2008).

Identifying fetuses at-risk for abnormal neurodevelopment in fetal medicine lays the basis to perform specific strategies to potentially improve both pre and postnatal outcome in the critical period of the first years of life. Simple strategies such as reinforcing breast feeding, early stimulation, the inclusion in Newborn Individualized Developmental Care and Assessment Programs (NIDCAP) have shown to improve neurobehavior, electrophysiology and brain structure when compared to those receiving standard care (Als 2012).

Moreover, the implications of these results open the door to the potential implementation of these biomarkers into other conditions in fetal medicine aiming to identify endophenotypes more susceptible to develop neurological disorders.

We finally conclude that SGA fetuses showed differences in their cortical development and corpus callosum microstructure and during their follow up presented worse neurodevelopmental outcome at 2-years. Based on these results we showed that fetal brain MRI cortical development and corpus callosum parameters have the potential value to predict an abnormal neurological outcome. These results support the value of brain

reorganizational changes as potential image biomarkers to identify those infants at risk for an abnormal neurodevelopment. Further research involving long-term follow-up is warranted to construct predictive models of abnormal neurodevelopment in fetuses with IUGR and other fetal conditions based on their prenatal brain assessment.

8. CONCLUSIONS

Final considerations of the contribution of this research work

With these five studies we add to the body of evidence that term small fetuses with normal umbilical artery Doppler, present differences in their brain cortical and corpus callosum microstructure as compared to controls. Furthermore a worse neurodevelopmental outcome was present which correlated with their brain microstructural alterations.

In this respect, the objectives of this research have been accomplished as follows:

1. Term SGA present deeper brain fissures, smaller volumes and different asymmetries.
2. Term SGA show thinner cortex and smaller cortical volumes in the insula which correlated to their neurobehavioral performance.
3. Small fetuses present abnormal corpus callosum morphology with smaller areas, mainly affecting its posterior portion as shown by MRI, which was further associated to their neurobehavioral performance.
4. These corpus callosum differences in term SGA shown by fetal MRI where also present in the neurosonographic assessment of late-onset IUGR as compared with controls.
5. Finally, we provided evidence that prenatal brain assessment of late-onset IUGR correlated with their neurodevelopmental outcome at 2 years. A combination of fetal brain imaging biomarkers can help to improve the characterization of late-onset IUGR and identify those fetuses at risk of an abnormal neurodevelopment.

9. ABBREVIATIONS

IUGR	Intrauterine growth restriction
SGA	Small for gestational age fetus
AGA	Adequate for Gestational Age
MRI	Magnetic resonance imaging
NBAS	Neonatal behavioral assessment scale
Bayley-III	Bayley scale for infant and toddler development
BPD	Biparietal diameter
PI	Pulsatility Index
ISUOG	International Society of Ultrasound in Obstetrics and Gynecology

10. REFERENCES

(2007). Sonographic examination of the fetal central nervous system: guidelines for performing the 'basic examination' and the 'fetal neurosonogram'. Ultrasound Obstet Gynecol 2007;29: 109-16.

Achiron, R. and A. Achiron. Development of the human fetal corpus callosum: a high-resolution, cross-sectional sonographic study. Ultrasound Obstet Gynecol 2001;18: 343-7.

Alexander, A. L., J. E. Lee, et al. Diffusion tensor imaging of the corpus callosum in Autism. Neuroimage 2007; 34: 61-73.

Allen, G. V., C. B. Saper, et al. Organization of visceral and limbic connections in the insular cortex of the rat. J Comp Neurol 1991; 311: 1-16.

Allin, M., C. Nosarti, et al. Growth of the corpus callosum in adolescents born preterm. Arch Pediatr Adolesc Med 2007; 161: 1183-9.

Alonso, I., M. Borenstein, et al. Depth of brain fissures in normal fetuses by prenatal ultrasound between 19 and 30 weeks of gestation. Ultrasound Obstet Gynecol 2010; 36: 693-9.

Als, H., F. H. Duffy, et al. NIDCAP improves brain function and structure in preterm infants with severe intrauterine growth restriction. J Perinatol 2012; 32: 797-803.

Anderson, N. G., I. Laurent, et al. Growth rate of corpus callosum in very premature infants. AJNR Am J Neuroradiol 2005; 26: 2685-90.

Arcangeli, T., B. Thilaganathan, et al. Neurodevelopmental delay in small babies at term: a systematic review. Ultrasound Obstet Gynecol 2012; 40: 267-75.

Arduini, D. and G. Rizzo. Normal values of Pulsatility Index from fetal vessels: a cross-sectional study on 1556 healthy fetuses. J Perinat Med 1990; 18: 165-72.

Augustine, J. R. Circuitry and functional aspects of the insular lobe in primates including humans. Brain Res Brain Res Rev 1996; 22: 229-44.

Back, S. A., N. L. Luo, et al. Late oligodendrocyte progenitors coincide with the developmental window of vulnerability for human perinatal white matter injury. J Neurosci 2001; 21: 1302-12.

Bahado-Singh, R. O., E. Kovanci, et al. The Doppler cerebroplacental ratio and perinatal outcome in intrauterine growth restriction. Am J Obstet Gynecol 1999; 180: 750-6.

Barker, D. J. The origins of the developmental origins theory. J Intern Med 2007; 261: 412-7.

Barker, D. J. Fetal origins of coronary heart disease. BMJ 1995; 311: 171-4.

Barkovich, A. J. and B. O. Kjos. Normal postnatal development of the corpus callosum as demonstrated by MR imaging. AJNR Am J Neuroradiol 1988; 9: 487-91.

Baschat, A. A. and U. Gembruch. The cerebroplacental Doppler ratio revisited. Ultrasound Obstet Gynecol 2003; 21: 124-7.

Batalle, D., E. Eixarch, et al. Altered small-world topology of structural brain networks in infants with intrauterine growth restriction and its association with later neurodevelopmental outcome. Neuroimage 2012; 60: 1352-66.

Bayley N. Bayley Scales of Infant and Toddler Development - Third Edition: Administration Manual. PsychCorp: San Antonio, TX, 2006.

Boger-Megiddo, I., D. W. Shaw, et al. Corpus callosum morphometrics in young children with autism spectrum disorder. J Autism Dev Disord 2006; 36: 733-9.

Bornstein, E., A. Monteagudo, et al. A systematic technique using 3-dimensional ultrasound provides a simple and reproducible mode to evaluate the corpus callosum. Am J Obstet Gynecol 2010; 202: 201 e1-5.

Brazelton, T. B. Working with families. Opportunities for early intervention. Pediatr Clin North Am 1995; 42: 1-9.

Brazelton, T. B. Preface. Neonatal Intensive Care Unit Network Neurobehavioral Scale. Pediatrics 2004; 113: 632-3.

Brisse, H., G. Sebag, et al. Prenatal MRI of corpus callosum agenesis. Study of 20 cases with neuropathological correlations. J Radiol 1998; 79: 659-66.

Canals, J., C. Hernandez-Martinez, et al. Neonatal Behavioral Assessment Scale as a predictor of cognitive development and IQ in full-term infants: a 6-year longitudinal study. Acta Paediatr 2011; 100: 1331-7.

Cao, Q., L. Sun, et al. The macrostructural and microstructural abnormalities of corpus callosum in children with attention deficit/hyperactivity disorder: a combined morphometric and diffusion tensor MRI study. Brain Res 2010; 1310: 172-80.

Chauhan, S. P., L. M. Gupta, et al. Intrauterine growth restriction: comparison of American College of Obstetricians and Gynecologists practice bulletin with other national guidelines. Am J Obstet Gynecol 2009; 200: 409 e1-6.

Chen, C. Y., R. A. Zimmerman, et al. MR of the cerebral operculum: topographic identification and measurement of interopercular distances in healthy infants and children. AJNR Am J Neuroradiol 1995; 16: 1677-87.

Chi, J. G., E. C. Dooling, et al. Gyral development of the human brain. Ann Neurol 1977; 1: 86-93.

Clatterbuck, R. E. and E. P. Sipos. The efficient calculation of neurosurgically relevant volumes from computed tomographic scans using Cavalieri's Direct Estimator. Neurosurgery 1997; 40: 339-42; discussion 343.

Clouchoux, C., A. J. du Plessis, et al. Delayed cortical development in fetuses with complex congenital heart disease. Cereb Cortex 2013; 23: 2932-43.

Cohen, J. D., J. R. Mock, et al. Morphometry of human insular cortex and insular volume reduction in Williams syndrome. J Psychiatr Res 2010; 44: 81-9.

Cohen-Sacher, B., T. Lerman-Sagie, et al. Sonographic developmental milestones of the fetal cerebral cortex: a longitudinal study. Ultrasound Obstet Gynecol 2006;27: 494-502.

Counsell, S. J., A. D. Edwards, et al. Specific relations between neurodevelopmental abilities and white matter microstructure in children born preterm. Brain 2008; 131: 3201-8.

Crespo-Facorro, B., J. Kim, et al. Insular cortex abnormalities in schizophrenia: a structural magnetic resonance imaging study of first-episode patients. Schizophr Res 2000; 46: 35-43.

Crispi, F., F. Figueras, et al. Cardiovascular programming in children born small for gestational age and relationship with prenatal signs of severity. Am J Obstet Gynecol 2012; 207: 121 e1-9.

Cruz-Martinez, R., F. Figueras, et al. Cerebral blood perfusion and neurobehavioral performance in full-term small-for-gestational-age fetuses. Am J Obstet Gynecol 2009; 201: 474 e1-7.

Davenport, N. D., C. Karatekin, et al. Differential fractional anisotropy abnormalities in adolescents with ADHD or schizophrenia. Psychiatry Res 2010; 181: 193-8.

Doctor, B. A., M. A. O'Riordan, et al. Perinatal correlates and neonatal outcomes of small for gestational age infants born at term gestation. Am J Obstet Gynecol 2001;185:652-9.

Dubois, J., M. Benders, et al. Mapping the early cortical folding process in the preterm newborn brain. Cereb Cortex 2008; 18: 1444-54.

Dubois, J., M. Benders, et al. Primary cortical folding in the human newborn: an early marker of later functional development. Brain 2008; 131: 2028-41.

Dubois, J., M. Benders, et al. Structural asymmetries of perisylvian regions in the preterm newborn. Neuroimage 2010; 52: 32-42.

Dubois, J., L. Hertz-Pannier, et al. Structural asymmetries in the infant language and sensori-motor networks. Cereb Cortex 2009; 19: 414-23.

Egaña-Ugrinovic, G., M. Sanz-Cortes, et al. Differences in cortical development assessed by fetal MRI in late-onset intrauterine growth restriction. Am J Obstet Gynecol 2013; 209: 126.e1-8.

Egaña-Ugrinovic, G., M. Sanz-Cortes, et al. Fetal MRI Insular Cortical Morphometry and its association with Neurobehavior in Late-Onset Small for Gestational Age Fetuses. Ultrasound Obstet Gynecol 2014 Mar 10. doi: 10.1002/uog.13360.

Egaña-Ugrinovic G, Sanz-Cortes M, Couve-Perez C, Figueras F, Gratacos E. Corpus callosum differences assessed by fetal MRI in late-onset intrauterine growth restriction and its association with neurobehavior. Prenat Diagn 2014 Apr 7. doi: 10.1002/pd.4381.

Eikenes, L., M. P. Martinussen, et al. Being born small for gestational age reduces white matter integrity in adulthood: a prospective cohort study. Pediatr Res 2012; 72: 649-54.

Eixarch, E., E. Meler, et al. Neurodevelopmental outcome in 2-year-old infants who were small-for-gestational age term fetuses with cerebral blood flow redistribution. Ultrasound Obstet Gynecol 2008; 32: 894-9.

Figueras, F. and E. Gratacos. Update on the Diagnosis and Classification of Fetal Growth Restriction and Proposal of a Stage-Based Management Protocol. Fetal Diagn Ther. 2014 Jan 23. [Epub ahead of print]

Figueras, F., E. Meler, et al. Customized birthweight standards for a Spanish population. Eur J Obstet Gynecol Reprod Biol 2008; 136: 20-4.

Figueras, F., D. Oros, et al. Neurobehavior in term, small-for-gestational age infants with normal placental function. Pediatrics 2009; 124: e934-41.

Foulon, I., A. Naessens, et al. A 10-year prospective study of sensorineural hearing loss in children with congenital cytomegalovirus infection. J Pediatr 2008; 153: 84-8.

Gardosi, J. Intrauterine growth restriction: new standards for assessing adverse outcome. Best Pract Res Clin Obstet Gynaecol 2009; 23: 741-9.

Garel, C., I. Cont, et al. Biometry of the corpus callosum in children: MR imaging reference data. AJNR Am J Neuroradiol 2011; 32: 1436-43.

Garel, C., E. Chantrel, et al. Fetal cerebral cortex: normal gestational landmarks identified using prenatal MR imaging. AJNR Am J Neuroradiol 2001; 22: 184-9.

Geva, R., R. Eshel, et al. Memory functions of children born with asymmetric intrauterine growth restriction. Brain Res 2006; 1117: 186-94.

Geva, R., R. Eshel, et al. Neuropsychological outcome of children with intrauterine growth restriction: a 9-year prospective study. Pediatrics 2006; 118: 91-100.

Gilliam, M., M. Stockman, et al. Developmental trajectories of the corpus callosum in attention-deficit/hyperactivity disorder. Biol Psychiatry 2011; 69: 839-46.

Glenn, O. A. Normal development of the fetal brain by MRI. Semin Perinatol 2009; 33: 208-19.

Goldstein, I., A. Tamir, et al. Corpus callosum growth in normal and growth-restricted fetuses. Prenat Diagn 2011; 31: 1115-9.

Gomez, O., F. Figueras, et al. Reference ranges for uterine artery mean pulsatility index at 11-41 weeks of gestation. Ultrasound Obstet Gynecol 2008; 32: 128-32.

Goodyear, P. W., C. M. Bannister, et al. Outcome in prenatally diagnosed fetal agenesis of the corpus callosum. Fetal Diagn Ther 2001; 16: 139-45.

Hadlock, F. P., R. B. Harrist, et al. Estimation of fetal weight with the use of head, body, and femur measurements--a prospective study. Am J Obstet Gynecol 1985; 151: 333-7.

Hagmann, C. F., N. J. Robertson, et al. Foetal brain imaging: ultrasound or MRI. A comparison between magnetic resonance imaging and a dedicated multidisciplinary neurosonographic opinion. Acta Paediatr 2008; 97: 414-9.

Harreld, J. H., R. Bhore, et al. Corpus callosum length by gestational age as evaluated by fetal MR imaging. AJNR Am J Neuroradiol 2011; 32: 490-4.

Hazlett, H. C., M. D. Poe, et al. Early brain overgrowth in autism associated with an increase in cortical surface area before age 2 years. Arch Gen Psychiatry 2011; 68: 467-76.

Hernandez-Andrade, E., H. Figueroa-Diesel, et al. Changes in regional fetal cerebral blood flow perfusion in relation to hemodynamic deterioration in severely growth-restricted fetuses. Ultrasound Obstet Gynecol 2008; 32: 71-6.

Hofer, S. and J. Frahm. Topography of the human corpus callosum revisited--comprehensive fiber tractography using diffusion tensor magnetic resonance imaging. Neuroimage 2006; 32: 989-94.

Huppi, P. S. Neuroimaging of brain development--discovering the origins of neuropsychiatric disorders? Pediatr Res 2008; 64: 325.

Jugovic, D., J. Tumbri, et al. New Doppler index for prediction of perinatal brain damage in growth-restricted and hypoxic fetuses. Ultrasound Obstet Gynecol 2007; 30: 303-11.

Kasprian, G., G. Langs, et al. The prenatal origin of hemispheric asymmetry: an in utero neuroimaging study. Cereb Cortex 2011; 21: 1076-83.

Kier, E. L. and C. L. Truwit. The normal and abnormal genu of the corpus callosum: an evolutionary, embryologic, anatomic, and MR analysis. AJNR Am J Neuroradiol 1996; 17: 1631-41.

Kok, J. H., A. L. den Ouden, et al. Outcome of very preterm small for gestational age infants: the first nine years of life. Br J Obstet Gynaecol 1998; 105: 162-8.

Langmeier, M., J. Pokorny, et al. Changes of the neuronal structure produced by prolonged hypobaric hypoxia in infant rats. Biomed Biochim Acta 1989; 48: S204-7.

Leitner, Y., A. Fattal-Valevski, et al. Neurodevelopmental outcome of children with intrauterine growth retardation: a longitudinal, 10-year prospective study. J Child Neurol 2007; 22: 580-7.

Lerman-Sagie, T., L. Ben-Sira, et al. Thick fetal corpus callosum: an ominous sign? Ultrasound Obstet Gynecol 2009; 34: 55-61.

Ley, D., E. Tideman, et al. Abnormal fetal aortic velocity waveform and intellectual function at 7 years of age. Ultrasound Obstet Gynecol 1996; 8: 160-5.

Lim, K. I., M. F. Delisle, et al. Cephalic index is not a useful sonographic marker for trisomy 21 and trisomy 18. Fetal Diagn Ther 2004; 19: 491-5.

Limperopoulos, C. and C. Clouchoux. Advancing fetal brain MRI: targets for the future. Semin Perinatol 2009; 33: 289-98.

Limperopoulos, C., W. Tworetzky, et al. Brain volume and metabolism in fetuses with congenital heart disease: evaluation with quantitative magnetic resonance imaging and spectroscopy. Circulation 2010; 121: 26-33.

Lindqvist, P. G. and J. Molin. Does antenatal identification of small-for-gestational age fetuses significantly improve their outcome? Ultrasound Obstet Gynecol 2005; 25: 258-64.

Lo, Y. C., W. T. Soong, et al. The loss of asymmetry and reduced interhemispheric connectivity in adolescents with autism: a study using diffusion spectrum imaging tractography. Psychiatry Res 2011; 192: 60-6.

MacDorman, M. F. and T. J. Mathews. Behind international rankings of infant mortality: how the United States compares with Europe. Int J Health Serv 2010; 40: 577-88.

Mailath-Pokorny, M., G. Kasprian, et al. Magnetic resonance methods in fetal neurology. Semin Fetal Neonatal Med 2012; 17: 278-84.

Malinger, G. and H. Zakut. The corpus callosum: normal fetal development as shown by transvaginal sonography. AJR Am J Roentgenol 1993; 161: 1041-3.

Malinger, G. and H. Zakut. Transvaginal visualization of the corpus callosum. Am J Obstet Gynecol 1994; 171: 1677.

Makhoul, I. R., M. Soudack, et al. Sonographic biometry of the frontal lobe in normal and growth-restricted neonates. Pediatr Res 2004; 55: 877-83.

McAnulty, G. B., F. H. Duffy, et al. Effects of the Newborn Individualized Developmental Care and Assessment Program (NIDCAP) at age 8 years: preliminary data." Clin Pediatr (Phila) 2010; 49: 258-70.

Milne, S., J. McDonald, et al. The use of the Bayley Scales of Infant and Toddler Development III with clinical populations: a preliminary exploration." Phys Occup Ther Pediatr 2012; 32: 24-33.

Moses, P., E. Courchesne, et al. Regional size reduction in the human corpus callosum following pre- and perinatal brain injury. Cereb Cortex 2000; 10: 1200-10.

Nakamura, K., Y. Kawasaki, et al. Multiple structural brain measures obtained by three-dimensional magnetic resonance imaging to distinguish between schizophrenia patients and normal subjects. Schizophr Bull 2004; 30: 393-404.

Nieuwenhuys, R. The insular cortex: a review. Prog Brain Res 2012; 195: 123-63.

Nosarti, C., T. M. Rushe, et al. Corpus callosum size and very preterm birth: relationship to neuropsychological outcome. Brain 2004; 127: 2080-9.

Owen, M., M. Shevell, et al. Brain Volume and Neurobehavior in Newborns with Complex Congenital Heart Defects. J Pediatr 2014; 164: 1121-1127.e1.

Pashaj, S., E. Merz, et al. Biometry of the fetal corpus callosum by three-dimensional ultrasound. Ultrasound Obstet Gynecol 2013; 42: 691-8.

Paul, L. K. Developmental malformation of the corpus callosum: a review of typical callosal development and examples of developmental disorders with callosal involvement. J Neurodev Disord 2011; 3: 3-27.

Penttila, J., M. L. Paillere-Martinot, et al. Global and temporal cortical folding in patients with early-onset schizophrenia. J Am Acad Child Adolesc Psychiatry 2008;47:1125-32.

Pistorius, L. R., P. Stoutenbeek, et al. Grade and symmetry of normal fetal cortical development: a longitudinal two- and three-dimensional ultrasound study. Ultrasound Obstet Gynecol 2010; 36: 700-8.

Pujol, J., P. Vendrell, et al. When does human brain development end? Evidence of corpus callosum growth up to adulthood. Ann Neurol 1993; 34: 71-5.

Rajagopalan, V., J. Scott, et al. Local tissue growth patterns underlying normal fetal human brain gyrification quantified in utero. J Neurosci 2011; 31: 2878-87.

Reichel, T. F., R. M. Ramus, et al. Fetal central nervous system biometry on MR imaging. AJR Am J Roentgenol 2003; 180: 1155-8.

Righini, A., C. Parazzini, et al. Early formative stage of human focal cortical gyration anomalies: fetal MRI. AJR Am J Roentgenol 2012; 198: 439-47.

Robinson, H. P. and J. E. Fleming. A critical evaluation of sonar "crown-rump length" measurements. Br J Obstet Gynaecol 1975; 82: 702-10.

Ruiz, A., C. Sembely-Taveau, et al. Sonographic cerebral sulcal pattern in normal fetuses. J Radiol 2006; 87: 49-55.

Sagiv, S.K., et al. Prenatal organochlorine exposure and measures of behavior in infancy using the Neonatal Behavioral Assessment Scale (NBAS). Environ Health Perspect 2008; 116: 666-73.

Sanz-Cortes, M., F. Figueras, et al. Fetal brain MRI texture analysis identifies different microstructural patterns in adequate and small for gestational age fetuses at term. Fetal Diagn Ther2013; 33: 122-9.

Sanz-Cortes, M., G. Egaña-Ugrinovic, et al. Brainstem and cerebellar differences and their association with neurobehavior in term small-for-gestational-age fetuses assessed by fetal MRI. Am J Obstet Gynecol 2013 Dec 4. pii: S0002-9378(13)02166-2. doi: 10.1016/j.ajog.2013.12.008

Sanz-Cortes, M., F. Figueras, et al. Abnormal brain microstructure and metabolism in small-for-gestational-age term fetuses with normal umbilical artery Doppler. Ultrasound Obstet Gynecol 2010; 36: 159-65.

Savchev, S., F. Figueras, et al. Estimated weight centile as a predictor of perinatal outcome in small-for-gestational-age pregnancies with normal fetal and maternal Doppler indices. Ultrasound Obstet Gynecol 2012; 39: 299-303.

Savchev, S., M. Sanz-Cortes, et al. Neurodevelopmental outcome of full-term small-for-gestational-age infants with normal placental function. Ultrasound Obstet Gynecol 2013; 42: 201-6.

Severi, F. M., C. Bocchi, et al. Uterine and fetal cerebral Doppler predict the outcome of third-trimester small-for-gestational age fetuses with normal umbilical artery Doppler. Ultrasound Obstet Gynecol 2022; 19: 225-8.

Stancak, A., E. R. Cohen, et al. The size of corpus callosum correlates with functional activation of medial motor cortical areas in bimanual and unimanual movements. Cereb Cortex 2003; 13: 475-85.

Skranes, J., T. R. Vangberg, et al. Clinical findings and white matter abnormalities seen on diffusion tensor imaging in adolescents with very low birth weight. Brain 2007; 130: 654-66.

Takahashi, T., M. Suzuki, et al. Bilateral volume reduction of the insular cortex in patients with schizophrenia: a volumetric MRI study. Psychiatry Res 2004; 131: 185-94.

Tang, P. H., A. I. Bartha, et al. Agenesis of the corpus callosum: an MR imaging analysis of associated abnormalities in the fetus. AJNR Am J Neuroradiol 2009, 30: 257-63.

Toft, P. B. Prenatal and perinatal striatal injury: a hypothetical cause of attention-deficit-hyperactivity disorder? Pediatr Neurol 1999; 21: 602-10.

Tolsa, C. B., S. Zimine, et al. Early alteration of structural and functional brain development in premature infants born with intrauterine growth restriction. Pediatr Res 2004; 56: 132-8.

Toro, R. and Y. Burnod. A morphogenetic model for the development of cortical convolutions. Cereb Cortex 2005; 15: 1900-13.

Tremblay, E., E. Therasse, et al. Quality initiatives: guidelines for use of medical imaging during pregnancy and lactation. Radiographics 2012; 32: 897-911.

Uno, H., L. Lohmiller, et al. Brain damage induced by prenatal exposure to dexamethasone in fetal rhesus macaques. I. Hippocampus. Brain Res Dev Brain Res 1990; 53: 157-67.

Vasung, L., N. Jovanov-Milosevic, et al. Prominent periventricular fiber system related to ganglionic eminence and striatum in the human fetal cerebrum. Brain Struct Funct 2011; 215: 237-53.

Volpe, P., D. Paladini, et al. Characteristics, associations and outcome of partial agenesis of the corpus callosum in the fetus. Ultrasound Obstet Gynecol 2006; 27: 509-16.

Walker, D. M. and N. Marlow. Neurocognitive outcome following fetal growth restriction. Arch Dis Child Fetal Neonatal Ed 2008; 93: F322-5.

Warren, D. J., D. J. Connolly, et al. Assessment of sulcation of the fetal brain in cases of isolated agenesis of the corpus callosum using in utero MR imaging. AJNR Am J Neuroradiol 2010; 31: 1085-90.

Witelson, S. F. Hand and sex differences in the isthmus and genu of the human corpus callosum. A postmortem morphological study. Brain 1989; 112: 799-835.

Youssef, A., T. Ghi, et al. How to image the fetal corpus callosum. Ultrasound Obstet Gynecol 2013; 42: 718-20.

Zhang, Z., S. Liu, et al. Development of fetal cerebral cortex: assessment of the folding conditions with post-mortem magnetic resonance imaging. Int J Dev Neurosci 2010; 28: 537-43.